Waikato Regional Council Technical Report 2016/32

Sources of eroded soils and their contribution to long-term sedimentation in the Firth of Thames

www.waikatoregion.govt.nz
ISSN 2230-4355 (Print)
ISSN 2230-4363 (Online)

Waikato
REGIONAL COUNCIL
Te Kaunihera ā Rohe o Waikato

Prepared by:
A. Swales, M. Gibbs, G. Olsen, R. Ovenden ,K. Costley (National Institute of Water & Atmospheric Research Ltd.), T. Stephens (Dairy NZ)

For:
Waikato Regional Council
Private Bag 3038
Waikato Mail Centre
HAMILTON 3240

May 2016

Document #: 8995024

Peer reviewed by:
Pete Wilson Date July 2016

Approved for release by:
Dominique Noiton Date June 2017

Disclaimer

This technical report has been prepared for the use of Waikato Regional Council as a reference document and as such does not constitute Council's policy.

Council requests that if excerpts or inferences are drawn from this document for further use by individuals or organisations, due care should be taken to ensure that the appropriate context has been preserved, and is accurately reflected and referenced in any subsequent spoken or written communication.

While Waikato Regional Council has exercised all reasonable skill and care in controlling the contents of this report, Council accepts no liability in contract, tort or otherwise, for any loss, damage, injury or expense (whether direct, indirect or consequential) arising out of the provision of this information or its use by you or any other party.

Summary

Sedimentation in the Firth of Thames

Over the past 90 years, fine sediments have been accumulating on intertidal and shallow subtidal areas in the southern Firth of Thames at rates that are up to an order of magnitude higher than in many other North Island estuaries. Excess fine sediment deposits can physically smother seafloor plant and animal communities, place additional stress on fish and water-filtering organisms such as shellfish, limit the amount of light available for photosynthesising plants (e.g., seagrass), and increase oxygen demand in the water column and surface sediments leading to hypoxia (low oxygen), or in extreme cases, anoxia (zero oxygen).

It is important to understand the source of these fine sediment deposits in order to inform and guide management actions that may reduce sedimentation in the Firth of Thames. In 2015, Waikato Regional Council, DairyNZ, and NIWA co-funded a study to investigate fine sediments that are transported into the marine area by the two largest rivers flowing into the Firth of Thames, the Waihou and Piako Rivers. The aim of this study was to determine:

1) likely sources of contemporary fine sediments that are deposited in the Firth of Thames by catchment and land use; and
2) how these sources and rates of deposition may have changed over the past 1000 years or so.

Determining sediment sources

To determine the sources of contemporary sediments deposited in the Firth of Thames, we established a reference library of soil fingerprints for representative land uses within the Waihou and Piako catchments including, dairy, sheep/beef, vegetable crops, pine forests, and native bush (Figure 1). Soil samples were collected from these land uses throughout each catchment and analysed to determine their soil fingerprints.

We also collected samples along the Waihou and Piako Rivers, their major tributaries, and their deltas/outlets in the Firth. These samples were used to determine the proportional contributions of sediments from the main stem of each river and their tributaries, including indicative assessments of ongoing sediment loss by land use to the river network.

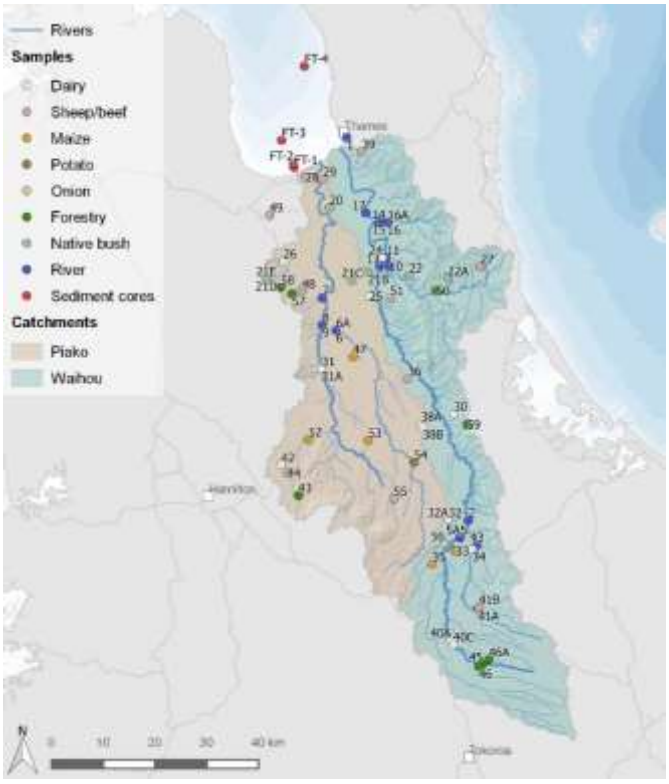

Figure 1: Sampling locations within the Waihou and Piako catchments and Firth of Thames.

To investigate how sources of sediment may have changed over the past ~1000 years, we analysed sediment accumulated in the Firth of Thames by collecting and dating marine sediment cores. We analysed sediment samples from different depths (age) down each core and compared the soil fingerprints with the established fingerprint library. The analysis of the cores required us to consider changes in land use over time from historical and pre-historic records and also the wider mix of land uses. The sediment cores also allowed

us to determine how sedimentation rates in the Firth have changed over the last 1000 years or so.

What we found

Contemporary sediment sources

The Waiomou Stream and Ohinemuri and Hikutaia Rivers collectively contribute 29% of the fine sediment delivered to the Firth of Thames by the Waihou River (Figure 2). The Waitoa River accounts for an estimated 65% of fine sediment load discharged by the Piako River into the Firth of Thames. Notably, previous WRC studies indicate that the Waihou River supplies about four times as much sediment to the Firth of Thames as the Piako River. Consequently, sediment sources in the Waihou catchment will dominate overall contemporary land-use derived sedimentation in the Firth of Thames.

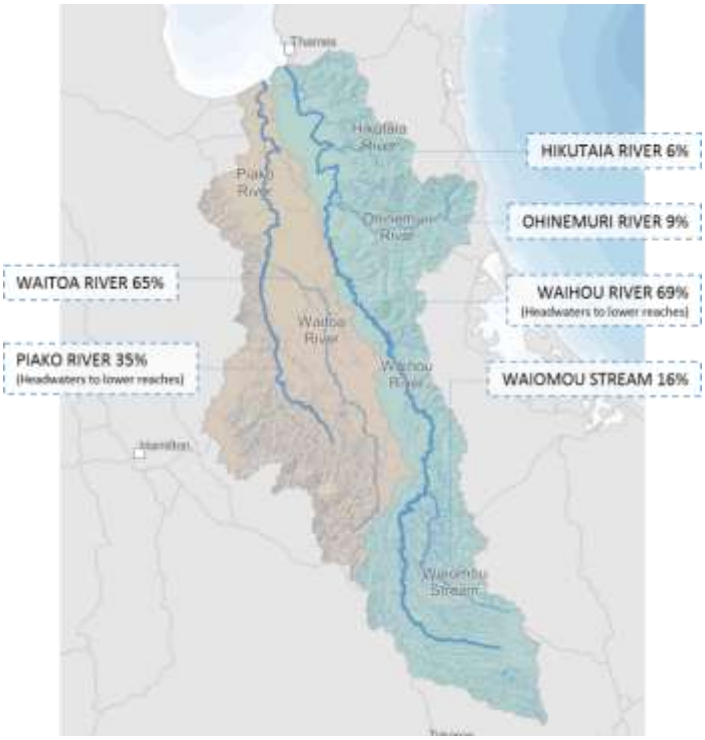

Figure 2: Proportional present-day sediment contributions (%) by major tributaries and main reaches of the Waihou and Piako Rivers to the Firth of Thames. This diagram does not illustrate the quantity of sediment per year supplied by each catchment – the Waihou carries approximately four times more sediment than the Piako. All estimates are indicative.

Changes in historic sediment sources

The results indicate that catchment subsoil is the largest source of fine sediment accumulating in the southern Firth of Thames (48–69%) and that this situation has persisted for the last 700 years or more (Figure 3). These soils no longer have a specific land use fingerprint and may be sourced from any land use in a deep erosion event (e.g., excavation, gullying, mass movement). Forest disturbance, both natural and human-influenced, is indicated by the contribution of bracken-labelled top soils (2–9%) in the cores. Interestingly, soils associated with pastoral farming (e.g., sheep & beef and dairy) make up a small proportion of sediments accumulating in the Firth of Thames since the early-20th century (< 7%) relative to the total extent of pasture in Waihou and Piako catchments (73%).

An unexpected result of the study is the substantial and increasing contribution of 'estuarine' or older reworked fine sediments accumulating in the southern Firth of Thames since the 1950-60's. The fingerprints of these estuarine sediments suggest that they are the result of mixing legacy river-borne sediments with organic sediments supplied by marine primary production over time (e.g., phytoplankton, diatoms, and sea grasses). Figure 3 shows that the proportion of these legacy 'estuarine' sediments has increased over time. These sediments are a legacy of previous soil erosion in the past (i.e., before, during and after large-scale deforestation and mining activities during the 1860s to early-1900s). Thus, both legacy and contemporary sources of sediment appear to be contributing to rapid sedimentation and development of intertidal mudflats in the southern Firth of Thames.

The sediment core dating results indicate that, even after large-scale deforestation in the catchment, which ended last century, contemporary sediment accumulation rates were still up to ~10-fold higher than before the mid-1800s.

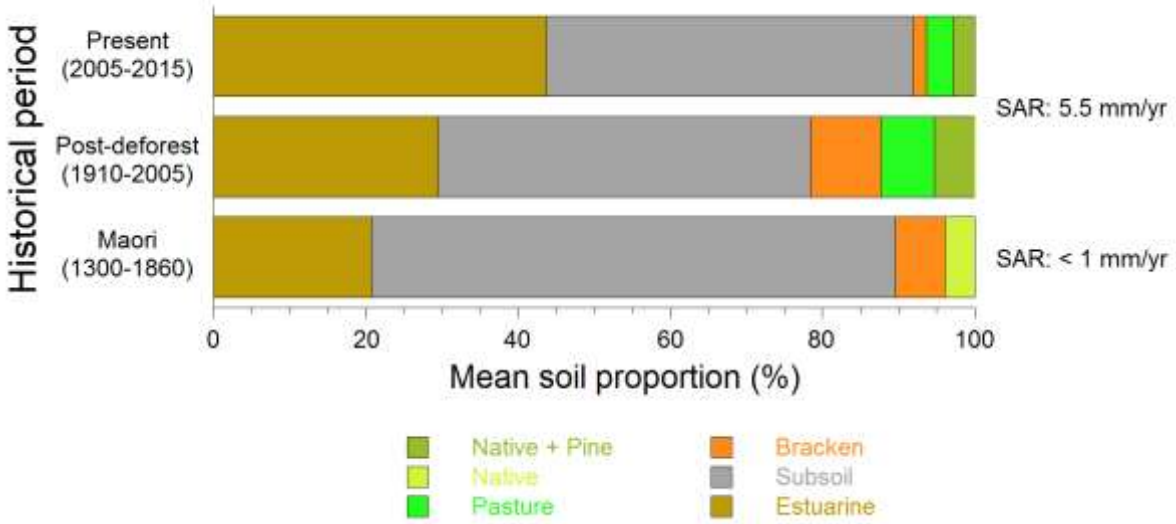

Figure 3: Summary of weighted-average soil source contributions (%) for three historical time periods. Long-term average contributions by land use were calculated for data from each of three cores (FT-1, FT-2, FT-4) by weighting % soil proportions by the time period (years) between individual dated samples and summing these for broad historical time periods. The source estimates for each core and historical period were then averaged between cores to construct Figure 3. Note that each time period comprises a different number of data points and the associated measurement errors are not presented in this figure. The sediment accumulation rate (SAR) for the post-deforestation to present time periods is also a weighted-average value based on lead-210 dating, whereas the Māori-period SAR is based on radiocarbon dating.

NIWA
Taihoro Nukurangi

Sources of eroded soils and their contribution to long-term sedimentation in the Firth of Thames

Prepared for Dairy NZ and Waikato Regional Council

May 2016

Prepared by:
A. Swales
M. Gibbs
T. Stephens[1]
G. Olsen
R. Ovenden
K. Costley

1. Dairy NZ

For any information regarding this report please contact:

Andrew Swales
Coastal & Estuarine Physical Processes Group
+64-7-856 7026
Andrew.Swales@niwa.co.nz

National Institute of Water & Atmospheric Research Ltd
PO Box 11115
Hamilton 3251

Phone +64 7 856 7026

NIWA CLIENT REPORT No: HAM2016-001
Report date: March 2016
NIWA Project: EVW15212

Quality Assurance Statement		
D. Thompson	Reviewed by:	
A. Wadhwa	Formatting checked by:	
D. Roper	Approved for release by:	

Contents

Executive summary

Waikato Regional Council (WRC), Dairy NZ and NIWA co-funded a study to determine contemporary and historical changes in the sources of fine sediment accumulating in the Firth of Thames and inflowing rivers from carbon isotopic analysis of catchment soils, river sediments and dated estuarine sediment cores. The cores, collected from the southern Firth, preserve records of environmental change over the last 1800 years, including the effects of large-scale catchment deforestation and subsequent conversion to land uses including pastoral agriculture and production forestry since the mid-1800s.

The specific objectives of the present study are to:

- Determine the sources of eroded soils and their relative contributions to the sediment deposition in the Firth of Thames (by land use and sub-catchment), including an assessment of the variability in fatty acid $\delta^{13}C$ signatures.
- Determine how sedimentary contributions have changed by land use source over the recent past (last 1000 years).

These objectives are addressed using: (1) compound specific stable isotope (CSSI) analysis of fatty acid (FA) labelled soils and sediments; (2) statistical determination of isotopically distinct land use sources; and (3) mixing models to estimate the proportions of these sources in contemporary fluvial sediments deposited in the Waihou and Piako Rivers, and estuarine sediments that have accumulated in the southern Firth over the last ~1000 years.

Information about indigenous plant communities prior to human arrival (i.e., ~1300 AD) and subsequent changes in land use was collated from previous studies and used to inform the selection of potential sources in the analysis of historic deposits in the Firth.

Three modelling approaches were used to estimate source contributions. Two-endmember and IsoSource models were used to estimate source proportions for fluvial deposits. A Bayesian mixing model, MixSIAR, was used to estimate source proportions over time in the dated sediment cores. MixSIAR offers the benefit of providing information on the statistical uncertainty in estimated contributions of each sediment source.

Differentiation of sources to fluvial deposits in the Waihou and Piako Rivers was refined using geographical constraints (i.e., upstream sources). Whereas, modelling of sedimentation in the Firth was aided by historical land use information to constrain possible sources. For the latter analysis, statistical tests determined the following six sources could be reliably distinguished over time using the MixSIAR model: native forest, bracken, native and pine combined and pasture topsoils combined, subsoil and estuarine sediments.

Currently in the Waihou system, the Waiomou, Ohinemuri and Hikutaia tributaries make relatively small contributions (i.e., <16%) to the fluvial sediments deposited downstream of their confluences. In contrast, the Waitoa makes a more substantive contribution (65%) to contemporary fluvial deposits in the Piako. Whilst eroding subsoils dominate fine sediment inputs to the Waitoa (~86%), bank erosion is the largest source of fluvial sediment in both the Waihou (~75–80%) and Piako Rivers (~68%). In both the Waihou and Piako, the origin of bankside deposits differs. For instance, in the headwaters of the Waihou where the vast majority (>90%) of sediment carried downstream originates, soils eroded from pine forest dominate (i.e., ~80-90% of bankside eroded material). Minor contributing sources to bankside deposits within the Waihou include sheep and beef pasture, dairy

pasture, native broadleaf forest and subsoils. In the Piako, eroding banks comprise sediment predominantly from dairy pasture (75%) with minor contributions by sheep and beef pasture, maize cropping, pine forest, broadleaf and podocarp native forest. Ultimately, by the time all fluvial sediment reach the estuarine deltas of the Waihou and Piako Rivers, these fluvial sediments represent 70% and 20% of contemporary fine sedimentation, respectively.

Modelling of current and historic soil source contributions to the Firth using MixSIAR generated soil-source summary statistics with moderate uncertainty. Nonetheless, modelling results are consistent with what is known about the pre-history and recent history of land use/plant communities in the Waihou and Piako catchments. During the last 1000 years, changes in soil source contributions and overall sedimentation rate match the history of human occupation in the catchment. Following European arrival, contributions of fluvial sediments to the Firth increased by up to an order of magnitude.

Changes in sediment accumulation rates (SAR) in the Firth follow similar patterns to those observed in other North Island estuaries, with pre-European SAR averaging less than 1 mm yr^{-1} and typically increasing tenfold thereafter. Over the last century, SAR in the southern Firth and Firth as a whole have averaged 5.5 mm and 4.3 mm yr^{-1} respectively. These values are in the upper range of average values measured in North Island estuaries (range 2.3 from 5.5 mm yr^{-1}).

Pre-human sedimentation in the Firth was dominated by the slow sediment accumulation over centuries to millennia, primarily composed of subsoils (76–81% of total), supplied by rivers draining catchments with indigenous forest and scrub cover. Estuarine muds, with isotopically enriched $\delta^{13}C$ FA signatures, were important secondary sources of sediment accumulating in the southern Firth (i.e., 15–27% of total). These isotopically-enriched estuarine sediments suggest the mixing of ancient fluvial sediments with organic sediments supplied by marine primary production over time (e.g., phytoplankton, diatoms, and sea grasses). Eroded bracken soils account for most of the remaining historic sedimentation (6–7.3%). The presence of bracken-labelled sediments hundreds of years prior to human arrival suggests that natural disturbance of the landscape was common within the Firth catchment.

Weighted-average contributions of eroded catchment topsoils (15–25%) substantially increased after the late ~1600-1800s and along with large subsoil contributions (43–56%) suggest substantial disturbance of the indigenous forest landcover. In terms of sediments derived from catchment erosion, sub-soil erosion accounted for 63–79% of the total net sedimentation overall. These weighted-average % source contributions are based on the length of time between the instantaneous % soil proportions of successive dated sediment samples.

In interpreting these source proportion results it is important to bear in mind that sediment accumulation rates since the late-1800s/early-1900s have increased by as much as ten-fold in comparison to the previous ~1,200 years. Consequently, the quantity of sediment deposited in the southern Firth associated with the various sediment sources has also substantially increased even if their percentage contributions did not change.

The $\delta^{13}C$ FA data do not enable these subsoils to be traced to a specific land use. Potential sources include processes such as slope failures during intense rainfall, stream bank erosion drainage clearance and exposure of subsoil and erosion from road cuttings, unsealed roads and tracks and other earthworks, particularly stop banks. Given the land use history, it is also likely that a significant fraction of ongoing deposition in southern Firth is legacy sediment associated with historic

deforestation and gold-mining activities contributing subsoil. Further discrimination of subsoil sources maybe possible using additional conservative tracers in a mixing model, such as MixSIAR. For example, a number of metals, such as gold, silver, lead, copper, tin antimony, mercury or arsenic but was not explored here.

The results of the present study indicate that the largest contemporary source of sediment to the Waihou and Piako River systems is bank erosion. These eroded river-bank sediments in turn are derived from upstream erosion of pine forest soils in the upper reaches of the Waihou and Waiomou Rivers, and eroded dairy pasture and subsoils in the Piako and Waitoa Rivers, respectively.

The relatively small contribution of pastoral top soils to sedimentation in the Firth of Thames over the last ~100 years, averaging 4–6%, is notable given the substantial areas of dairying, sheep and beef farming in the Waihou and Piako catchments. These pastoral land uses account for 73% of the combined area of the Waihou and Piako catchments. By comparison, the combined contribution of native forest and pine averaged 5–8% during the same period from 20.3% of the combined catchment area. These topsoil sources are, however, relatively minor compared with subsoil contributions averaging 63–79% per year.

The apparent discontinuity between the make-up of contemporary sediment sources in Waihou and Piako Rivers compared to those of the southern Firth, can be explained by ongoing contributions of legacy subsoil delivered to the Firth during the historic period of mining and large-scale deforestation (i.e., mid-1800s to early 1900s). These legacy subsoils have in all likelihood been progressively transported onshore under the influence of wind, wave and current action and substantially account for the rapid accretion of the intertidal flats (i.e., centimetres per year) since the early 1900s.

1 Introduction

Waikato Regional Council (WRC), Dairy NZ and NIWA have co-funded a study to determine contemporary and historical changes in the sources of fine sediment accumulating in the Firth of Thames using compound specific stable isotope (CSSI) analysis of three dated sediment cores. The cores, collected from the southern Firth preserve records of environmental change over the last 1800 years, including the effects of large-scale catchment deforestation and subsequent conversion to land uses including pastoral agriculture and production forestry since the mid-1800s.

The specific objectives of the present study are to:

- Determine the sources of eroded soils and their relative contributions to sediment deposition in the Firth of Thames (by land use and sub-catchment), including an assessment of the variability in fatty acid $\delta^{13}C$ signatures (within end members).
- Determine how sedimentary contributions have changed by land use source over the recent past (present to 1000 years before present, BP).

These objectives are addressed using CSSI analysis and modelling of: (1) potential sources of terrigenous sediments and sediments deposited in the Waihou and Piako River networks and ultimately in the Firth of Thames within the last 1000 years. Terrigenous sediments were sampled at multiple sites in the Waihou and Piako catchments including topsoils associated with major contemporary and historical land use types, subsoils and fluvial sediments from the river network; and (2) sediments derived from three dated cores collected from intertidal and subtidal areas of the southern Firth.

1.1 Sediment source tracing

The quantities of sediment yielded by soil erosion can vary by land use, between sub-catchments and over time. Furthermore, the area occupied by a particular land use may not be directly proportional to the sediment yield of an area, due to spatial variations in slope, precipitation, geology, soil properties and land use and management practices. Consequently, sediment accumulation rates in the Firth of Thames provide an estimate of how much sediment is being deposited but not where it originated. In order to determine where the soil is coming from, we used a recently developed forensic stable isotope technique, using the compound specific stable isotope (CSSI) signatures of soil organic biomarkers bound to soil to discriminate and apportion the source of sediment from different land uses (Gibbs 2008).

The application of CSSIs as sediment source tracers is based on the concept that plant communities label soils with a range of organic compounds that are primarily exuded by their roots. Fatty acids (FAs) in particular have attributes that make them particularly suitable as sediment tracers of land use, as defined by plant community composition, being bound to fine-sediment particles and persisting over long time scales (i.e., decades–centuries) (Gibbs, 2008, Blake et al. 2012; Wildhaber et al. 2012; Hancock & Revill 2013). Although the pool or concentration of FAs in a sediment may reduce over time due to microbial decay, the carbon-13 to carbon-12 isotopic ratios (i.e., delta carbon-13, $\delta^{13}C$) are fixed. This is the key concept on which isotopic studies of sediment source tracing studies are based.

Fatty acids, particularly of medium chain lengths (i.e., C14 to C24), are slightly water soluble but highly polar so that they spread through the soil in the root zone and ionically bind to the soil particles. Although all plants produce these same biomarkers, the stable isotopic signature of those

biomarkers is different for each plant species or plant community. For example, the understory plant community in an exotic pine forest will impart additional biomarkers to that soil, which are not present in soil from a similar exotic forest without an understory.

For agri-environmental investigation, the CSSI technique is based on the delta carbon-13 ($\delta^{13}C$) natural abundance isotopic signatures of specific organic compounds such as natural FAs in soils and sediments. The FAs selected are those exuded from the plant community associated with each land use. The full suite of FA $\delta^{13}C$ values from carbon chain lengths of 12 (C12:0) to 24 (C24:0) thereby provides a unique 'fingerprint' for different plant communities. Ideally the suite of FA $\delta^{13}C$ values will be measurably different between types of plant communities. By linking these CSSI fingerprints of land use to the sediment in depositional environments, this approach has been shown to be a useful technique for determining the source of eroded soil and informing management of soil-based (i.e., fine sediment) effects on water quality (Blake et al. 2012; Wildhaber et al. 2012; Hancock & Revill 2013; Alewell et al. 2016).

The CSSI sediment tracing technique can also be applied to quantify the contribution of fluvial sediments transported by differing tributaries, the contribution of bank erosion processes as well as disaggregating the sources of these fluvial sediments by land use (i.e., sub-catchment and land use contributions). Applied as an iterative process through a river catchment, from its upper reaches to its outlet, the CSSI technique can identify the relative importance of each sub-catchment by analysing sediment up and downstream at river-tributary confluences and, by summation of the proportions from each sub-catchment and the main river, it can provide an estimate of the importance of a specific land use or land use practice to the sediment discharge into the estuary from the catchment as a whole.

Estuarine and coastal sediments are typically mixtures of soils and marine sediments from various sources.

To identify the sources of sediment in a deposit, the isotopic signatures of individual end members or sources must be determined from sampling soils for each land use or vegetation type in the catchment (i.e., under native forest, pine, pasture, cropping). The feasible soil sources in each sediment mixture are then evaluated using an isotopic mixing model.

In the present study, contemporary sources of terrigenous sediments deposited in the Waihou and Piako Rivers were evaluated using the CSSI method (Gibbs 2008) and the US EPA IsoSource mixing model (Phillios and Gregg, 2001, 2003). A simple two-endmember mixing model was also used to evaluate the contribution of main stem and tributaries as sediment sources to downstream fluvial sediment deposits at river confluences.

A modified version of the CSSI method and more complex Baysian mixing model MixSIAR (Stock and Semmens, 2015) was required to analyse dated sediment cores that preserve the history of sedimentation over the last 800–1000 years, from a wider and more complex pool of sources than those upstream of tributary mixtures. A key advantage of the MixSIAR model is that it can incorporate and account for uncertainty in the source signatures of isotopes and resulting estimates of source contributions to a mixture (Parnell et al. 2013; Phillips et al. 2014).

A more detailed description of the CSSI methods is provided in Appendix C.

1.2 Land use change and estuary sedimentation

In this section, catchment land use history and information on sedimentation in the Firth is briefly reviewed to provide context for the interpretation of results.

1.2.1 Land use history

The Holocene pre-history of vegetation communities that characterised the Hauraki lowlands and Firth of Thames catchments has been reconstructed largely from plant-pollen assemblages preserved in freshwater wetland and estuarine sediments (McGlone et al. 1984; Pocknall et al. 1989; Newnham et al. 1995). The lowlands north of the existing shoreline began to be inundated by rising sea levels from about 10,000 years BP, with the shoreline located close to Paeroa by 6,000 years BP (Newnham et al. 1995). Mangrove forests fringing an earlier shoreline in the outer Firth and now 35 m below present sea level that existed in the early Holocene, were also inundated by rising sea levels and evidence of this is preserved in marine sediments (Pocknall et al. 1989).

Kahikatea (*Dacrycarpus dacrydioides*) swamp forests began to develop from about 6000 years BP along the western margin of the Kopouata bog/wetlands. Wetland species included abundant *Empodisma* spp., *Sproadanthus* sp., *Gleichenia* spp., *Leptospermum scoparium* (manuka) and Cyperaceae (*Baumea rubiginosa* and *Schoenus* spp.). Between 10,750 and 5,500 years BP, grassland decreased markedly in extent, replaced by dryland podocarps forests, fringing the Kopouata wetlands that included rimu (*Dacrydium cupressinum*), matai (*Prumnopitys taxifolia*) and red beech (*Nothofagus fusca*). Kauri forest (*Agathis australis*) expansion (5,500-700 years BP) displaced rimu forests, also with expansion of red beech forest at higher elevations in the ranges fringing Hauraki Lowlands (Newnham et al. 1995).

Human settlement and land use changes

The Hauraki lowlands east of the Piako River were covered by extensive kahikatea swamp forest seaward of the present-day Kerepehi township, immediately prior to the arrival of people. These extensive forests and marshes fringed the river margins. Mixed kahikatea and podocarp forest interspersed with peat bogs occurred further inland, with podocarp forests dominating the Coromandel ranges (Trustrum and Crippen, 1986, Fig 2.6 Phillips, 2000). Māori arrived around 1300 A.D., based on dating of rat-gnawed seeds, rat bones, and volcanic tephra in the upper North Island and which demonstrate that the Pacific rat was introduced to both main islands of New Zealand at about this time (Wilmshurst et al. 2008). Settlement initially occurred along the river banks, particularly on the higher levee deposits along the banks of the Waihou and Piako Rivers. Forest clearance was mainly restricted to the immediate areas around settlements and on the flood plain between the Waihou River and the Coromandel ranges and foothills typically up to 150 m above sea level (Phillips, 2000).

A key land disturbance indicator in sedimentary records from lakes and estuaries is the bracken fern (*Pteridium esculentum*). Evidence primarily from palynological studies shows that bracken scrubland became abundant in New Zealand after the arrival of Māori in the early 1300s, when deforestation affected most lowland catchments (McGlone et al. 2005). The abundance of bracken over large areas, particularly in the North Island was primarily a result of forest burning by Māori and subsequently by European settlers from the mid-1800s. In fact, bracken was a major weed of pastoral areas well into the 20th century (McGlone et al. 2005). In the Firth of Thames, sediment cores analysed by Hume and Dahm (1992) also indicated that bracken spores became come common following arrival of Māori.

The major period of European settlement began in the mid-1800s. Although timber extraction began in the early 1800s, with kauri logging in the Hikutaia catchment, the main phase of deforestation occurred during the period 1860s–1910 (Phillips, 2000). Large-scale deforestation along with gold-mining in the Coromandel ranges substantially increased sediment loads to the Firth. The conversion of the Hauraki Plains to pastoral agriculture was delayed until drainage works began in 1905. A stop bank was constructed along the southern shore of the Firth and the tidal reaches of the Waihou and Piako Rivers. By 1920 some 162 km^2 of swamp had been converted to pasture (Brownell, 2004). The 1938 storm flooded the entire Hauraki Plains and consequently the height of the stop banks was increased. These engineering works constrained floodwaters to the river channels and are likely to have increased sediment delivery to the Firth.

Present-day land use in the Waihou and Piako catchments is dominated by pastoral agriculture (65%) with native forest and scrub accounting for about 20% (Van der Roovart et al. 2006). Production forestry is an important secondary land use on the Mamaku plateau, upper Waihou catchment, covering 180 km^2, and accounting for about 9% of the 1,966 km^2 Waihou catchment (Table 1-1). These data show that dairy farming is the most prevalent land use, although the proportion varies substantially between smaller sub-catchments, from 0% in the Kauaeranga River to 69% in the Waitoa sub-catchment of the Piako system (Vant, 2011). Approximately 60,000 people live in the Hauraki rivers catchment; many of them (~60 %) in one of seven moderate-sized towns (3500–7000 people each) (Vant, 2011).

Table 1-1: Summary of contemporary land use for the Waihou and Piako River catchments. Data source: Van der Roovart (2016).

Land use	Combined area		Waihou-Ohinemuri-Hikutaia			Piako-Waitoa		
	Ha (000)	%	Ha	% Sub-catchment	% Combined	Ha	% Sub-catchment	% Combined
Dairy platform	177.3	55.3	86,203	45.5	24.7	91,138	63.3	26.1
Dairy support	19.3	6.0	9,467	5.0	2.7	9,857	6.8	2.8
Dry stock	39.0	12.1	21,932	11.6	6.3	17,060	11.8	4.9
Horticulture	4.2	1.3	1,841	1.0	0.5	2,364	1.6	0.7
Lifestyle	5.9	1.9	3,239	1.7	0.9	2,703	1.9	0.8
Exotic Forestry	17.8	5.5	15,431	8.2	4.4	2,345	1.6	0.7
Native forest	47.7	14.8	44,558	23.5	12.8	3,095	2.2	0.9
Wetland	9.8	3.0	0	0	0	9,770	6.8	2.8

1.2.2 Historical sedimentation

Sediments deposited in estuaries and coastal marine areas can provide detailed information about how these receiving environments have changed over time, which include the effects of human activities on the land. In New Zealand, major changes have occurred in estuaries and coastal ecosystems over the last several hundred years due to large-scale clearance of native forests for land use. This deforestation began shortly after initial colonisation by Māori in ~1300 A.D. (Wilmshurst et al. 2008) and accelerated following the arrival of European settlers in the early–mid 1800s. Forest clearance associated with slash and burn agriculture by early Māori, and subsequent timber extraction, mining and land conversion to pastoral agriculture by European settlers triggered large increases in fine-sediment loads from catchments. During the peak period of deforestation in the mid-1800s to early 1900s, sediment loads are believed to have increased by a factor of ten or more (Brownell, 2004). In many estuaries, this influx of fine sediment resulted in a shift from sandy to more shallow, turbid and muddy environments and large increases in sediment accumulation rates (SAR). Studies mainly in North Island estuaries indicate that in pre-Polynesian times (i.e., before

~1300 A.D.) SAR averaged 0.1–1 millimetres per year (mm yr^{-1}). In comparison the rates have increased to 2–5 mm yr^{-1} in these same systems today (Hume and McGlone, 1986; Sheffield et al. 1995; Swales et al. 1997; 2002a, 2002b, 2005a,b, 2007, 2008, 2011, 2012, 2013, 2015b). Sedimentation rates in tidal creeks, mangrove forests and in estuaries near large catchment outlets are even higher and typically in the range of 10–30 mm yr^{-1} (e.g., Hume and McGlone, 1986; Swales et al. 2002a).

Previous studies conducted in the Firth of Thames suggest that this system has been substantially impacted by soil erosion and resulting sedimentation (Hume and Dahm, 1992; Healy, 2002; Brownell, 2004; Swales et al. 2015b). In the southern Firth, intertidal flats have experience rapid vertical accretion, with lead-210 (^{210}Pb) SARs of 30–100 mm yr^{-1} being among the highest measured in a New Zealand estuary (Swales et al. 2015b). By comparison, ^{210}Pb SAR in the outer Firth (i.e., 20–40 m water depth) of 1.6–2 mm yr^{-1} are an order of magnitude lower (Figure 1-1, de Baere, 2006). This offshore reduction in SAR is consistent with distance from major river-borne sediments sources. Evidence of the longer-term historical changes in sedimentation rates and patterns in the Firth of Thames are sparse. Hume and Dahm (1992) analysed sediment cores collected from three subtidal sites located in the southern Firth between Tararu and Waiomu (i.e., 0–5 m below chart datum, Figure 1-1). Pollen profiles indicated that sediments below 15-cm depth were composed of native-forest species, with bracken spores, indicative of land disturbance, being common in sediments above that depth. Background SAR before Māori settlement averaged less than 0.2 mm yr^{-1}, increasing by up to ten-fold following large-scale catchment disturbance associated with forest clearance for farm establishment and gold mining from the mid-1800s (Hume and Dahm, 1992).

The Austrian geologist Ferdinand von Hochstetter's 1859 map of the Firth of Thames clearly shows the presence of extensive intertidal flats and river deltas in the southern Firth (Figure 1-2). The German text *Weicher schlamm* shown on the intertidal tidal flats translates to *soft mud*. This is significant because it suggests that muds were accumulating in the Firth before large-scale catchment deforestation by European settlers had begun.

Hydrographic surveys conducted by the Public Works Department in 1882 and 1918 indicated that approximately 7 x 10^6 m^3 of sediment was deposited within a 16 km^2 area of the lower Waihou River and its tidal delta during this period. An additional ~37 x 10^6 m^3 was estimated to have been deposited in a 210 km^2 area of the Firth south of Tararu (Brownell, 2004), which is equivalent to a layer of sediment averaging 0.18 m thick.

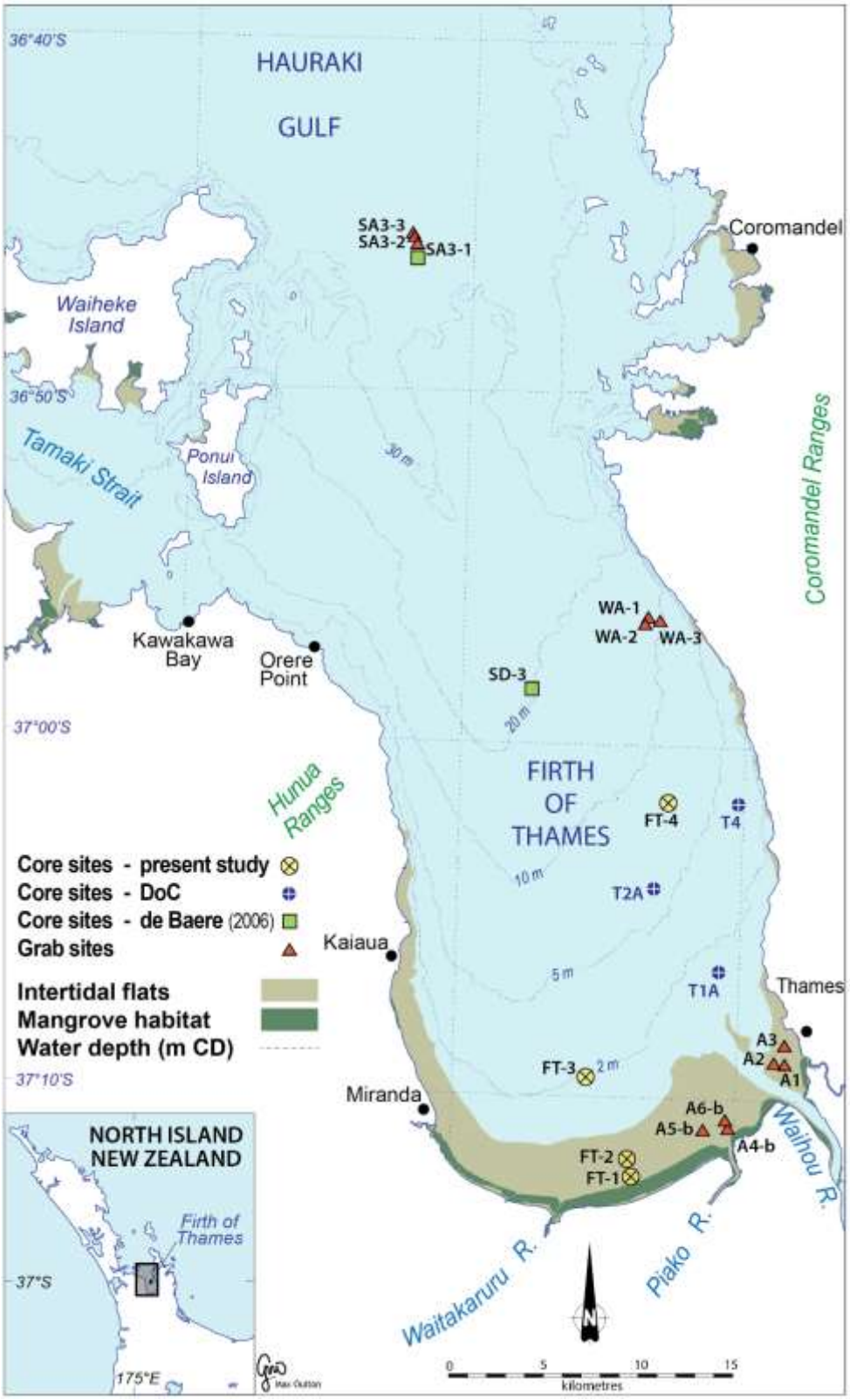

Figure 1-1: Location of sediment cores and surficial grab samples collected in the Firth of Thames. Present study (January and March 2015) as well as previous coring studies undertaken by Hume and Dahm (1992) and de Baere (2006).

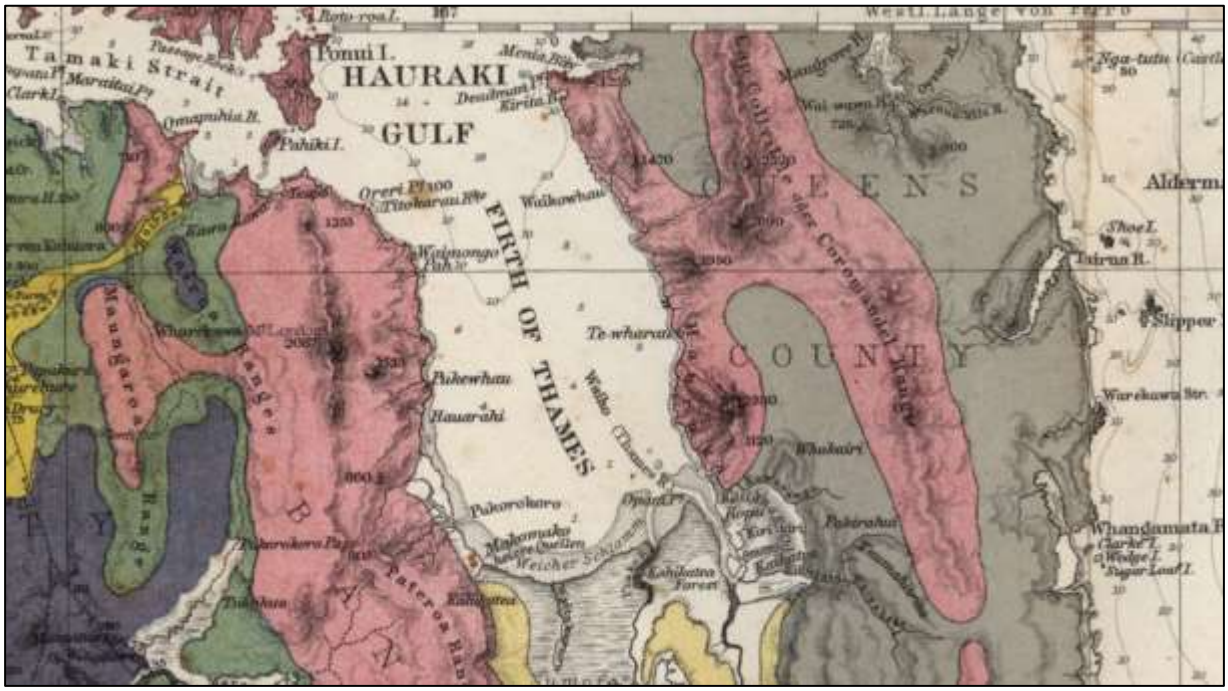

Figure 1-2: Hochstetter's 1859 map of the Auckland – Waikato regions. Acknowledgement: University of Auckland Libraries and Learning Services and the Early New Zealand Book Collection. Note: map cropped to Firth of Thames – Coromandel region.

Mangroves (*Avicennia marina* subsp *australasica*) have colonised the rapidly accreting intertidal flats in the southern Firth since the early 1960s. Captain James Cook visited the Firth in 1769 and noted the presence of mangroves along the banks of the lower Waihou River (Beaglehole, 1968). Aerial photographs of the southern Firth in the 1940s and early 1950s show that mangrove habitat was restricted to delta deposits flanking the mouths of the Waitakaruru, Piako and Waihou Rivers. Today, mangroves occupy some 7 km^2 of former intertidal flat between the Piako and Waitakaruru Rivers and 11 km^2 in the southern Firth as a whole (Brownell, 2004). The biogeomorphic evolution of the intertidal flat/mangrove forest complex has been reconstructed by Swales et al. (2015b). This study showed that the mangrove forest developed as a result of rapid vertical accretion of the intertidal flats and that mangrove forest has not measurably enhanced sediment accumulation rates.

1.2.3 Fine sediment fate

The fate of eroded catchment soils and river sediment in the Firth of Thames primarily depends on the dispersal and deposition of river plumes that deliver fine suspended sediments to the Firth. This knowledge is of value in determining core locations to target areas of high deposition.

Pritchard et al. (2015) simulated the Waihou River storm-discharge plume behaviour and sediment deposition in the Firth of Thames using a calibrated Delft-3D 3-dimensional hydrodynamic model and uncalibrated sediment transport module (i.e., regular 500 m × 500 m grid). The spectral wave model SWAN was also used to simulate gravity wave generation and was dynamically coupled to the Delft-3D model to incorporate the effect of wave-current interactions on sediment transport.

The models were used to simulate river-plume behaviour and fine-sediment fate over 30-day periods under calm conditions as well as for prevailing south-west winds and the north-east winds that often coincide with rainstorms generated by extra-tropical cyclones. Under calm weather conditions, the decelerating river outflow and sediment plumes do no spread far from the river mouth (i.e., within a

1-2 km radius). By contrast, wind stress forcing substantially enhance the dispersion of buoyant river plumes and their suspended sediment load downwind. This results in a larger, and more diffuse, deposition footprint occurs (Figure 1-3). Under north-east wind conditions the Waihou River plume is deflected to the west, along the Firth's southern shore, whereas under south-west wind conditions, the storm-discharge river plume is deflected north east, with deposition maxima in the eastern Firth as well as on the river delta.

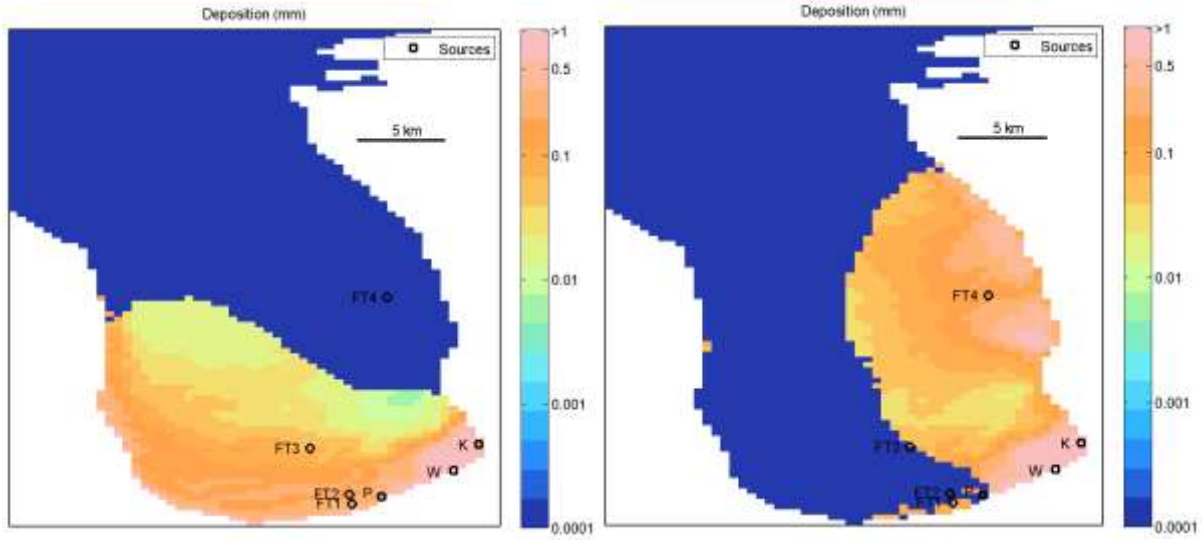

Figure 1-3: Predicted sediment deposition (mm) at the end of 30 day period in Firth of Thames under: (a) NE and (b) SW wind conditions. Note that simulated deposition footprints for storms based on synthetic sedigraphs, with maximum suspended sediment concentration of 1,200 mg l^{-1} at peak flood discharge, so that event deposition values are indicative. The location of core sites in the present study are also shown (FT-1 to FT-4). Source: Pritchard et al. (2015).

2 Methods

2.1 Present-day land use and soil erosion sources

Samples of catchment topsoils, subsoils and fluvial deposits in river channels were collected during February, March and May 2015 to assemble a library of stable isotope $\delta^{13}C$ signatures of FA compounds associated with major land use types (Figure 2-1). Specifically, $\delta^{13}C$ data for a suite of FA's are used to develop a library of $\delta^{13}C$ signatures for potential major sources of topsoils and subsoils deposited in: (1) the contemporary river channels of the Waihou and Piako systems; and (2) over the last several hundred years in the Firth of Thames.

These topsoils associated with specific land uses, subsoils and estuarine sediments are used to represent end member sources in the isotopic mixing models that we use in the present study to apportion the contributions of various sources to a particular fluvial or estuarine sediment mixture.

2.1.1 Land use

To identify sites for collection of catchment soil samples, land use information was overlaid with erosion risk factors (e.g., precipitation isopleths; drainage class from the NZLRI; landslide delivery risk from the NZEEM; and slope) (Figure 2-2). In total, 53 replicate topsoil sampling sites were selected for major land use types, defined as being land uses that account for more than 5% of present catchment areas (Figure 2-3). These replicates were spatially distributed to cover many categories of erosion risk within the constraints of the maximum sample size that could be analysed. In addition, the persistence of these major land uses were determined by comparison of the LCDB-2 and LCDB-4 land use data (i.e., same land use coded between February 2002 and December 2012). This ensured that the land use at each soil sampling site had been stable long enough for characteristic $\delta^{13}C$ signatures of the FA biomarkers for a given land use to develop. For example, recent conversion from dry stock to dairying could alter topsoil biomarker $\delta^{13}C$ signatures due to differences in farm management practices. In particular, changes in pasture types, variation in cropping practices, and application or excretion of supplementary feeds can alter the topsoil FA $\delta^{13}C$ signature (e.g., palm kernel is rich in the FA biomarker palmitic acid [C16:0]).

Overall, this sampling design provided information on eight land use classes:

- dairy
- sheep and beef
- maize
- goat
- lifestyle
- horticulture
- production forestry (*Pinus radiata*)
- native forest and scrub communities.

Of these land use classes only four occurred in both the Waihou and Piako catchments (e.g., dairy, sheep & beef, production forestry and native forest and scrub communities).

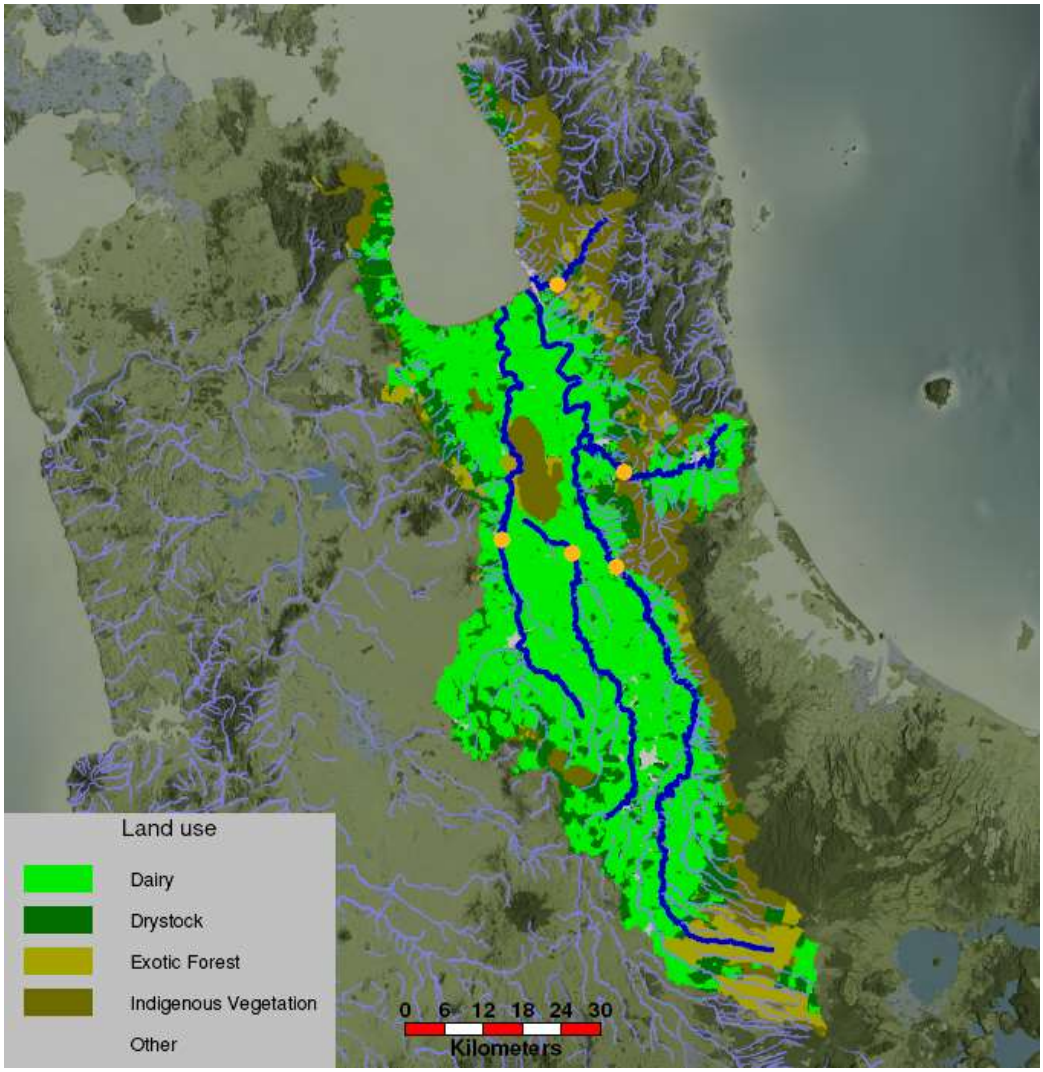

Figure 2-1: Firth of Thames catchment land cover and main rivers. Source: Waikato Regional Council.

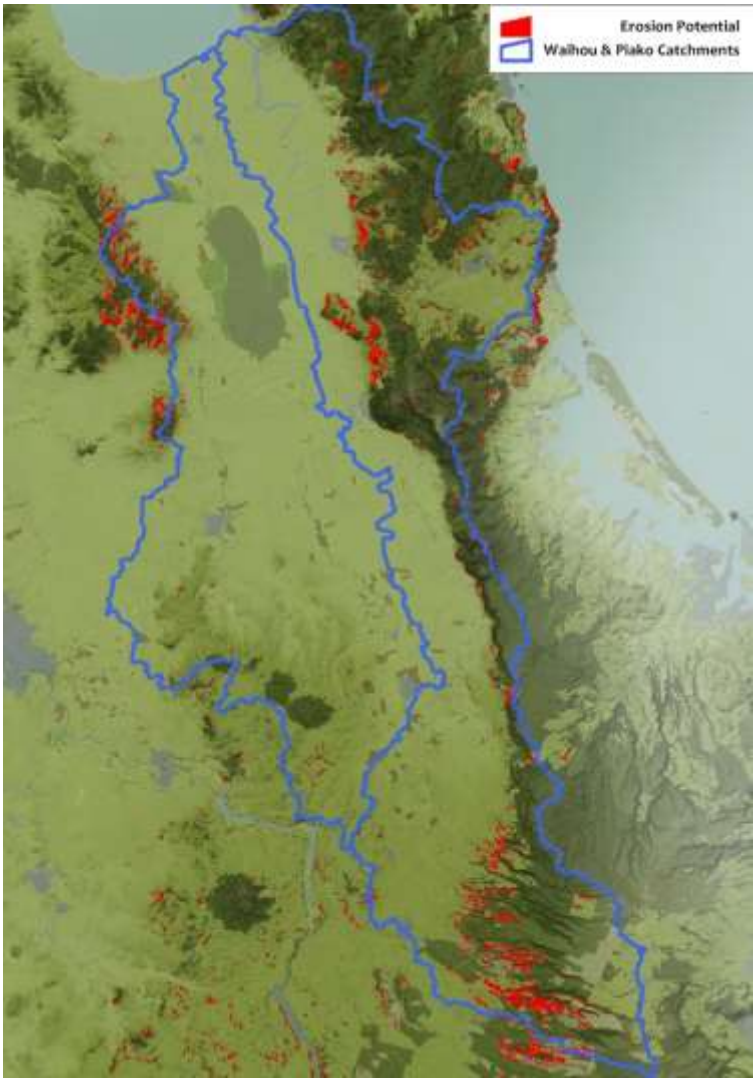

Figure 2-2: Land areas in the Waihou and Piako catchments identified as having high landslide delivery risk. Source: Waikato Regional Council.

2.1.2 Subsoils

Subsoil samples were collected from five sites distributed across the Waihou (3) and Piako (2) catchments, to represent deeper erosional inputs to sediment deposits in the river channels and Firth of Thames. Subsoil erosion processes include hillslope failure and stream-bank erosion as well as subsoil released to the river network by human activities such as mining. These subsoil erosion and delivery processes may differ from those associated with topsoil erosion. Furthermore, it should be appreciated that subsoil erosion will be associated with land uses although the $\delta^{13}C$ FA signatures of these subsoils are typically substantially different from those of the overlying topsoils that are labelled/defined by the plant community and land management practices that define land use.

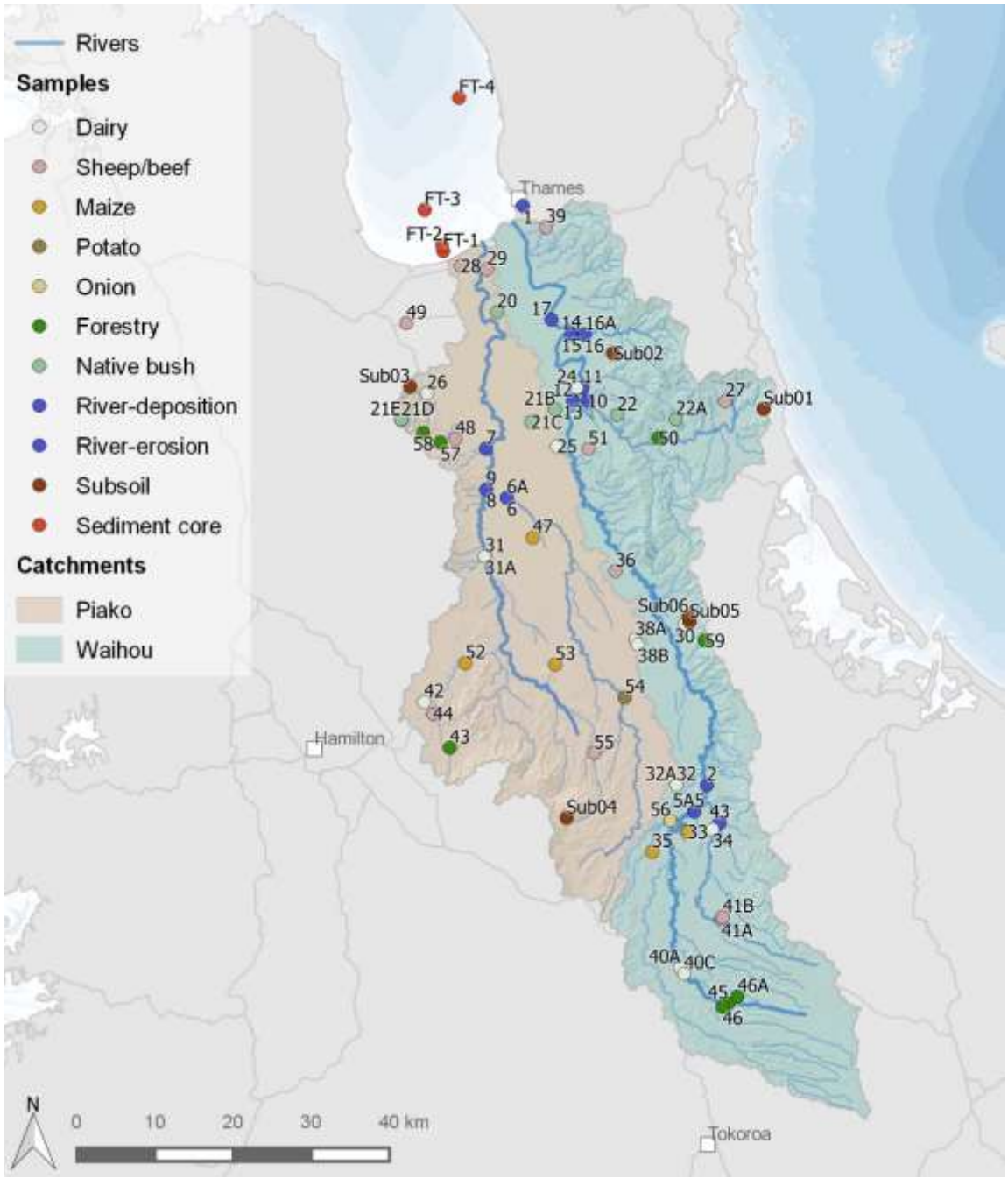

Figure 2-3: Locations of soil and fluvial sediment deposits collected for determination of the stable isotope signatures of potential sources. Field sampling of top soils and river sediments conducted February–March and May 2015 and subsoil samples collected November 2015. Source: Waikato Regional Council.

2.1.3 River sub-catchments

River sediments were collected at the confluence of major tributaries with the Waihou and Piako Rivers, as marked in dark blue dots on Figure 2-3. A set of three samples were collected – one in the main river channel (i.e., first end member), one in the tributary channel upstream of the confluence (i.e., second end member), and a third downstream of the confluence (i.e., mixture) at sufficient distance to allow mixing of sediment from both upstream channel sources.

2.2 Soil sampling

Topsoil and subsoil samples were collected at each of the 53 sampling sites as composites of at least 10 subsamples collected within a ~100 m^2 area. Each sub-sample was collected using a purpose-built hand corer to ensure equivalent soil volumes were collected to prevent bias in the composite sample (Figure 2-4).

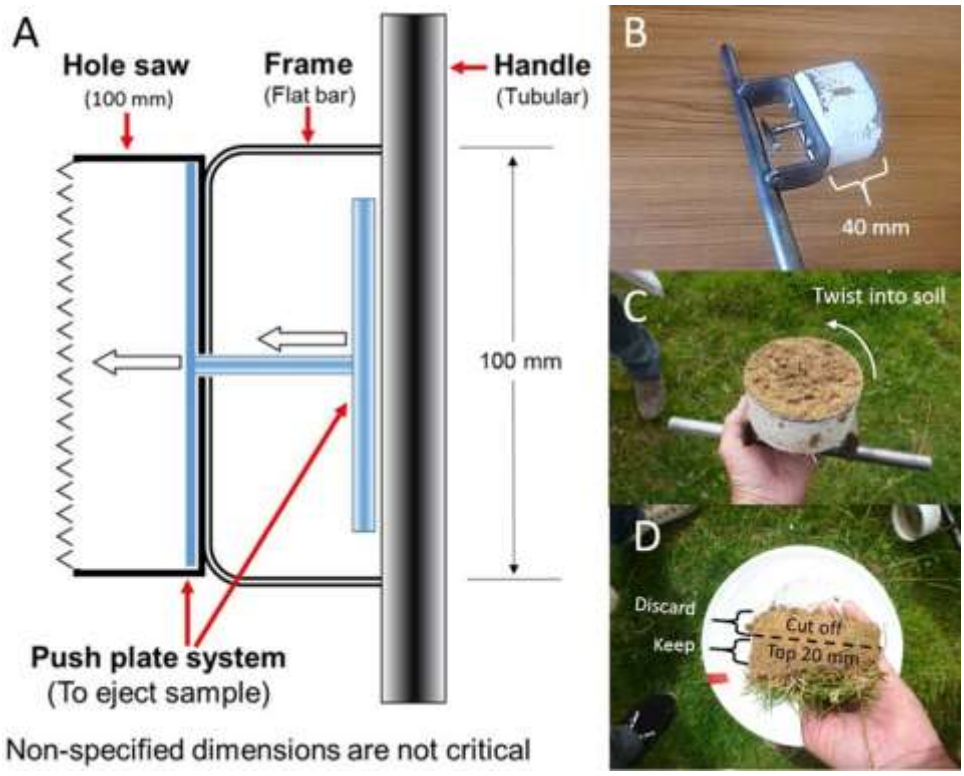

Figure 2-4: Hand corer used for land use sampling. A) Schematic cross section showing the push plate system used to extrude the soil from the corer after collection, B) side view of the hand corer showing the push plate handle ready for coring, C) a view of the inverted corer after collecting a pasture core, and D) the soil plug extruded from the corer ready for trimming to 20 mm thickness before combining in the composite sample.

To use, the hand corer is first cleaned of any residual soil from a previous location by brushing out any soil or plant material then twisted into the soil of the site to be sampled. The soil plug collected is extruded and discarded. Any material now in the corer will be from the site to be sampled, limiting cross contamination risk. The ~ten or more subsamples were collected at intervals of about five paces from the first subsample point selected at random or in a grid pattern over an area of about 100 m^2. At each location the corer is twisted into the soil using the saw teeth to cut through the root sward in the ground. The corer barrel is about 40 mm long and provides enough friction for the soil plug to come out of the ground inside the corer (Figure 2-4C).

The side of the corer barrel has slots through which it is possible to see the edge of the push plate. Using this as a guide, the soil plug can be partially extruded leaving the 0–20 mm depth section inside the hand corer and allowing the exposed 20-40 mm depth section to be cut off and discarded. Alternatively, the whole soil plug can be extruded and the bottom 20 mm cut off and discarded. The soil in the upper 0–20 mm depth layer is crumbled from the plant root mass and combined into a bulk composite sample in a 20-L plastic bucket. Obvious sticks, stones, leaves, roots, seeds, worms

and insects are removed by hand picking. The combined soil is mixed thoroughly before a 200–400 g aliquot of the mixture is sealed in zip-lock type sealable plastic bag as one of the 53 representative land use and subsoil samples in the soil library.

2.2.1 Fluvial sediments

Fluvial sediments were collected from deposition zones on the river bed by taking several scoops of the surface layer (i.e., top-most 20 mm) and combining these into a single composite sample. This approach recognises that sediment comprised of various sources has been homogenised during transport prior to deposition.

Hence, fluvial sediment deposits sampled from the river bed represent a mixture of all of the upstream sources that contributed to the deposit.

The sampled surface layer represents recent sediment deposits. The actual time span represented by a surface deposit will vary depending on local sediment accumulation rate, which reflects local hydraulic conditions, river discharge and upstream soil erosion episodes. Typically, these surficial sediments represent deposits laid down within the previous several years at most and can therefore be related to contemporary upstream land use and sediment erosion.

2.3 Estuarine sediment sampling

Replicate sediment cores were collected at four sites in the Firth of Thames during January and March 2015. The core sites were located along a gradient of depth from the mid-intertidal to subtidal zone, characteristic of the southern Firth (Figure 1-1). Cores from three sites were analysed to determine historical changes in sediment sources.

The location of the core sites was informed by Pritchard et al's. (2015) modelling of storm-discharge river plume dispersal and sedimentation, including the effects of the prevailing south-west wind direction and the typical north-east winds driven by extra-tropical cyclones (Figure 1-3). This modelling indicated mud depocentres on the intertidal flats in the southern Firth as well as the shallow subtidal zone to about 10-m below chart datum in the eastern Firth north of Thames. A large subtidal area of muddy, sandy shell gravel in the south-west Firth suggests that this represents an environment where deposition rates of river-borne muds are relatively low and/or fine-sediment deposits are being winnowed by currents and/or wave action. The location of the intertidal core sites was also selected to coincide with a (north–south) transect of cores collected in the mangrove forest fringing the southern Firth, some five kilometres west of the Piako River mouth (Swales et al. 2015b). This enabled the sedimentation regime from the lower to upper intertidal along a gradient of tidal inundation, wave exposure and sediment supply to be considered. Thus, core sites were selected:

- on the mid-to-lower intertidal flats (FT-1 and FT-2) in line with the mangrove-forest core transect
- subtidal fine-sediment winnowing zone (FT-3)
- Subtidal mud depocentre located north of Thames (Figure 1-3).

2.3.1 Sediment cores

Replicate sediment cores were collected at four sites on 27 January and 10 March 2015 in water depths ranging from 1 m above chart datum (mid-intertidal flat) to 8 m below chart datum (CD) (Figure 1-1). Subtidal cores up to 2.2 m long were collected using a 10-cm diameter gravity Corer,

loaded with up to 160 kg of lead weight (Figure 2-5) and intertidal cores up to 2.3 m long were collected using a 10-cm diameter Livingston piston corer deployed from the R.V. Rangitahi III. Both types of corer were deployed with core catchers attached to the PVC pipe to reduce loss of sediment from the PVC core barrel during extraction from the seabed.

The PVC barrel containing the sediment was separated from the corer on the boat, sealed at both ends, labelled and secured in racks for shipment. Replicate cores were collected at each site, with one used for radioisotope dating, particle size and bulk density analyses and the second core prepared for x-ray imaging and subsequent sub-sampling for analysis of stable-isotope signatures for sediment source determination. A third replicate core was collected at sites FT-2 to FT-4 for archiving.

Figure 2-5: Sediment coring from R.V. Rangitahi lll. Retrieving a Gravity Corer used to collect sediment cores in the Firth of Thames (photo: Rod Budd, NIWA, Hamilton).

Table 2-1 provides details of the sediment-core sites collected from the Firth of Thames during January and March 2015.

Table 2-1: Sediment cores collected in southern Firth of Thames, January and March 2015. Lengths of each core retained indicated. Note: water depth (m) is the range during the time taken to collect cores.

Site	Location description	Date	Time (NZST)	Water depth (m)	Latitude	Longitude	Core lengths A-B-C(cm)
FT-1	Mid intertidal	27/01/15	1310	0.9	37° 12.224’ S	175° 26.503’ E	132, 166
FT-2	Lower intertidal	27/01/15, 10/03/15	1550	1.2–0.9 1.4–1.2	37° 11.744’ S 37° 11.8371’ S	175° 26.3800’ E 175° 26.3832’ E	105, 132, 170
FT-3	Sub-tidal	27/01/15	1117	3.7–2.9	37° 09.390’ S	175° 24.806’ E	107, 210, 210
FT-4	Sub-tidal	27/01/15	1238	8.2	37° 1.541’ S	175° 27.505’ E	220, 237, 160

2.3.2 Estuarine surficial sediments

Surficial sediment samples were also collected using a grab sampler at several locations in the Firth of Thames to measure bulk and compound specific $\delta^{13}C$ values to inform the evaluation of sediment sources (Figure 1-1).

2.4 Sediment composition

The sediment cores were processed in the laboratory and prepared for x-ray imaging and sub-sampling for dating, stable isotope analysis and determination of basic sediment properties as described below.

Sediment cores selected for radioisotope dating were cut open length-wise using a skill saw with a 125 mm diameter blade. After cutting the core barrels along their entire lengths on both sides, thin stainless steel sheets were pushed through the sediment to split the core into two separate halves. The cores were first logged, including description of any obvious sediment layers before sub-sampling for radioisotope, particle size and bulk density analyses.

Information on the composition and stratigraphy of the sediment cores was provided by x-ray imaging (Figure 2-6). An x-ray image or x-radiograph provides information on the fine-scale sedimentary fabric of sediment deposits. Density differences (due to particle size and composition, porosity) between layers of silt and sand or animal burrows that are infilled with mud make these often subtle features easily recognisable in the x-ray image even though they may not be visible to the naked eye.

Figure 2-6: NIWA digital x-ray system, with a sediment slab mounted on the detector plate ready for imaging. (Photo: Ron Ovenden, NIWA Hamilton).

X-radiographs were made of each sediment core prior to dating. To do this, each core was first split lengthways and sectioned into 40 cm long and 2 cm thick longitudinal slabs. These slabs were then imaged using a Varian PaxScan 4030E amorphous silicon digital detector panel (Figure 2-6). X-rays were generated using an Ultra EPX-F2800 portable x-ray source with a typical exposure of 25 mAs (milliamp seconds) and 50–60 kiloelectron Volts (keV). The raw x-ray images were post-processed using the Image-J software package.

Particle size distributions (PSD, 0.1–300, 10–2000 μm) of sediment-core samples were determined using an Eye-Tech stream-scanning laser system, employing the time-of-transition (TOT) method to measure the diameters of individual particles (e.g., Jantschick et al. 1992).

Dry-bulk sediment density (ρ_b) profiles were determined for each core. The ρ_b was calculated as the dry mass per unit volume of sediment in each 1-cm thick core slice prepared for radioisotope dating. The slice volume was 78 cm^3 for the 10-cm diameter cores. Samples were processed by first weighing on a chemical balance to the nearest 0.01 g, dried at 70°C for 24 hours and reweighed to obtain the dry-sample weight. The ρ_b is expressed in units of grams per cubic centimetre (g cm^{-3}) and was calculated from the dry sample weight and sample volume.

The ρ_b reflects the bulk characteristics of the sediment deposit, in particular sediment porosity (i.e., proportion of pore-space volume) and particle characteristics, such as size distribution and mineralogy. For example the ρ_b of an estuarine sand deposit is of the order of 1.5–1.7 g cm^{-3}, whereas a mud deposit with high water content can typically have a ρ_b of ~ 0.5 g cm^{-3}.

2.5 Radioisotope dating and sediment accumulation rates

2.5.1 ^{210}Pb, ^{137}Cs and ^{7}Be

Sediment accumulation rates were estimated from radioisotope activities measured in each core. Radioisotopes are strongly attracted to the surfaces of clays and silt particles and this makes them particularly useful as "mud meters" (Sommerfield et al. 1999).

In the present study, historical SARs over the last 800 to 1,200 years were quantified based on caesium-137 (^{137}Cs), lead-210 (^{210}Pb) and carbon-14 (^{14}C) dating (Wise, 1977; Robbins and Edgington, 1975; Olsen et al. 1981; Richie and McHenry, 1989). The short-lived radioisotope beryllium-7 (^{7}Be) also provided information on the depth of the surface mixed layer (SML) (Sommerfield et al. 1999). The SML is the surface layer in which seabed sediments are mixed by the activities of benthic animals and current- and/or wave-driven sediment transport. These radioisotope dating techniques are described in detail in Appendix B.

The activity of excess ^{210}Pb, ^{137}Cs and ^{7}Be in each core was determined by gamma spectrometry of 40–60 g dry samples (1-cm slices) of sediment taken at increasing depths in each core. The radioisotope activity of a sediment sample is expressed as Becquerel (number of disintegrations per second) per kilogram (Bq kg^{-1}). The radioactivity of samples was counted at the ESR National Radiation Laboratory for 23 hours using a Canberra Model BE5030 hyper-pure germanium detector. The excess ^{210}Pb activity was determined from the (^{226}Ra, $t_{1/2}$ 1622 yr) assay. The excess ^{210}Pb profiles in each core were used to determine time-averaged SAR from regression analysis of natural-log transformed data. The maximum depth of ^{137}Cs in the cores was used to estimate time-averaged SAR since the early 1950s. This included a correction for downward mixing of ^{137}Cs, based on the maximum depth of ^{7}Be. In New Zealand, ^{137}Cs deposition from the atmosphere was first detected in 1953 (Matthews, 1989).

2.5.2 AMS ^{14}C dating

Pre-human SAR were estimated by atomic mass spectrometry (AMS) radiocarbon (^{14}C) dating of marine/estuarine carbonate shell valves preserved in the sediment cores. Individual and articulated valves of the common suspension-feeding bivalve *Austrovenus stutchburyi* (cockle) and the Dawn/Morning Star shell (*Tawera spissa*) were selected from the lower sections of cores FT-1, FT-2 and FT-4 for dating (Table 2-2). Two samples of whole shell valves collected from individual animals

in each core were dated. New Zealand cockle is suitable for radiocarbon dating as they have ^{14}C concentrations in cockles are similar to those found in marine shellfish (Hogg et al. 1998) so that marine reservoir effects can be accounted for using the marine ^{14}C calibration curve (Petchy et al. 2008).

Table 2-2: Summary of bivalve shell sub-sampled from the Firth cores and submitted for AMS ^{14}C dating.

Core	Depth increment (cm)	Sample type	Wk number
FT-1	148–149	Cockle shell valve (*Austrovenus stutchburyi*)	Wk-42301
	149–150	Cockle shell valve (*Austrovenus stutchburyi*)	Wk-42302
FT-2B	98–99 (A)	Cockle shell valve (*Austrovenus stutchburyi*)	Wk-41785
	98–99 (B)	Cockle shell valve (*Austrovenus stutchburyi*)	Wk-41786
FT-4	76–80	Cockle (*Austrovenus stutchburyi*)	Wk-43449
	78–80	Cockle (*Austrovenus stutchburyi*)	Wk-43450
	175–176	Morning Star shell valve (*Tawera spissa*)	Wk-41787
	175–176	Morning Star shell valve (*Tawera spissa*)	Wk-41788

Shell samples were acid-washed in 0.1 N hydrochloric acid, rinsed and dried prior to AMS analysis. The AMS dating results are expressed as conventional ages in years before present (B.P., 1950 AD, Stuiver and Polach, 1977). Duplicate samples were analysed from the same depth interval in several cores to evaluate the likelihood of shell material being reworked from its original stratigraphic position.

2.6 Sediment sources

The general concepts of CSSI sediment source tracing are summarised in section 1.1 and described in detail in Appendix C. There are two fundamental decisions required in any sediment source tracing study:

- **Which tracers to use**? This decision should be based on the ability of a suite of tracers to discriminate potential sediment sources. In the present study, the $\delta^{13}C$ values of FAs are used to inform which FA to include.
- **Which potential sources to include**? Where possible, the definition of sources should include a statistical evaluation of the differences in the $\delta^{13}C$ FA values of each potential source. Individual sources should be combined of they cannot be distinguished from each other on the basis of parametric (e.g., difference of means, median %ile) and/or non-parametric tests. A further key requirement for the selection of tracers and potential sources is that must conform to the isotopic polygon principle, which is the basis of isotopic mixing models. Specifically, the $\delta^{13}C$ values of the mixture samples must be enclosed with a polygon (two tracers) or hyper-volume (three or more tracers) defined by the $\delta^{13}C$ values of potential sources.

Decisions on both varied between fluvial and estuarine mixtures in line with analytical good practice (e.g., Phillips et al. 2014). The methods employed in the present study to make these decisions on which tracers and sources to include in the isotopic modelling ae described below.

2.6.1 CSSI methodology

The CSSI technique uses two different sets of stable isotope signatures — the bulk $\delta^{13}C$ values and percentage carbon (%C) of the whole soil, after acidification to remove inorganic carbonates, and the $\delta^{13}C$ values of individual FAs bound to soil particles after these have been extracted from the unacidified soil samples. Because the FAs are highly polar, they cannot be analysed directly as they will bind to the gas chromatograph (GC) column during analysis. Consequently, they must be derivatised into their methyl esters, which are non-polar, using a catalyst such as boron trifluoride (BF_3) in methanol (MeOH). Each FA methyl ester (FAME) consists of the FA carbons plus one carbon from the MeOH used for the derivatisation step. The analytical values from the GC-combustion-isotope ratio mass spectrometer (GC-C-IRMS) were corrected for the added carbon in a methyl-group from methanol to obtain the CSSI value for each FA using the equation:

$$\delta^{13}C_{FA} = (\delta^{13}C_{FAME} - (1-X) * \delta^{13}C_{Methanol})/X \quad (1)$$

where FA is the fatty acid and X is the fractional contribution of the FA to the FAME. X can be calculated from the number of carbons in the FA molecule divided by the number of carbon atoms in the FAME derived from the FA. For example, the FA stearic acid (C18:0) has 18 carbon atoms whereas the FAME produced, methyl stearate, has nineteen carbon atoms, including one added carbon from the methanol and thus has an X value of 18/19 or 0.9474. $\delta^{13}C_{FA}$ is the FACSSI value corrected for the methyl- group, $\delta^{13}C_{FAME}$ is the uncorrected isotopic value for the FAME and $\delta^{13}C_{Methanol}$ is the isotopic value for the methanol used in the derivatisation step.

The CG-C-IRMS analysis uses FA standards, both internal and external, of known CSSI $\delta^{13}C$ value for the calibration of the soil FAMES and uses the retention times of the standards to confirm the identity of each FA being measured. This methyl-group correction was applied to all FAMEs.

Several corrections are applied to the raw data to enable direct comparison of data between batches and for samples of varying ages (in the case of the sediment cores):

- Methyl-group (MeOH, FAME only) corrections to the $\delta^{13}C$ signature of each batch.
- Inter-batch corrections for individual FAs were applied relative to the main batch containing soil samples using a NIWA FAME standard analysed with each batch.
- These inter-batch and methyl-corrected $\delta^{13}C$ data were finally adjusted for the Suess Effect to the year 2015 AD (i.e., sediment cores only). The Suess Effect describes the progressive depletion of the atmospheric CO_2 signature, which is largely due to the combustion of fossil fuels since the early 1700s. This process also results in a depletion of soil $\delta^{13}C$ signatures as plants utilise CO_2 in photosynthesis and subsequently label potential soil sources (Verburg, 2007, Gibbs et al. 2014). The annual rate of delta $^{13}CO_2$ depletion in New Zealand is -0.025‰ (per mil) per year (source: NIWA).

  This Suess Effect correction is critical to enable direct comparison of sediment deposits with sources of varying ages, which has resulted in a ~2.15‰ depletion in $\delta^{13}C$ values since 1700. Full details of the CSSI method are included in Appendix C.

2.6.2 Modelling of fluvial sediments sources at river confluences

Two-endmember mixing model

The $\delta^{13}C$ isotopic signatures of the bulk soil and the FAs extracted from the soil were collated with the %C values. The river bed deposition samples were separated into confluence triplicates (Section 2.1.3) and the proportional contribution of the tributary at each confluence was determined using a two-endmember linear mixing model. This model assumes that the $\delta^{13}C$ isotopic values of the downstream site sediment mixture is the sum of the $\delta^{13}C$ isotopic values of inputs from each upstream source, **A** and **B**, where A can be the tributary and B can be the main stem of the river.

$$\delta^{13}C_{mixture} = fA\delta^{13}C_A + fB\delta^{13}C_B \quad (2)$$

Where fA and fB are the fractions or proportions of each source. This equation can also be rewritten

$$1 = fA + fB \quad (3)$$

To solve for fA, the equation is rewritten as:

$$fA = (\delta^{13}C_{mixture} - \delta^{13}C_B)/(\delta^{13}C_A - \delta^{13}C_B) \quad (4)$$

and for fB, the equation is rewritten as:

$$fB = (\delta^{13}C_{mixture} - \delta^{13}C_A)/(\delta^{13}C_B - \delta^{13}C_A) \quad (5)$$

The caveat for the two-endmember mixing model is that the $\delta^{13}C$ value of the mixture must be between the $\delta^{13}C$ values of the sources A and B. Theoretically, this should be the case where only tributaries upstream contribute to the mixture downstream, and where both upstream sources are dissimilar. However, because we are dealing with a flowing river system where the sediments can be reworked by the current flow, there can be variability in the isotopic signatures in the deposition zone mixtures, when these isotopic signatures are similar, which will allow some combinations of FAs to fall outside this criterion, resulting in non-valid values for f. Interpretation of feasible results from the full suite of two-endmember mixing model results may need to call on flow information for the sources where extreme ranges occur, and with more evenly balanced results.

Multiple source mixing models

The sub-catchments of the Waihou River were assessed at major confluences by treating the two upstream sites (A and B) as the mixture for their respective catchments and using a stable isotope mixing model (SIMM) to deconstruct the sediment mixture into the isotopic proportions of feasible sources that could have contributed to the mixture. The potential sources used were the eight land uses that were sampled at the 53 sites, which comprise the reference library for the Waihou and Piako River catchments. The US EPA software package IsoSource (Philips and Gregg, 2003) was used to analyse land use contributions to fluvial sediments deposited at the confluences of the Waihou and Piako river networks.

IsoSource estimates the isotopic proportions of feasible sources (end members) contributing to a mixture by iteratively calculating every possible combination of end member isotopic signatures that could result in the mixture isotopic composition. IsoSource then selects all feasible solutions (that sum to 100%) that satisfy the isotopic mass balance conservation within a user-defined tolerance of

the observed isotopic signature of the mixture. The user-defined tolerance is reduced iteratively to a minimum value that will produce a valid solution. Philips and Gregg (2003) define a minimum tolerance that avoids discounting a feasible solution, which depends on (1) the isotopic ($\delta^{13}C$) increment value (I); and (2) maximum difference in $\delta^{13}C$ values between potential sources (δ–max), and is calculated as δ–max*I*0.5.

The remaining feasible solutions are taken as the best fits of the sources to the mixture. Unless the catchment system is relatively simple, there are likely to be several valid combinations of sources in varying proportions from this process. IsoSource produces a histogram of all feasible mixture solutions, plotting the frequency of occurrence against the feasible proportion for each percentage of that source in the mixture. Because these results are simply calculations from the data supplied, each feasible proportion could be the actual value and, consequently, the whole range of feasible proportions should be presented in the results. The number 'n' of feasible solutions as well as the range of isotopic proportions for each source provides an indication of the level of uncertainty in the results. For example, the lower the value of n, the smaller the uncertainty, with n = 1 being a unique solution.

Results with n >1 include pseudo statistics of mean, max, min, 95% confidence intervals and standard deviation. As the value of n increases, the uncertainty in the results increases and values of n >1000 are at best only indicative. Notwithstanding this, the level of uncertainty may stem from one source being very similar in isotopic fingerprint to another. If this is the case and the sources are of similar land use origin, then these can be combined and IsoSource re-run with the revised data.

Limitations of IsoSource are (1) information on uncertainty (i.e., variance) of the source isotopic values cannot be included. Typically an average or median value is employed were replicate sample data are available; (2) the model can only accommodate up to five isotopes and ten sources. While the general ecological view of an isotope is that it is ^{13}C (for carbon) or ^{15}N (for nitrogen), in the CSSI technique each FA can be used as a discrete isotope; (3) data must be entered manually rather than as input files.

MixSIAR is a recently developed Bayesian isotopic mixing model, which incorporates advances in mixing model theory and builds on the earlier MixSIR and SIAR models (Stock and Semmens, 2015, 2016). Model-fitting to the observed data is based on a Markov Chain Monte Carlo (MCMC) method whereby the isotopic proportions of potential sources are estimated by repeated random sampling and discarding those which are not "probabilistically consistent with the data" (Phillips et al. 2014). Subsequent estimates are required to be similar to previous ones, thereby creating a Markov Chain (Phillips et al. 2014). The model output consists of a sample of the posterior proportions derived from the MCMC simulation. Unlike IsoSource, the outputs of Bayesian models represent true probability distributions of source proportions that can be summarised by various descriptive statistics, including the 95% credible interval.

MixSIAR includes two diagnostic tests to determine convergence of the MCMC on the posterior distributions for all variables in the model:

- Gelman-Rubin test requires more than one MCMC to be calculated (default = 3), with a value of 1 at convergence. A value of less than 1.1 is generally acceptable. In the present study, most model variables had G-R values of less than 1.05 (Stock and Semmens, 2015).

- Geweke test. A two-sided z-test comparing the means of chain segments. At convergence these means should be the same, with large z-scores indicating rejection (Stock and Semmens, 2015).

In the present study the MCMC settings in MixSIAR were: three chains, chain lengths of 300,000, "burn in" of 200,000 and "thin" value of 100. This generated model output containing 3000 samples of posterior source proportions (sum = 1). A continuous effects model, with a process only (i.e., *n* = 1) error structure, was employed to estimate the posterior distributions of sources for each individual sediment mixture sampled from the dated cores. The process-only error structure implements the MixSIR model (Moore and Semmens, 2008) within the MixSIAR suite, so that uncertainty includes the source variance only and no distinction is made from sources of variance associated with the trophic discrimination factors (TDF, Stock and Semmens, 2015, 2016). Specification of TDF to account for differences in the isotopic values of consumers' tissues and diet is a major source of uncertainty in estimating source contributions in food-web applications (Phillips et al. 2014; Stock and Semmens, 2016). In the context of the present study, the fact that TDF are not required for sediment tracing studies, as well as the application of historical information to constrain potential sources, are key advantages.

The results of model runs incorporating all FAs (C14 to C24) as well as medium-chain length FAs (C14 to C18:1) were compared. This step was undertaken as only core FT-1 (mid-intertidal flat) contained the entire suite of FAs for all dated sediment samples, whereas samples from cores FT-2 and FT-4 consistently contained only the C14 to C18:1 fatty acids. Comparison of the diagnostic tests indicated that the four-tracer model runs (i.e., C14 to C18:1) provided the most reliable results.

Bayesian estimates of source proportions can be informed by reliable priors based on data and thereby constrain the model and reduce uncertainty. For example, in food web studies, the gut contents of fish (i.e., prey species and relative abundance) can be used to construct priors in MixSIAR. In the present study, reliable/semi-quantitative information on the relative contributions of various sediment sources was unknown so that an "uninformative prior" was applied. An uninformative prior is one were all combinations of isotopic proportions (sum = 1) are equally likely (Stock and Semmens (2015).

2.6.3 Selection of sources and tracers

The selection of sources to be used in the SIMM is critical to the credibility of the results obtained. Best practices for the use of SIMM are reviewed by Phillips et al. (2014). Key recommendations include: (1) selecting potential sources in an informed way, based on prior information; (2) use of isotopic biplots to ensure that mixtures fall within potential source polygons; (3) combine sources if sample variability is such that individual sources cannot be distinguished based on parametric tests (e.g., difference of means, median %ile) and non-parametric statistical tests. Statistical analysis can also be used to determine the level of discrimination of sources provide by each tracer (e.g., FA); (4) incorporate uncertainties; and (5) report distributions of source proportion estimates. Ultimately, whatever methods are used, the selection of potential sources and tracers must conform to the isotopic biplot polygon principle, where the mixture must be enclosed with the polygon area (two tracers) or hyper-volume (three or more tracers) defined by the isotopic values of potential sources.

To inform best practice application of MixSIAR, statistical analyses (PCA, ANOVA) of the bulk carbon and fatty acid $\delta^{13}C$ data were employed to determine the extent to which both potential sediment sources and the biotracers could distinguished from each other, within one or more FA biomarkers. Appendix D provides a detailed description of this statistical analysis, with a brief summary below.

Prior to all analyses, samples were filtered to exclude outlier signatures. Any bulk or FA $\delta^{13}C$ signature was omitted if more than ±4‰ of the corresponding land use class arithmetic mean (i.e., comparing a dairy sample C16:0 FA $\delta^{13}C$ signature to the corresponding average of all dairy C16:0 FA $\delta^{13}C$ signatures). The lack of replicates of goat dairying required omission of the only dedicated sample and a mixed goat/dairying sample, whilst two further maize samples were omitted for repeated outlying signatures across several FA's. Cleaning the dataset resulted in nine potential sediment sources being analysed for discriminant ability.

Replicate estuarine sediment samples (3 per site) were also collected at several sites in the Firth of Thames to obtain $\delta^{13}C$ signatures for an estuarine/marine endmember to include in the MixSIAR source modelling.

Discriminant analyses were conducted in two steps:

- **Step one**: one-way Analysis Of Variance (ANOVA) was employed to test if statistically significant differences (p <0.05) in mean $\delta^{13}C$ signatures existed between the nine sources, repeating analysis for each of the isotopic biomarkers (i.e., single factor of land use, nine classes within). Residuals were inspected for normality and equivalence of variance. Post-hoc testing of between-class differences was undertaken using Tukey Honest Significant Difference routines. All analyses were undertaken in R using inbuilt functions (R Core Development Team, 2016). A subset of 42 land cover samples across the nine potential sources were also subject to principal components analysis (PCA[1]). PCA determines the underlying pattern of change (variance) across the nine isotopic biomarkers, to generate composite or 'principal components' that maximise those isotopic differences between samples. A biplot of the 42 samples distributed along the first and second principal components, was used with ANOVA output to determine which land cover classes were alike or dissimilar.

- **Step two**: output from step one was used to merge and exclude several of the original land use classes to enhance differences between the revised classes, testing these again with a one-way ANOVA design (i.e., single factor of land use, five classes within). Step one demonstrated no significant difference between the $\delta^{13}C$ signatures of the native forest and exotic pine topsoil samples, across all nine FAs so that only a merged exotic and native forest source class could be justified. Likewise the lack of any significant differences between the dairying and sheep & beef topsoil samples, across all nine FA $\delta^{13}C$ signatures indicated a merged pasture class was appropriate. Several other land uses were also infrequently discriminated from others in step one, including cropping (other than maize) and lifestyle classes (i.e., differing significantly in <20 of 72 possible pairings to other land uses). Based on their widely varying FA $\delta^{13}C$ signatures and limited replicates, neither class could be merged reliably with other classes. Both classes were thus excluded from the modelling of sediment sources in step two. Output from step two demonstrated that a more limited mix of land uses offered greater discriminant ability than the original nine land uses. This more limited mix of land use end members consisted of:

    - pasture (dairying and sheep and beef classes combined)

[1] PCA requires an observed $\delta^{13}C$ signature on all nine FA and bulk biomarkers, for each sample included, whereas 11 of the original 53 land use samples required one or more biomarker signatures being omitted as an outlier. Hence, the ordination of only 42 samples.

- forest (native and exotic forestry combined)
- subsoil
- maize
- mussel (i.e., isotopically enriched estuarine sediment).

On average significant differences were detected between any one of five classes and at least two of four others (see Appendix D), across all nine $\delta^{13}C$ biomarkers. Further testing on the revised forestry and pasture classes also demonstrated no significant differences within each class, by catchment for eight and nine $\delta^{13}C$ biomarkers, respectively. Thereby demonstrating that whereas land use was fundamental to determining the $\delta^{13}C$ biomarker composition, there were insignificant differences between forestry or pasture samples collected in the Waihou and Piako catchments (however, see point below about longitudinal differences along a river network being probable).

It should be noted that by amalgamating all replicate samples within a land use class in steps one and two above, more fine-scale spatial patterns within each sub-catchment can be masked. For example, despite there being insignificant difference between the mean of all dairying and of all sheep and beef $\delta^{13}C$ signatures for each of the nine biomarkers, there are spatial differences between sources at more localised scales. For example, the $\delta^{13}C$ signatures of sheep and beef are visibly different from dairying land use within the Piako for the C18:1 and C24:0 FA biplot (Figure 2-7). Importantly, Figure 2-7 also suggests a likely difference in dairying $\delta^{13}C$ signatures for C18:1 and C24:0 between dairying in the Piako and Waihou. This emphasises again that best-practice selection of end-members should occur in an informed way for sub-catchments (e.g., using nine classes), based on prior information whereas receiving environments like the Firth should approach selection from a whole-of-catchment statistical basis (e.g., using five classes only). In both instances, we are restricted by our limited understanding of the true variability of FA $\delta^{13}C$ signatures for each land use. Although this study includes the most exhaustive analysis of land use replicates to date in a New Zealand study, the potential remains for pasture or feed practices to differ within or between sub-catchments. This can result in differing FA $\delta^{13}C$ signatures within a land use class.

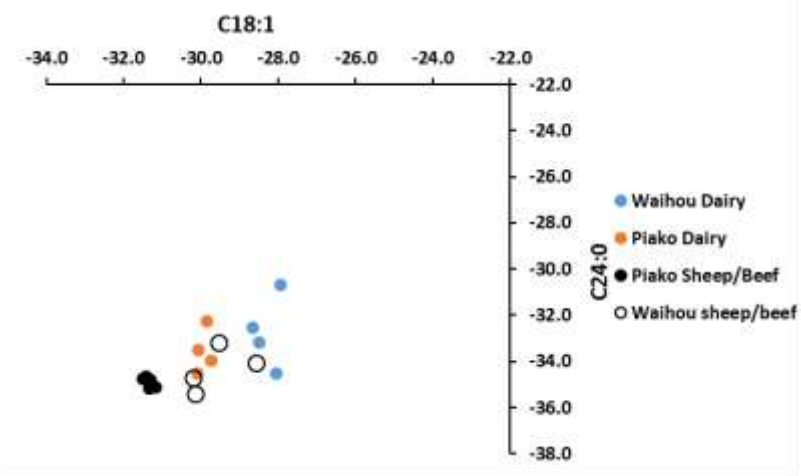

Figure 2-7: Isotopic biplot using the FA isotopes C18:1 versus C24:0 to show the separation between Waihou Dairy, Piako Dairy and Piako sheep and beef signatures. Each dot is a separate sample. The Waihou sheep and beef samples did not form a cluster but spread across the whole range of these samples.

Where equivalent land use class samples produce well defined clusters in a biplot, the isotopic signatures of the sample FAs of the component soils in each cluster can be combined to produce a mean value and standard deviation suitable for use in a SIMM. In the example (Figure 2-7), the Waihou sheep and beef class of FA signatures did not conform to a tight cluster. Rather they spread across the full isotopic range of the clusters shown meaning that the sheep and beef FA signatures from the Waihou River catchment would benefit from merger with the dairy FA signatures to produce a mean and standard deviation for a new land use class "pasture", which is consistent with the ANOVA and PCA results. Using a different pair of FA isotopes in the biplot may have resolved the difference between Waihou River catchment sheep and beef and dairy land use classes, allowing a better level of discrimination between these sources in the SIMM. Consequently, the isotope selection is just as important as the land-use source selection. Ultimately, all selections are under-pinned by the assumption that variability in source δ^{13}C FA composition has been accurately sampled before generating biplots or undertaking discriminant analysis. To reiterate, this study represents the most exhaustive attempt to date to do so within a catchment, in New Zealand, and on that basis represents the most robust modelling of source contributions for any receiving environment.

Further analysis of the data using the isotopic biplots applied to all classes of land use at each confluence showed that it was possible to discriminate between most of the original nine classes in confluence sediments collected within the Waihou River and in the Piako River. There was, however, less discrimination in the lowland Waihou River confluences. This suggests that there were longitudinal differences within several land use class isotopic signatures along the river course (e.g., pine, dairy, sheep and beef). Such upstream–downstream differences in FA δ^{13}C values within a land use class are likely to be associated with the erosion of soil from upland catchments and deposition further downstream, thereby producing a new downstream mixture/source signature.

2.6.4 Modelling sources by sub-catchment

Because Waihou and Piako River catchments are large and elongated, it is not reasonable to expect the CSSI technique to resolve sediments sources by land use for the catchment as a whole. While selecting sources and isotopes it was apparent that there were differences between the two river catchments and between the upper and lower catchment, especially in the Waihou. Consequently, the catchments were analysed in sections based on the sub-catchments above each river confluence points analysed. Each branch of the river system above the confluence was assessed using polygons to determine which sources to include. Example biplots for C18:0 and C20:0 FA data are presented in Figure 2-8. These biplots show that Waihou sediment mixture (A) is more closely associated with sheep/beef, dairy and broadleaf native forest sources, whereas the Waiomou sediment mixture (B) is more closely associated with pine forest and broadleaf native forest sources. Both sediments have a component of bank erosion and dairy land use but less association with maize, subsoils and podocarp native forest sources. Sources were initially analysed in IsoSource at coarse (5%) increment to determine which sources were likely to contribute to the mixture. The ellipses drawn on each biplot enclose sources to be used in the SIMM. Sources outside the ellipses did not contribute to the mixture. Note that modelling of these sediment mixtures was undertaken using several FA tracers, which define a isotopic hypervolume: C18:0, C18:1, C18:2, C20:0, C22:0 (A, B and C) and C24:0 instead of C22:0 for (D).

The isotopic values for the upstream site on the Waihou River below the confluence of the upper Waihou and the Waiomou streams (C), is a source for the Waihou River upstream of the Ohinemuri River (D).

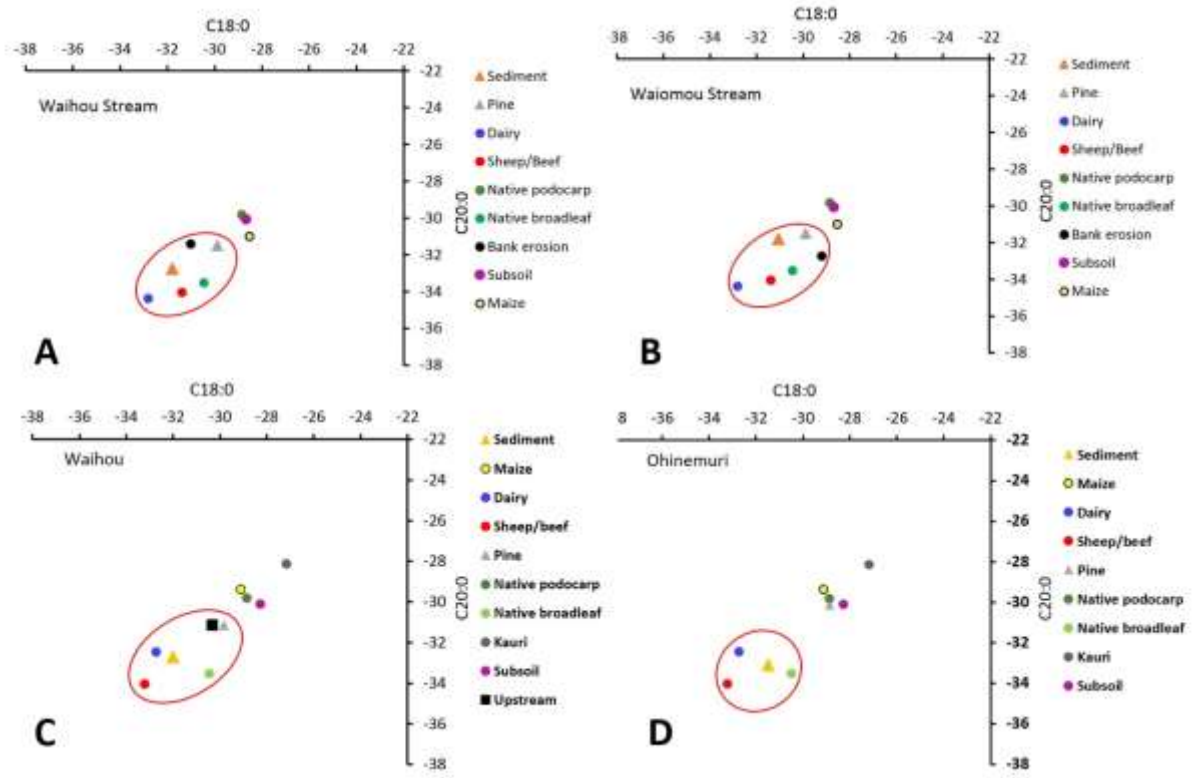

Figure 2-8: Comparison of sub-catchment polygons from the confluence between A) upper Waihou and B) the Waiomou streams, and C) the mid Waihou and D) Ohinemuri rivers. Source samples are the means of 3-4 individual samples. The sediment sample is a single bulked composite from the deposition zone upstream of the confluence. The ellipse encloses potential sources to be used in the SIMM. The standard deviation error bars have been omitted for clarity.

2.6.5 Modelling of sources in estuarine sediments

The corrected $\delta^{13}C$ values of the FA-labelled sediment mixtures preserved in the dated estuarine cores, along with data for potential sediment sources identified in the PCA-ANOVA statistical analysis (Appendix D), were used to model sources of sediment accumulating in the southern Firth over the last 800–1000 years. The data were initially compared using isotopic biplots to identify which combination of FA tracers would satisfy the requirement for mixtures to be constrained within polygons defined by the potential sources (Phillips et al. 2014).

Inspection of these isoplots suggested a missing source with a highly depleted $\delta^{13}C$ values (i.e., -34 to -38‰) that was not sampled in the field programme (Figure 2-9 to Figure 2-14). The outputs from mixing models are highly sensitive to missing sources. A potential candidate source (with a highly depleted $\delta^{13}C$ signature) is bracken soils, which are a ubiquitous land disturbance indicator preserved in New Zealand's sedimentary records. The abundance of bracken over large areas of the North Island following human arrival (McGlone et al. 2005) as well as the presence of bracken spores in cores previously collected in the Firth (Hume and Dahm, 1992) indicate that the inclusion of a bracken source was justified.

Stable isotope (FA) data for bracken soils sampled in the Mangemangeroa catchment (Howick, east Auckland) were subsequently included in the analysis after applying MeOH and inter-batch corrections. These samples were collected in 2012 as replicates of six separate composite samples collected using the same methods used in the present study.

Figure 2-9 to Figure 2-14 present each combination of isotopes as biplots for sediment mixtures and potential sources for the even-numbered FA tracers C14:0 to C24:0. These biplots show that the mid-chain length FAs (C14 to C18:2) have the largest source polygons defined by end members within which the sediment core samples (mixtures) are largely constrained (Figure 2-9 to Figure 2-10). The bracken endmembers have $\delta^{13}C$ values that are typically -8 to -12‰ more depleted than the surficial estuarine sediments end members of the Outer Firth. In many of the biplot combinations, the FA $\delta^{13}C$ values of the surficial estuarine sediments (i.e., Outer Firth, Mussels, Waihou and Piako River deltas) are very similar and can be treated as a single source type. It is also apparent that the size of the source polygons collapse and/or no longer constrain the sediment core (mixture) samples as FA chain lengths increase (Figure 2-11 to Figure 2-14). These data indicate that the C14:0 to C18:2 combinations most closely conform to the fundamental principles of isotopic source modelling. The biplots also critically show that the FA $\delta^{13}C$ signatures of many of the sources display substantial degree of variability. Along with the linear biplot structure of the higher chain-length FAs (i.e., paired $\delta^{13}C$ FA values of potential sources display apparent correlation [e.g., C16 – C18:2]), this variability influences the uncertainty of the isotopic proportions of sources estimated by MixSIAR.

The suite of FA tracers available in the cores varied between sites. Only core FT-1 contained a complete suite (C14:0 to C24:0). Core FT-2 contain a complete suite in sediments down to 33 cm depth (i.e., mid-1950s) but consistently only the C14:0 to C18-1 FA below that depth. Core FT-4 contained the C14:0 to C18-1 FA with few exceptions (Appendix A). In the subsequent modelling of source contributions, both the C14:0 to C18:1 and C14:0 to C24:0 suites were used to compare results.

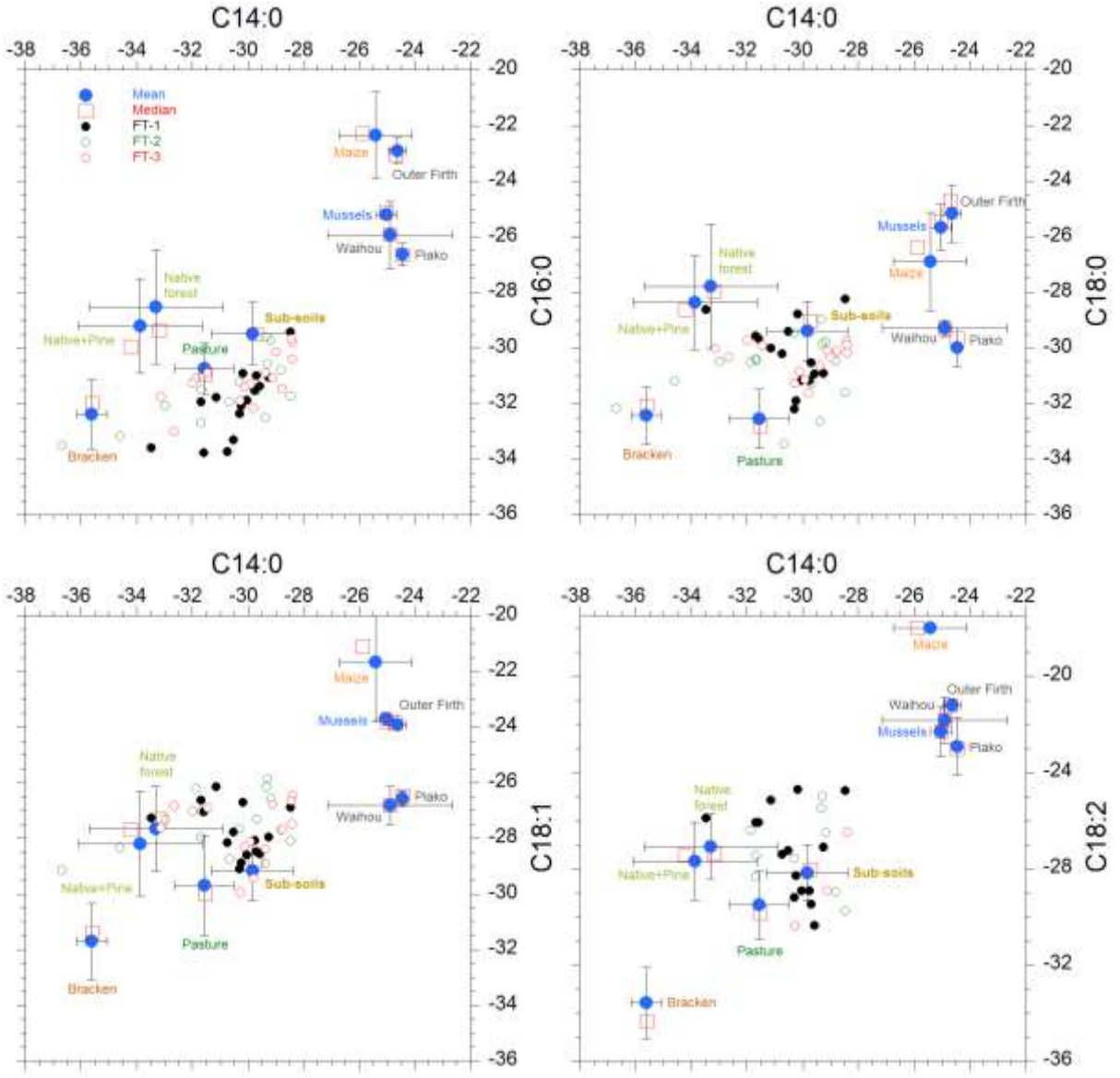

Figure 2-9: Sample isotopic biplots of average fatty acid d13C values (C14:0 and C16:0 to C18:2) for potential sediment sources and estuarine sediment mixtures in the dated cores. Notes: (1) Refer to Figure 1-1 for location of Outer Firth (SA3 sites) Waihou and Piako River delta (A sites), and mussel (WA sites) sampling locations and cores (FT); (2) all isotope data corrected to present (2015 AD) with methyl and inter-batch corrections applied; (3) one standard deviation values shown.

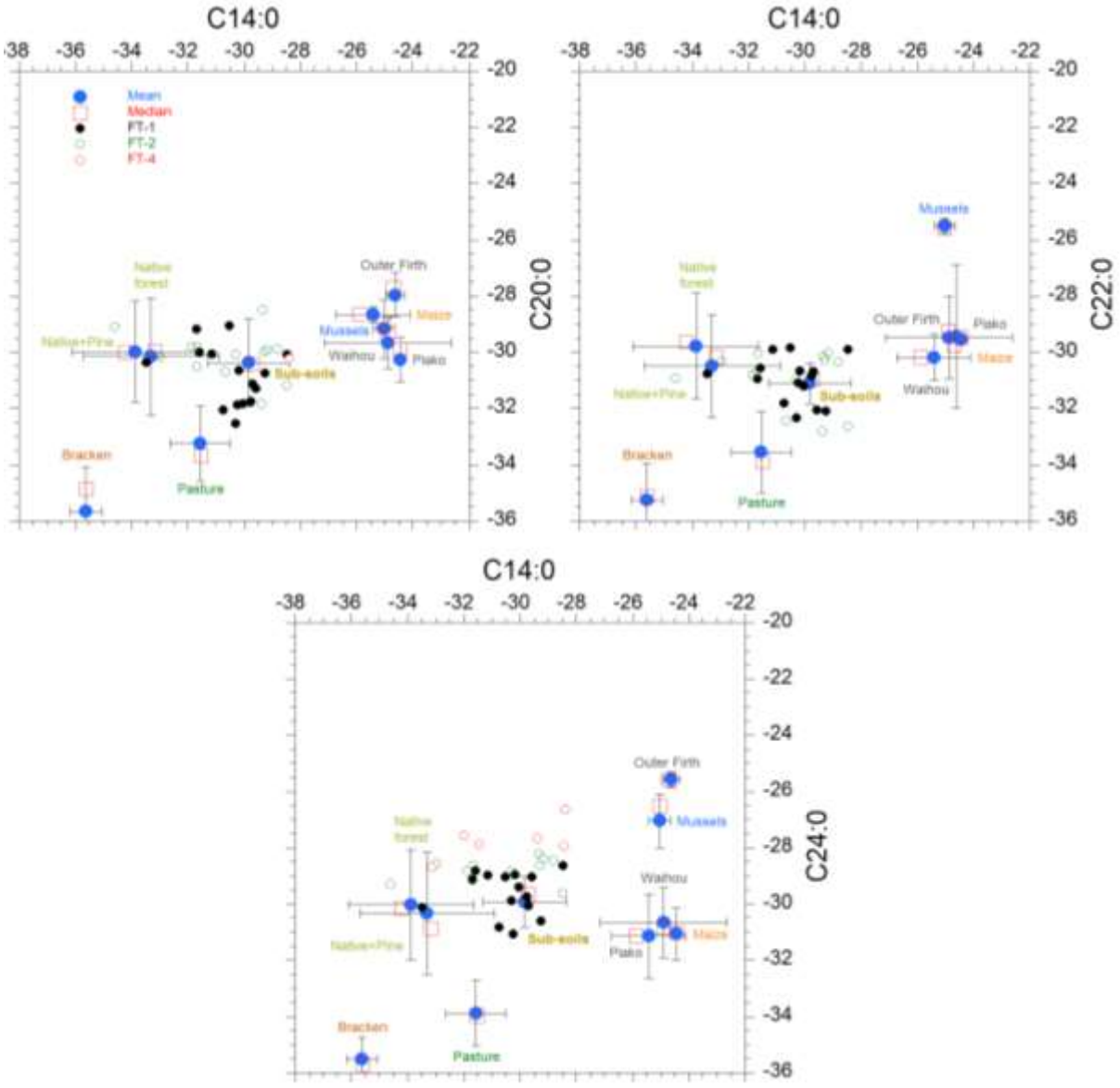

Figure 2-10: Sample isotopic biplots of average fatty acid d13C values (C14:0 and C20:0 to C24:0) for potential sediment sources and estuarine sediment mixtures in the dated cores. Notes: (1) Refer to Figure 1-1 for location of Outer Firth (SA3 sites) Waihou and Piako River delta (A sites), and mussel (WA sites) sampling locations and cores (FT); (2) all isotope data corrected to present (2015 AD) with methyl and inter-batch corrections applied; (3) one standard deviation values shown.

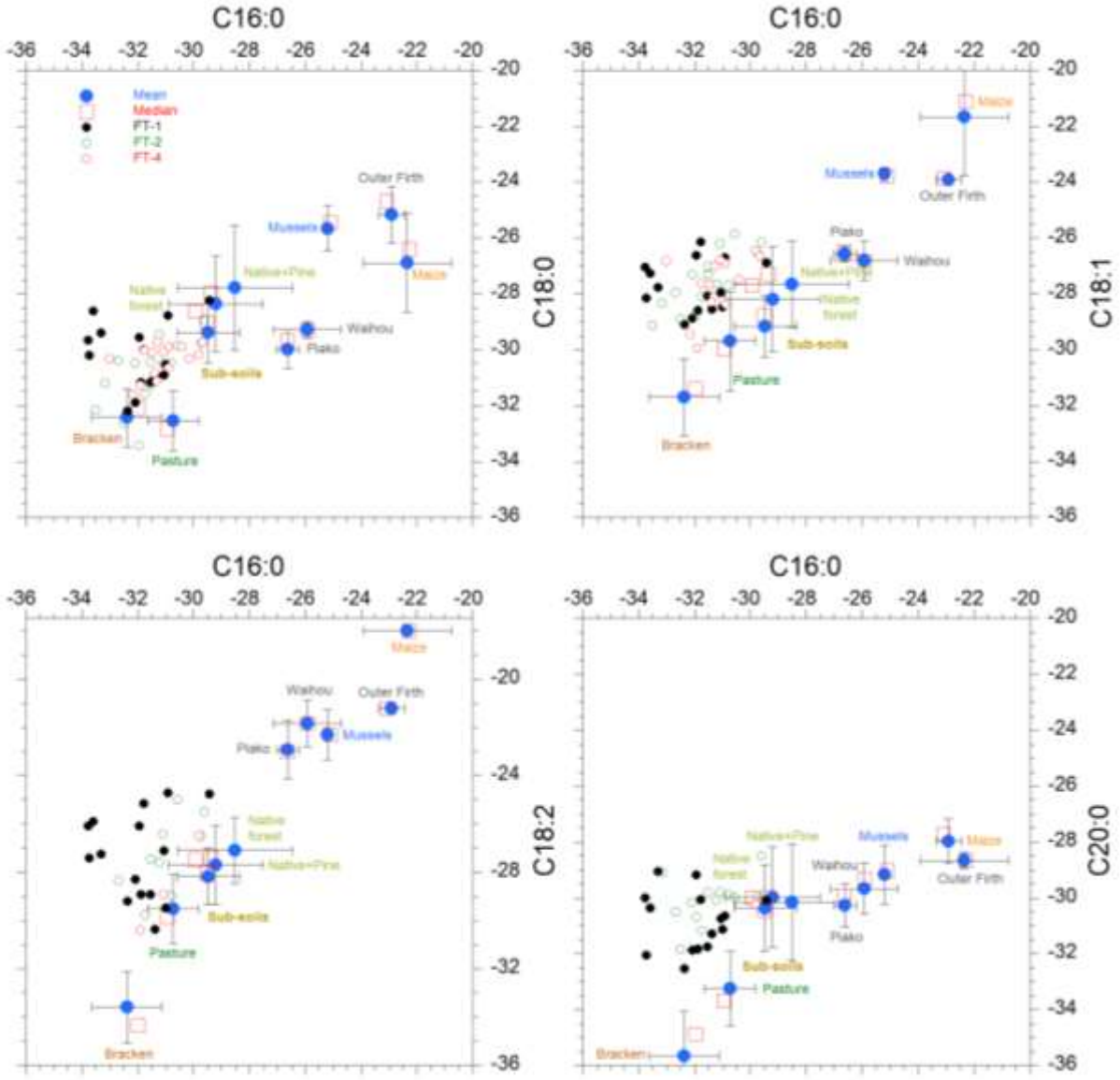

Figure 2-11: Sample isotopic biplots of average fatty acid d13C values (C16:0 and C18:0 to C24:0) for potential sediment sources and estuarine sediment mixtures in the dated cores. Notes: (1) Refer to Figure 1-1 for location of Outer Firth (SA3 sites) Waihou and Piako River delta (A sites), and mussel (WA sites) sampling locations and cores (FT); (2) all isotope data corrected to present (2015 AD) with methyl and inter-batch corrections applied; (3) one standard deviation values shown.

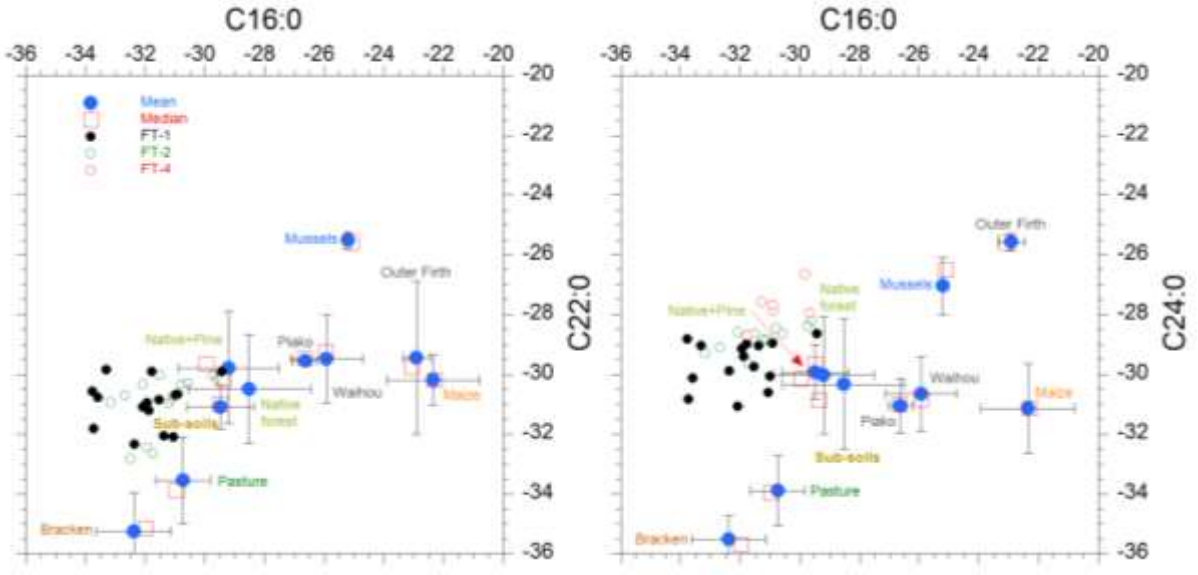

Figure 2-12: Sample isotopic biplots of average fatty acid d13C values (C16:0 and C22:0 to C24:0) for potential sediment sources and estuarine sediment mixtures in the dated cores. Notes: (1) Refer to Figure 1-1 for location of Outer Firth (SA3 sites) Waihou and Piako River delta (A sites), and mussel (WA sites) sampling locations and cores (FT); (2) all isotope data corrected to present (2015 AD) with methyl and inter-batch corrections applied; (3) one standard deviation values shown.

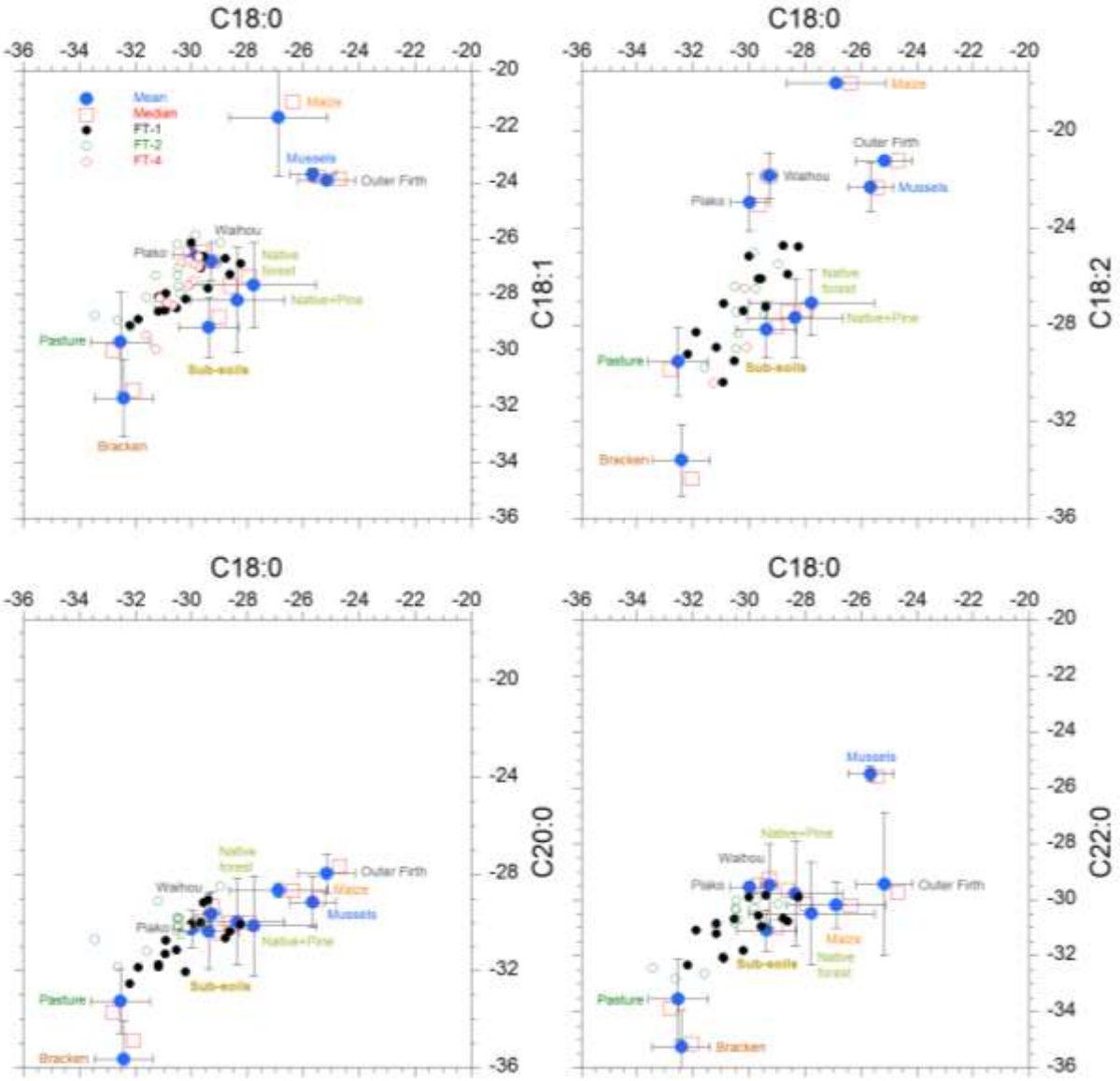

Figure 2-13: Sample isotopic biplots of average fatty acid d13C values (C18:0 and C18:1 to C22:0) for potential sediment sources and estuarine sediment mixtures in the dated cores. Notes: (1) Refer to Figure 1-1 for location of Outer Firth (SA3 sites) Waihou and Piako River delta (A sites), and mussel (WA sites) sampling locations and cores (FT); (2) all isotope data corrected to present (2015 AD) with methyl and inter-batch corrections applied; (3) one standard deviation values shown.

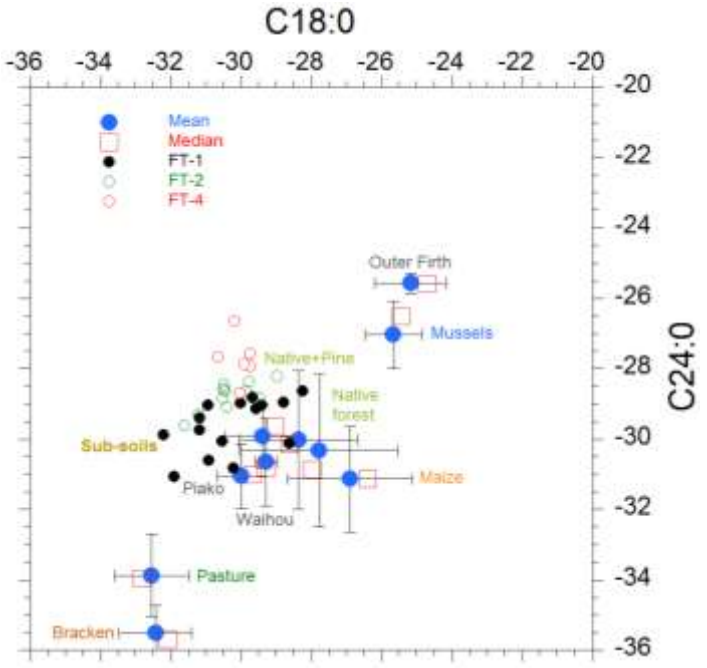

Figure 2-14: Sample isotopic biplots of average fatty acid d13C values (C18:0 and C24:0) for potential sediment sources and estuarine sediment mixtures in the dated cores. Notes: (1) Refer to Figure 1-1 for location of Outer Firth (SA3 sites) Waihou and Piako River delta (A sites), and mussel (WA sites) sampling locations and cores (FT); (2) all isotope data corrected to present (2015 AD) with methyl and inter-batch corrections applied; (3) one standard deviation values shown.

2.6.6 Conversion of SIMM results from isotopic to soil proportions

The outputs from both IsoSource and MixSIAR are in isotopic proportions (sum = 1), based on the model fits to the observed isotopic signatures of the FAs in the soils and sediment deposits. Soil comprises minerals and organic matter including carbon, with the %C in the whole soil or sediment ranging from less than 0.5% to greater than 30% (Appendix A). The FAs in the soil amount to about 0.002 – 0.01% of this soil/sediment carbon pool. To convert the isotopic proportions to soil proportions, a linear scaling equation is used, based on the %C content in each source soil:

$$\%source_n = \frac{I_n / \%C_n}{\sum_n^1 (I_n / \%C_n)} x100$$

where I_n is the mean feasible proportion of source n in the mixture as estimated from isotopic values of carbon by in the SIMM, and $\%C_n$ is the % carbon in the source n soil.

Because this calculation only uses the %C of the source soils for scaling, the proportional contribution of each source soil is independent of any loss of total carbon or FA in the sediment mixture through biodegradation.

This linear-scaling equation was applied directly to each of the 3000 realisations of isotopic proportions output from each MixSIAR model run. This enabled a probability distribution of soil proportions to be constructed for each of the dated sediment core samples.

3 Results

3.1 Sources of sediments by river tributary

Results of the river confluence analyses are presented in Table 3-1.

Table 3-1: Proportional contribution of main stem and tributary sources to downstream confluence samples from two-endmember modelling. Results shown are the mean and standard deviation contributions of each source to the confluence mixture, with number (No.) of valid tracers. Note: the accuracy implied by the decimal point is not real but is as calculated. Mean annual flow* estimates from Vant (2011) and ~flows from the NIWA Fish Database.

Confluence		Proportional contribution			Flow*
		Mean	±SD	No.	($m^3 s^{-1}$)
Upper Waihou and Waiomou Rivers	**Site 2**				
Waihou River	Site 5	84.4	2.8	4	
Waiomou River	Site 3	15.6	2.8	4	
Mid- Waihou and Ohinemuri Rivers	**Site 13**				
Waihou River	Site 11	90.2	3.1	3	37.2
Ohinemuri River	Site 10	9.8	3.1	3	11.1
Lower Waihou and Hikutaia Rivers	**Site 17**				
Waihou River	Site 15	94.0	5.3	2	
Hikutaia River	Site 16	6.0	5.3	2	
Waihou River delta (Mud)	**Site A3**				
Waihou River	Site 17	68.0	15.9	5	~70
River delta	Site A1	32.0	15.9	5	
Piako and Waitoa Rivers	**Site 7**				
Piako River	Site 9	35	6.6	3	6.9
Waitoa River	Site 6	65	6.6	3	4.8
Piako River delta (Mud)	**Site A4**				
Piako River	Site 7	19.9	9.0	3	~24
River delta	Site A6	80.1	9.0	3	

The river delta sample river proportions are best estimates based on using the inshore mud sample as the river delta mixture and the most seaward of each delta triplicate sample as the Firth of Thames sediment component (e.g., sites A3 and A4, Figure 1-1). These samples are indicative that the Waihou River is producing more sediment than the Piako River.

3.2 Contemporary sources of catchment sediments

Results of land use contributions at river confluences are presented in Table 3-2.

With the exception of the Waitoa and Ohinemuri Rivers, the largest source of sediment to both the Waihou and Piako River systems was from bank erosion. In contrast with the low contributions of local bankside material downstream of the confluence with the Ohinemuri, the majority of sediment in the Waihou was sourced from upstream (~90%) where bankside erosion was dominant (~75-80% of sediment). Analysis of bank erosion material demonstrated that in the upper reaches of the Waihou and Waiomou Rivers, it was mostly from pine forestry (Table 3-3).

The dominant land use source to bank erosion material in the Piako River was dairying (Table 3-3). Whereas, subsoil was the dominant contributor directly into and indirectly via bank erosion to the Waitoa River.

Table 3-2: The soil proportions contributing to each river confluence sample. Values are mean % land use source (±SD), where the SD is the range of feasible solutions around the mean. Where the mean soil % is <10 and the SD approaches or exceeds the mean, the uncertainty is high, and it is possible that that source may not be present. It was not possible to deconstruct the Waihou River and Hikutaia River sediments at sites 15 and 16 without the use of the downstream sediment signature from site 17 as a source sample.

Sub-catchment	Site ID	n	Bank erosion	Sheep/Beef	Dairy	Maize	Native Broadleaf	Pine	Upstream	Downstream	Subsoil
Waihou	5	362	80.0 (2.9)	12.5 (3.1)	0.3 (1)	0.4 (0.4)	0.5 (2.8)	6.3 (7.2)			0
Waiomou	3	686	74.6 (1.3)	0.3 (1.3)	7.4 (2.6)	14.3 (2.0)	0.2 (1.5)	3.4 (4.5)			0
Waihou	11	87	0	0.1 (0.8)	4.3 (3.2)	0.1 (0.1)	5.0 (3.7)	0.4 (1.3)	90.2 (0.8)		0
Ohinemuri	10	1	0	25.9 (0)	0	0	74.2 (0)	0	0		0
Waihou	15	5	3.8 (2.4)	0	0.2	0	0	0	62.7 (1.6)	33.4 (0.7)	0
Hikutaia	16	5	0.5 (0.4)	0	14.7 (1.1)	0	0	0	2.2 (1.7)	82.6 (0.4)	0
Piako	9	279	68.3 (5.7)	2.8 (2.9)	1.9 (2.5)	0	0.1 (0.5)	26.7 (2.9)			0
Waitoa	6	6	0.3 (0.4)	14.1 (0.8)	0.2 (0.8)	0	0	0			85.5 (0.5)

Table 3-3: Soil proportions contributing to each bank erosion sample in Table 3-2 greater than 1%.

Bank	Site ID	n	Sheep/Beef	Dairy	Maize	N Broadleaf	N Podocarp	Pine	Upstream	Downstream	Subsoil
Waihou	5A	52	2.1 (1.0)	16.4 (1.7)	0	1.1 (2.0)	0	80.4 (2.0)			0
Waiomou	4	382	0.8 (1.1)	2.4 (1.8)	0	3.5 (5.4)	<0.1 (0.3)	90.7 (4.9)			2.7 (0.3)
Waihou	14	3	0	8.4 (0.6)	0	5.0 (3.7)		20.5 (0)	3.7 (0.6)	67.4 (1.0)	0
Piako	8	46	0.8 (1.0)	75.3 (1.3)	3.7 (0.9)	0.1 (0.5)	0.6 (2.3)	7.5 92.1)			11.9 (2.1)

3.3 Sediment core geochronology and sedimentation

3.3.1 Summary of sediment accumulation rates

The geochronology of the sediment cores collected in the present study has been reconstructed from analysis of sediment core properties, x-radiographs and radioisotope dating. The results of the radioisotope dating of the sediment cores is summarised in Table 3-4 and presents estimates of time-averaged SAR in the Firth system over the last 700 to 1800 years. These estimates are based on ^{137}Cs and ^{210}Pb dating of sediments and ^{14}C dating of carbonate shell valves preserved in discrete sediment layers below the excess ^{210}Pb profiles. The ^{14}C SAR represents the time average value for sediments deposited above the dated shell layer to the base of the excess ^{210}Pb and includes the pre-deforestation, Māori (post-1300s) and European (post-1820s) periods.

These results indicate that sediments accumulated at a relative low rate in the Firth of Thames (0.2–0.9 mm yr^{-1}) over the 700–1600 years prior to the late-1800s/early 1900s. The ^{210}Pb dating of European period sediments show that time-average SAR over the last 90–145 years (3.4–18.1 mm yr^{-1}) are an order of magnitude higher than the pre-European period. Core FT-1 (mid intertidal flat) captures a period of changing sediment accumulation rates since the 1870s, with ^{210}Pb SAR increasing from 2.9 to 18.1 mm yr^{-1} in the early 1960s. This high-SAR period persisted for only a decade, with SAR averaging 10.1 mm yr^{-1} since the mid-1970s.

Comparison of the time-averaged ^{137}Cs SAR (corrected for ^{7}Be SML depth) with the ^{210}Pb estimates shows poor agreement in core FT-3 but reasonable agreement between these two dating techniques in cores FT-1, FT-2 and FT-4 (Table 3-4).

Despite this, several factors suggest that the ^{137}Cs data should be used with caution: (1) ^{137}Cs activity has substantially reduced even since the early-1960s ^{137}Cs deposition peak (i.e., $t_{1/2}$ = 30 years) so that ^{137}Cs activities are below detectable levels in deeper deposits and the maximum ^{137}Cs is increasingly under-estimated; (2) we assume that the ^{7}Be SML is assumed to be constant over time, when in fact deeper mixing over annual–decadal time scales is indicated by some of the ^{137}Pb profiles so that mixing maybe deeper, with the result that the maximum ^{137}Cs is over-estimated; (3) the early-1960s ^{137}Cs deposition peak observed in New Zealand wetland deposits (Gehrels et al. 2008), and the most reliable ^{137}Cs time-horizon for dating, is typically absent in New Zealand estuarine and coastal marine sediments (Appendix B).

It should be noted that the maximum age of sediments dated using ^{210}Pb profiles depends on the maximum depth of excess ^{210}Pb in each core. The maximum depth of excess ^{210}Pb in turn varies depending on the SAR, surface activity of excess ^{210}Pb, particle size and degree of sediment reworking after deposition (i.e., radioisotope activity generally increase with mud content). Small amounts of excess ^{210}Pb may occur below the apparent maximum depth but are below detectable levels.

Table 3-4: Summary of sediment accumulation rates (SAR), Firth of Thames cores. Time-average SAR (mm yr^{-1}) estimated from ^{137}Cs, excess ^{210}Pb and ^{14}C dating from historical to pre-human periods. Information on linear regression fits to log-transform $^{210}Pb_{ex}$ data included. The ^{137}Cs SAR is estimate assuming deposition since 1953.

Core site	^{137}Cs max (cm)	^{137}Cs SAR	^{210}Pb and ^{14}C depth and age ranges (cm, AD)	^{210}Pb SAR (r^2, *n*)	^{14}C SAR	Time Period (years)
FT-1	65	10.5	0-41 (*2015–1974*)	10.1 (*0.56, 8*)		41
			41–91 (*1974–1963*)	18.1 (*0.6, 9*)		11
			91–111 (*1963–1870*)	2.9 (*0.54, 6*)		93
			111–150 (1870–1320)		0.69	550
FT-2	26	4.1	0-61 (*2015–1906*)	5.6 (*0.83, 10*)		109
			61–150 (1906–1340)		0.43	570
FT-3	2	*0.3*	0–21 (*2015–1924*)	3.4 (*0.72, 6*)	N/A	109
FT-4	16	2.5	0–61 (*2015–1924*)	6.7 (*0.96, 7*)		91
			61–80 (*1924–1039*)		0.21	885
			80–150 (*1039–290*)		0.93	749

3.3.2 Radiocarbon dating results

The time-averaged ^{14}C SAR for the sediment cores range from 0.2 to 0.9 mm yr^{-1} and spanning time periods of 540 to 1630 years prior to the late 1800s– early 1900s. These time periods incorporate background sedimentation rates prior to human arrival in ~1300 A.D. as well as the effects of deforestation by Māori and European settlers. In cores FT-1 and FT-2, the SAR estimates largely reflect sedimentation during the period of Māori occupation whereas core FT-4 includes a ~1100 year period prior to human arrival. These data suggest that forest clearance by Māori had a minimal impact on sedimentation rates in the Firth of Thames. However, these ^{14}C SARs are averaged over centuries and do not capture sedimentation peaks that may have occurred over annual–decadal time scales, associated with shorter periods of forest clearance.

Conventional radiocarbon ages (AMS ^{14}C) obtained for pairs of estuarine shell samples taken from cores FT-1, FT-2 and FT-4 are presented in Table 3-5. The ages of the shell samples taken from two different animals in each core show a high level of agreement, with age differences of less than 15 years for the intertidal cores FT-1 and FT-2.

Table 3-5: Atomic Mass Spectrometry ^{14}C dating results and sediment accumulation rates for Firth of Thames cores. Age is the conventional age BP (Before Present, 1950 AD), with one standard deviation error shown. Note: Wk number is the Waikato University Radiocarbon Dating Laboratory sample identification.

Core	Depth (cm)	Wk number	Age (years BP)	±(± years)	^{14}C SAR (mm yr^{-1})	Time period
FT-1	148–149	Wk-42301	637	22	0.68	1313–1870 A.D.
	149–150	Wk-42302	622	21	0.70	1328–1870 A.D.
FT-2	98–99 (A)	Wk-41785	816	20	0.43	1134–1905 A.D.
	98–99 (B)	Wk-41786	804	20	0.44	1146–1905 A.D.
FT-4	76–80 (A)	Wk-43449	913	24	0.19	1037–1924 A.D.
	78–80 (B)	Wk-43450	908	20	0.22	1042–1924 A.D.
	175–176	Wk-41787	1,872	20	1.0	78–1039 A.D.
	175–176	Wk-41788	1,660	20	1.28	290–1039 A.D.

The substantially larger age difference for the two samples at 175–176 cm depth in core FT-4 (i.e., 212 years) is partially offset by their substantially older ages (i.e., 1,872, 1660 years BP) in comparison to the intertidal cores (i.e., 622–816 years BP). Reworking of older sediments and shell, and subsequent re-deposition in more recent deposits is a potential explanation for this age difference. The small sigma errors in the radiocarbon ages of about ±20 years, as well as the similar ages of the shell samples provide confidence in these data and derived estimates of long-term SAR.

3.3.3 Core FT-1

X-radiographs for core FT-1 display a range of sediment fabrics: finely laminated muds and fine sands (0–90 cm depth) containing rare fragments of shell valves (Figure 3-1). This surface layer of mud caps a layer of poorly-laminated muddy sands, with numerous shall fragments and whole valves of the trough shell (Cyclo*mactra ovata,* Māori: Ruheruhe), large wedge shell (*Macomona liliana,* Māori: Hanikura) and cockle-shell valves being common below ~90-cm depth. Duplicate samples of articulated cockle-shell valves from 148–149-cm depth were ^{14}C dated.

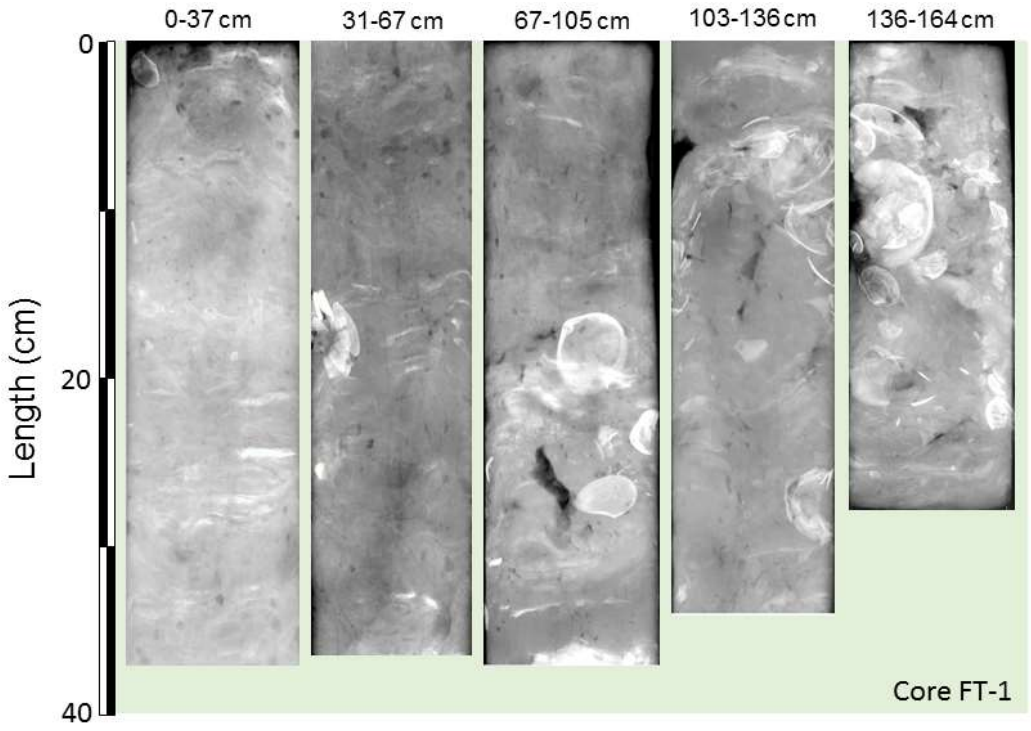

Figure 3-1: Core FT-1 (mid-intertidal flat) X-radiographs. (0–164 cm). These images have been inverted so that relatively high-density objects appear white (e.g., shell valves) and low-density materials such as muds or organic material appear as darker areas (format: 8bit tiff, export: 256 greyscale, scale 400%, png).

Figure 3-2 summarises the radioisotope dating and physical properties of sediments preserved in core FT-1. Dry-bulk sediment density (ρ_b) profiles for the cores provide information on the composition of the sediment deposits. For example, ρ_b values for estuarine sand deposits are typically of the order of 1.5–1.7 g cm^{-3}, whereas a mud deposit with high water content can typically have a ρ_b value as low as 0.4 g cm^{-3}.

Core FT-1 displays a gradual increase in ρ_b values with depth, from~ 0.4 g cm^{-3} in near-surface sediments to 0.5–0.6 g cm^{-3} in basal sediments at 150 cm depth (Figure 3-2b). Particle size profiles, are consistent with this gradual increase in dry bulk sediment density, with a gradual increase in mean particle size (~20 to ~40 microns) and reduction in mud content (~100 to 80%) with depth (Figure 3-2c–d). These basal muddy sands below ~100 cm depth coincide with the low-SAR phase prior to the late 1800s (Figure 3-2a).

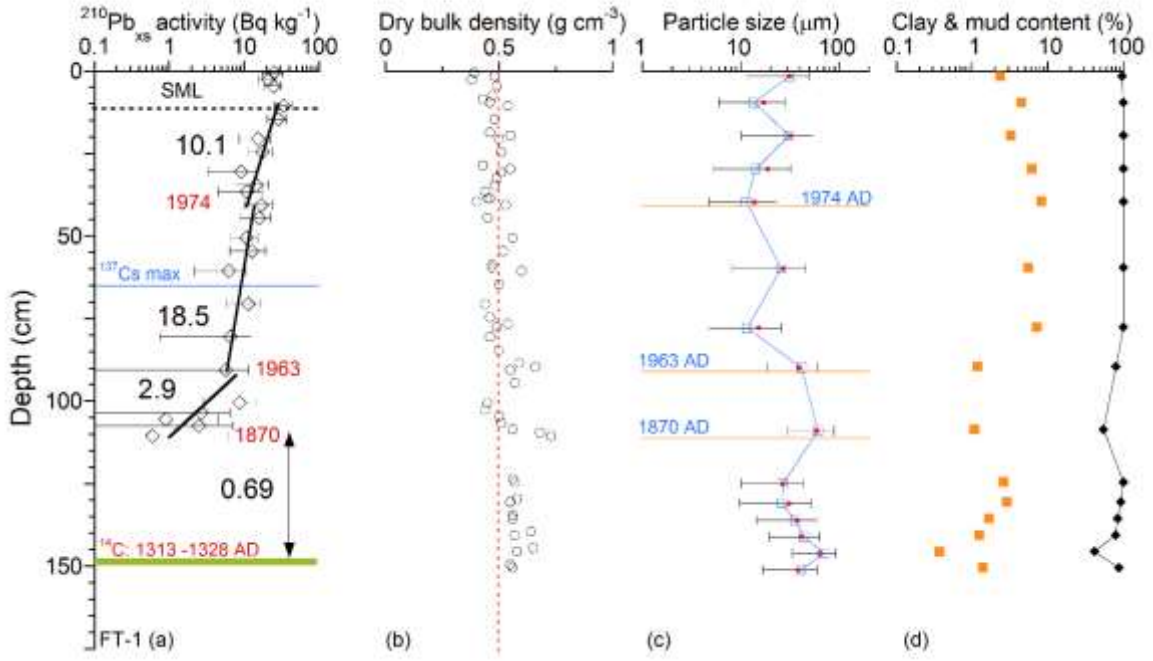

Figure 3-2: Core FT-1 (Intertidal) - ages of sediment layers and sediment accumulation rates (SAR), and sediment properties. (a) Excess ^{210}Pb activity profiles with 95% confidence intervals shown. Time-averaged SAR (Black text) derived from regression fit to natural log-transformed ^{210}Pb data and ^{14}C ages of bivalve shells. Estimated ages of depth horizons (red text). Surface mixed layer (SML) inferred from excess ^{210}Pb profiles. Maximum depth of caesium-137 (^{137}Cs) indicated. Radioisotope activity expressed in units of Becquerels (Bq). (b) Sediment dry bulk density; (c) mean (red) and median particle diameters with standard deviation; (d) clay and mud content as percentage of sample by particle volume.

3.3.4 Core FT-2

X-radiographs for core FT-2 (lower intertidal flat) display a range of sediment fabrics. Stratigraphy is generally better preserved than in core FT-1, particularly with increasing depth (Figure 3-3). Sediments contain abundant valves of small nut shell (*Nucula hartvigiana,* Māori: NA) of ~1 cm diameter. Occasional fragments and whole of the trough shells and large wedge shells also occur. A thick layer of shell hash and valves occurs at 40–52-cm depth, with several other layers of shell valves occurring at intervals down to the base of core FT-1. Bedding is particularly well developed in sediments below ~70-cm depth, which consist of alternating layers of low-density mud (dark layers) and millimetre-to-centimetre thick layers of sand (white layers, Figure 3-3). Duplicate samples of articulated cockle-shell valves from 98–99-cm depth were ^{14}C dated.

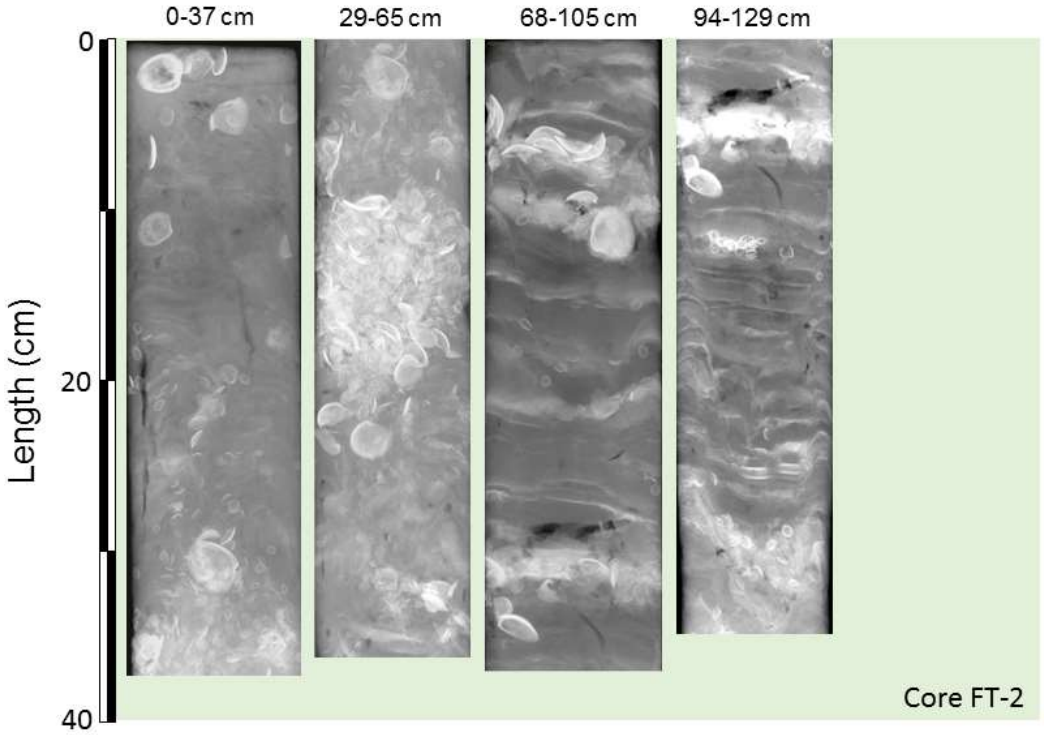

Figure 3-3: Core FT-2 (lower-intertidal flat) X-radiographs. (0–129 cm). These images have been inverted so that relatively high-density objects appear white (e.g., shell valves) and low-density materials such as muds or organic material appear as darker areas (format: 8bit tiff, export: 256 greyscale, scale 400%, png).

Dry-bulk sediment densities in core FT-2 clearly vary between the sediment layers. Low density muds (i.e., ~0.5 g cm^{-3}) occur above and below the shell layer at 40-50-cm (~1 g cm^{-3}) depth (Figure 3-4b). Particle size and composition vary between these mud and shell layers, with mean particle size of the mud–sand matrix gradually increases with depth (Figure 3-4c–d). As for core FT-1, muddy sands below ~50 cm depth coincide with the low-SAR phase prior to the early 1900s (Figure 3-4a).

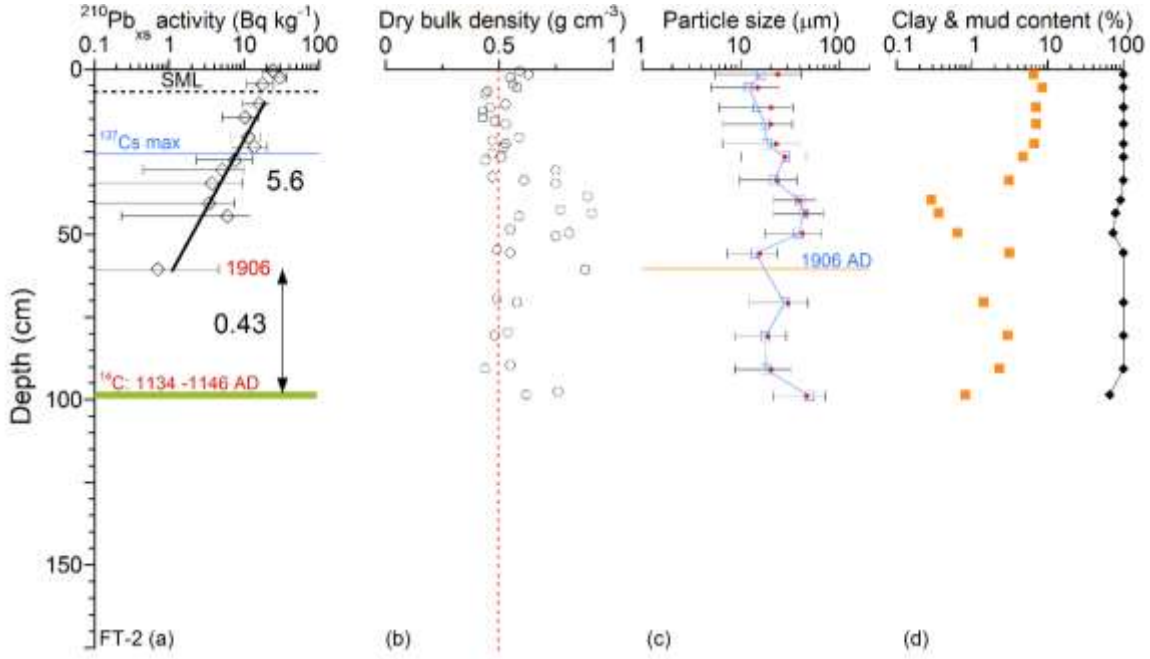

Figure 3-4: Core FT-2 (Intertidal) - ages of sediment layers and sediment accumulation rates (SAR), and sediment properties. (a) Excess ^{210}Pb activity profiles with 95% confidence intervals shown. Time-averaged SAR (Black text) derived from regression fit to natural log-transformed ^{210}Pb data and ^{14}C ages of bivalve shells. Estimated ages of depth horizons (red text). Surface mixed layer (SML) inferred from excess ^{210}Pb profiles. Maximum depth of caesium-137 (^{137}Cs) indicated. Radioisotope activity expressed in units of Becquerels (Bq). (b) Sediment dry bulk density; (c) mean (red) and median particle diameters with standard deviation; (d) clay and mud content as percentage of sample by particle volume.

3.3.5 Core FT-3

Core FT-3 was collected from shallow subtidal flats within a large area of surficial sediments characterised as muddy-calcareous gravels (section 1.2.5). The X-radiographs show a surface layer of shell-lag gravel composed of pipi (*Pahies australis*) and large wedge shell (*Macomona Liliana*) extending to 20-cm depth (Figure 3-5). Shell-lag layers such as these are indicative of fine-sediment winnowing by waves and/or currents. The shell-lag layer caps a sequence of strongly-laminated alternating layers of low-density mud (dark layers) and millimetre-to-centimetre thick layers of sand. There is a general down-core trend of increasing sand content, which is demonstrated by the increasing frequency and thickness of mm-to-cm thick sand layers. Shell fragments and valves are rare below the surface shell-lag layer. Dry-bulk sediment densities of up to ~1 g cm^{-3} occur in the shell-lag layer and abruptly decline to 0.5 g cm^{-3} in the underlying laminated muds (Figure 3-6).

The exponential decline in $^{210}Pb_{ex}$ activity in the mud matrix within the shell-lag layer suggests that this thick shell layer is decades old and that mud has accumulated (i.e., 3.4 mm yr^{-1}) in the interstitial voids over this period, with $^{210}Pb_{ex}$ decay occurring over time (Figure 3-6a). The winnowing of mud from the shell layer is also indicated by apparent absence of ^{137}Cs in all but the top-most 2 cm of the core. Given that atmospheric deposition of ^{137}Cs was not detected in New Zealand since the mid-1980s (Mathews, 1989), the presence of this radioisotope is most likely due to relatively recent sediment reworking, dispersal and re-deposition within the Firth.

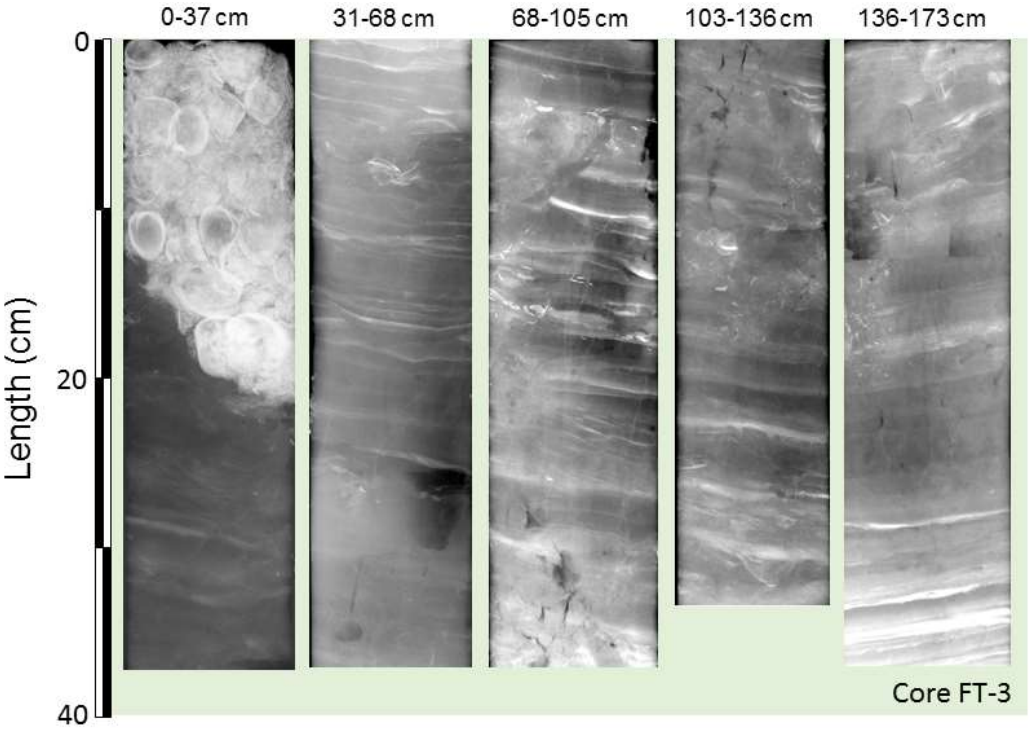

Figure 3-5: Core FT-3 (shallow subtidal) X-radiographs. (0–173 cm). These images have been inverted so that relatively high-density objects appear white (e.g., shell valves) and low-density materials such as muds or organic material appear as darker areas (format: 8bit tiff, export: 256 greyscale, scale 400%, png).

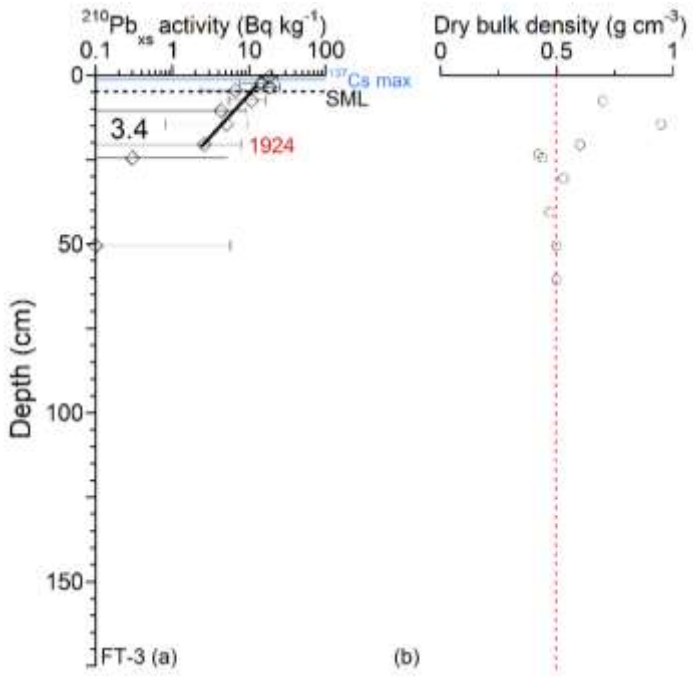

Figure 3-6: Core FT-3 (Subtidal) - ages of sediment layers and sediment accumulation rates (SAR), and sediment properties. (a) Excess ^{210}Pb activity profiles with 95% confidence intervals shown. Time-averaged SAR (Black text) derived from regression fit to natural log-transformed ^{210}Pb data. Estimated ages of depth horizons (red text). Surface mixed layer (SML) inferred from excess ^{210}Pb profiles. Maximum depth of caesium-137 (^{137}Cs) indicated. Radioisotope activity expressed in units of Becquerels (Bq). (b) Sediment dry bulk density.

3.3.6 Core FT-4

Core FT-4 was collected from the subtidal mud-depocentre predicted by the sediment-transport modelling (Section 1.2.4). The x-radiographs for this core show a diverse range of sediment fabric (Figure 3-7). The upper 46-cm of the core is composed of finely-laminated muds and sands with abundant shell fragments occurring in layers at 0–8 and 12–20 -cm depth. This unit caps a thick layer of shell fragments and valves extending to ~90-cm depth. Common species include large articulated cockles up to 5-cm diameter and individual trough shell valves. Below this shell layer, a sequence of finely laminated mud with mm-scale sand and shell layers units extends to ~130-cm depth. In turn, these muds cap a shell layer containing abundant valves of small nut shell, and juvenile trough shell and some specimens of dawn shell (*Tawera spissa*). Duplicate samples of dawn shell from ~175 cm depth were ^{14}C dated.

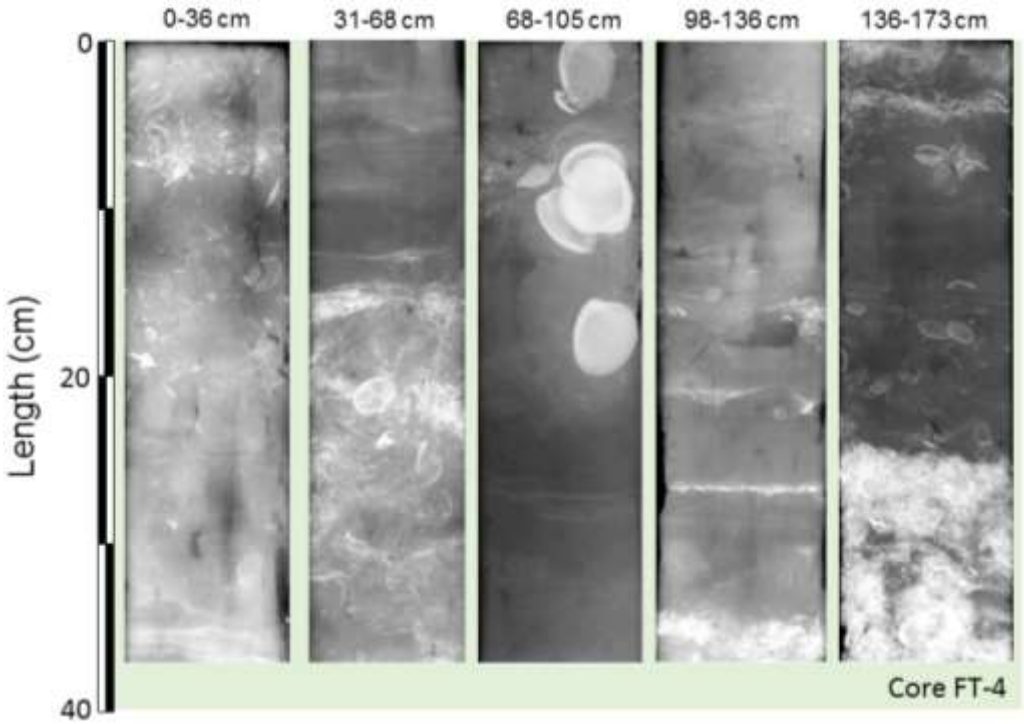

Figure 3-7: Core FT-4 (subtidal) X-radiographs. (0–173 cm). These images have been inverted so that relatively high-density objects appear white (e.g., shell valves) and low-density materials such as muds or organic material appear as darker areas (format: 8bit tiff, export: 256 greyscale, scale 400%, png).

Dry-bulk sediment densities in core FT-4 show no clear trend with depth, varying from 0.4 to 0.6 g cm^{-3}) to 100 cm depth (maximum sample depth) (Figure 3-8b). Particle size and composition of the sediment matrix is also relatively uniform with depth, consisting of clay-rich muds (up to 20% by particle volume) with mean particle diameters varying from 6 to 20 microns (Figure 3-8c–d). The low-density, clay-rich muds in the top-most ~60 cm of the core coincide with the maximum depth of $^{210}Pb_{ex}$ and relatively rapid SAR (6.7 mm yr^{-1}) since the 1920s (Figure 3-8a).

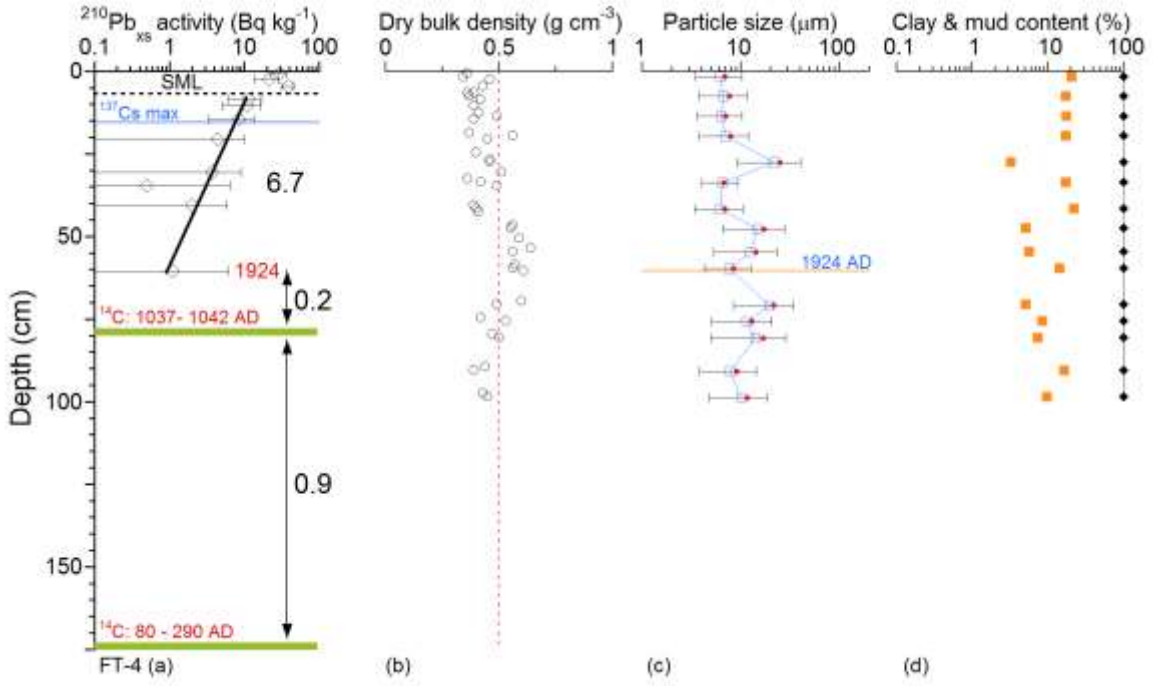

Figure 3-8: Core FT-4 (Subtidal) - ages of sediment layers and sediment accumulation rates (SAR), and sediment properties. (a) Excess ^{210}Pb activity profiles with 95% confidence intervals shown. Time-averaged SAR (Black text) derived from regression fit to natural log-transformed ^{210}Pb data and ^{14}C ages of bivalve shells. Estimated ages of depth horizons (red text). Surface mixed layer (SML) inferred from excess ^{210}Pb profiles. Maximum depth of caesium-137 (^{137}Cs) indicated. Radioisotope activity expressed in units of Becquerels (Bq). (b) Sediment dry bulk density; (c) mean (red) and median particle diameters with standard deviation; (d) clay and mud content as percentage of sample by particle volume.

Additional radiocarbon dating of cockle-shell valves from two animals sampled at 76–80 cm depth in core FT-4 indicates that sedimentation rates during the period ~1040–1920 AD (~0.2 mm yr^{-1}) were lower than during the prior 1000 years (~1 mm yr^{-1}). This latter ~900 year time period coincides with the transition from undisturbed catchments to the arrival of Māori and European settlers and subsequent deforestation and conversion to pastoral agriculture.

3.4 Historical changes in sources of sediments accumulating in the Firth of Thames system

3.4.1 Contribution of catchment and estuarine sources to long-term sedimentation

The results of the MixSIAR modelling allow us to reconstruct how the major sources of sediment have contributed to the sedimentation of the southern Firth and how these contributions have changed over the last ~1,200 years. Summary statistics (i.e., mean, median, σ) of the soil proportion probability distribution for each dated sediment core sample are presented in

Table 3-7 to

Table 3-9. Figure 3-9 to present the time series of mean sediment proportion data by source. We distinguish catchment sediments, which have isotopic signatures characteristic of native forest and pine, native forest, pasture, bracken or subsoil sources, from estuarine sediments, as described in section 2.6.3. These estuarine sediments have characteristically enriched $\delta^{13}C$ FA signatures (Figure 2-9 to Figure 2-14).

In interpreting these plots, it should be noted that subsoil sources encompass all land uses and represents erosion of material from the B horizon below the carbon-rich topsoil layer (A horizon), which contain most of the FA biomarkers. These subsoils are likely to be mobilised by deep-seated erosion or slope failure during intense rainfall events and derived from road cuttings or erosion of stream banks. The sources reported by land use relate only to the eroded top soils that are defined by the plant community growing on it and labelling these soils with a suite of FA biomarkers with characteristic of $\delta^{13}C$ signatures. In addition, the time-period represented by each 10-mm thick section within the cores varies between samples with differences in sediment accumulation rate. For example in core FT-1, SARs have averaged 10 mm yr^{-1} since the mid-1970s, whereas SARs were ten times lower prior to the 1870s (0.7 mm yr^{-1}). Furthermore, mixing of sediments in the surface layer to several centimetres depth by wave resuspension and/or bioturbation will blend the initial source signatures so that they will represent varying windows of time dependent on SAR (i.e., averages over several years for high SAR or decades for low SAR). This is generally acceptable given that the focus of the present study relates to changes in sources since the mid-1800s when land use rapidly changed resulting in increased catchment soil erosion and consequent higher SAR in the Firth (Section 1.2.1). Finally, the up to ten-fold increases in SAR following large-scale catchment deforestation from the mid-1800s should also be borne in mind when interpreting these plots of source contributions.

To begin, Figure 3-9 summarises how the proportion of sediments derived from the Firth of Thames catchment has changed over time. Prior to the arrival of Māori in the early 1300s, catchment sediments (i.e., native forest, bracken or subsoil) accounted on average for 70–90% of the sediment accumulating in the southern Firth. The remaining 10–30% of sediments having a distinctive isotopically enriched $\delta^{13}C$ FA signature characteristic of estuarine sediments. These estuarine sediments are comprised of ancient fluvial sediments mixed with organic sediments derived from in situ marine primary production (section 4.3). The proportion of catchment sediments has gradually reduced to 50–60% of the net sedimentation, particularly since the mid-1970s. This apparent reduction in the contribution of eroded soil and subsoils to deposition in the southern Firth is due to increasing contributions from estuarine sources. This apparent reduction in catchment contributions is most pronounced in sediments deposited on the mid–upper intertidal flats (i.e., sites FT-1 and FT-2) since the mid-2000s. Despite core FT-4 being located ~18 km north of FT-1 and FT-2, the cores display similar patterns of long-term change in catchment sediment source proportions.

In interpreting these results it is important to bear in mind that time-averaged sediment accumulation rates since the late-1800s/early-1900s have increased by as much as ten-fold in comparison to the previous ~1,200 years. Consequently, the absolute mass deposition in the southern Firth associated with the various sediment sources has also increased even if their percentage contributions have not changed over time.

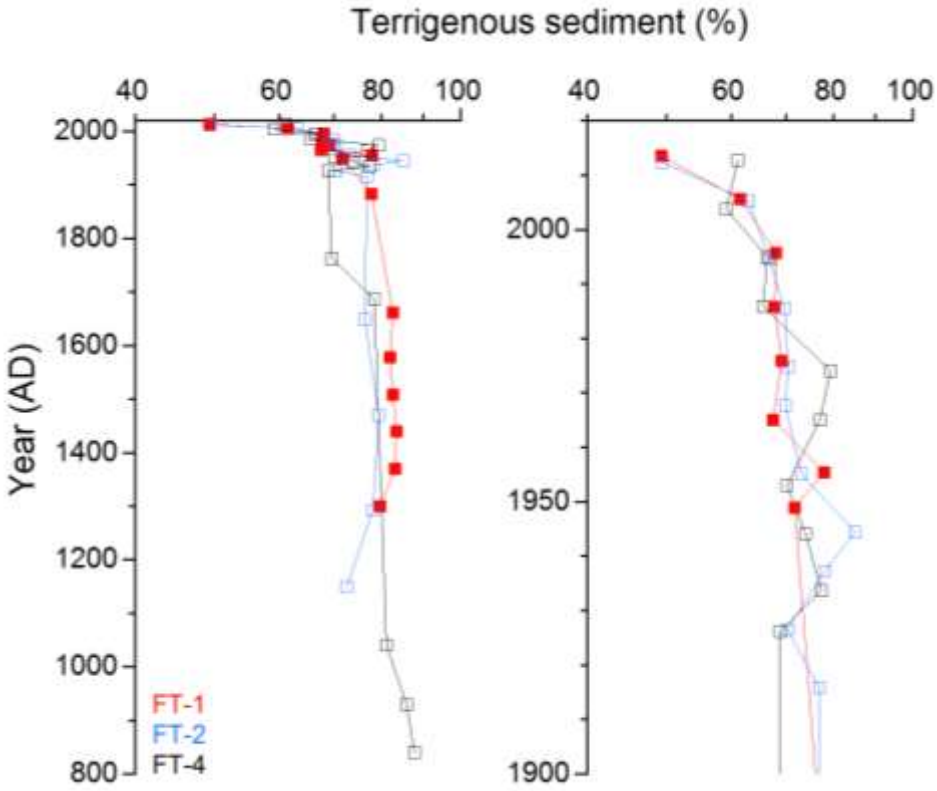

Figure 3-9: Firth of Thames cores: temporal changes in proportion of sediment derived from catchment sources (840-2015 AD). Sum of terrigenous sources: native forest, combined native and pine, pasture, bracken and subsoils. Note: log scale.

Figure 3-10 to summarise the temporal patterns of changing sediment proportions of both catchment and estuarine sources in each of the sediment cores. These results are presented in two ways: (1) summary stack plots of contributions of major sediment sources to sedimentation in each of the analysed core samples; (2) temporal changes in the sources of sediment accumulating at each core site over the last 700 to 1175 years.

In this section, source contributions (%) are reported as either time-specific averages as presented in the stack plots and associated summary statistic tables or as long term weighted-average values (

Table 3-6). These weighted-average % source contributions are calculated based on the time period between successive pairs of dated samples in each of the sediment cores and the total length of record representing the particular historical time period. The length of these time periods in each core are given by the ^{210}Pb and ^{14}C dating.

Table 3-6: Firth of Thames - fluvial sediment source contributions as time-weighted averages. Values are % soil proportions weighted by the time period between dated samples and summed for each historical time period. The estuarine source component (%) = 100-Sum. Note: based on the ages of dated sediment samples, the pre-European period includes all samples deposited before 1800 AD.

Time period	Core	Native + Pine (Euro) Native (pre-Euro)	Bracken (%)	Pasture (%)	Subsoil (%)	Sum (%)
European	FT-1	5.9	5.2	4.3	55.8	71
	FT-2	3.6	15.3	6.2	42.7	68
	FT-4	3.4	5.2	6.4	55.7	71
Pre-European	FT-1	3.2	7.1		70.7	81
	FT-2	5.3	7.3		63.7	76
	FT-4	3.3	6.0		69.0	78
Post-1300 AD	FT-1	3.7	6.7		68	78
Post-1150 AD	FT-2	5.2	8.2		61	74
Post-840 AD	FT-4	3.3	5.9		68	77

Eroded subsoils have dominated sedimentation at site FT-1 (mid-intertidal) since the 1300s, although Figure 3-10 and Figure 3-11 clearly show a gradual decline in this contribution over time (from 75 to 50%) primarily due to the increase in the proportion of estuarine sediments and, until the 1970s, eroded catchments topsoils. The contribution of bracken-labelled soils peaked in the late-1500s and again in the mid-1970s (~10%). Figure 3-10 also shows that topsoil contributions from all sources peaked in the mid-1970s at 30% of the total mass deposition at site FT-1. Contributions from pasture sources at this time accounted for less than 5% of the total mass deposition, and less than the peak contribution from pasture of ~8% that occurred in the mid-1950s. Native and pine forest soils have typically contributed less than 5% of the total sediment deposition at the cores sites, although at site FT-1 forest soil contributions peaked at ~15% during the mid-1970s.

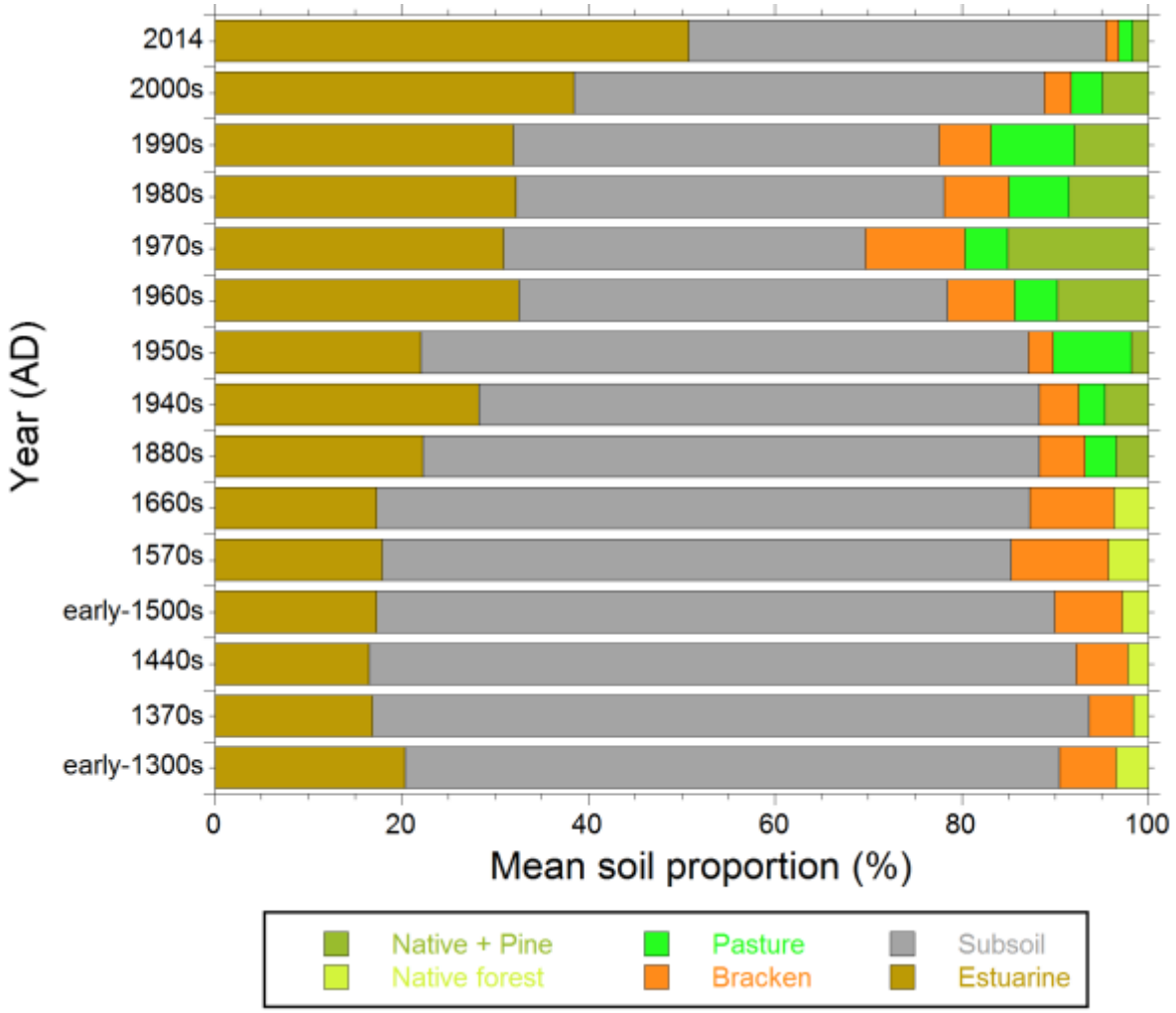

Figure 3-10: Core FT-1: summary stack plot of temporal changes in the contributions of major sediment sources to estuarine sedimentation (1300–2013 AD). Data are mean soil proportions calculated from isotopic source proportions determined using the MiXSIAR model. Notes: (1) Year of estimated sediment deposition indicated to the nearest decade, with exception of surface sample; (2) time scale on the y-axis is not linear.

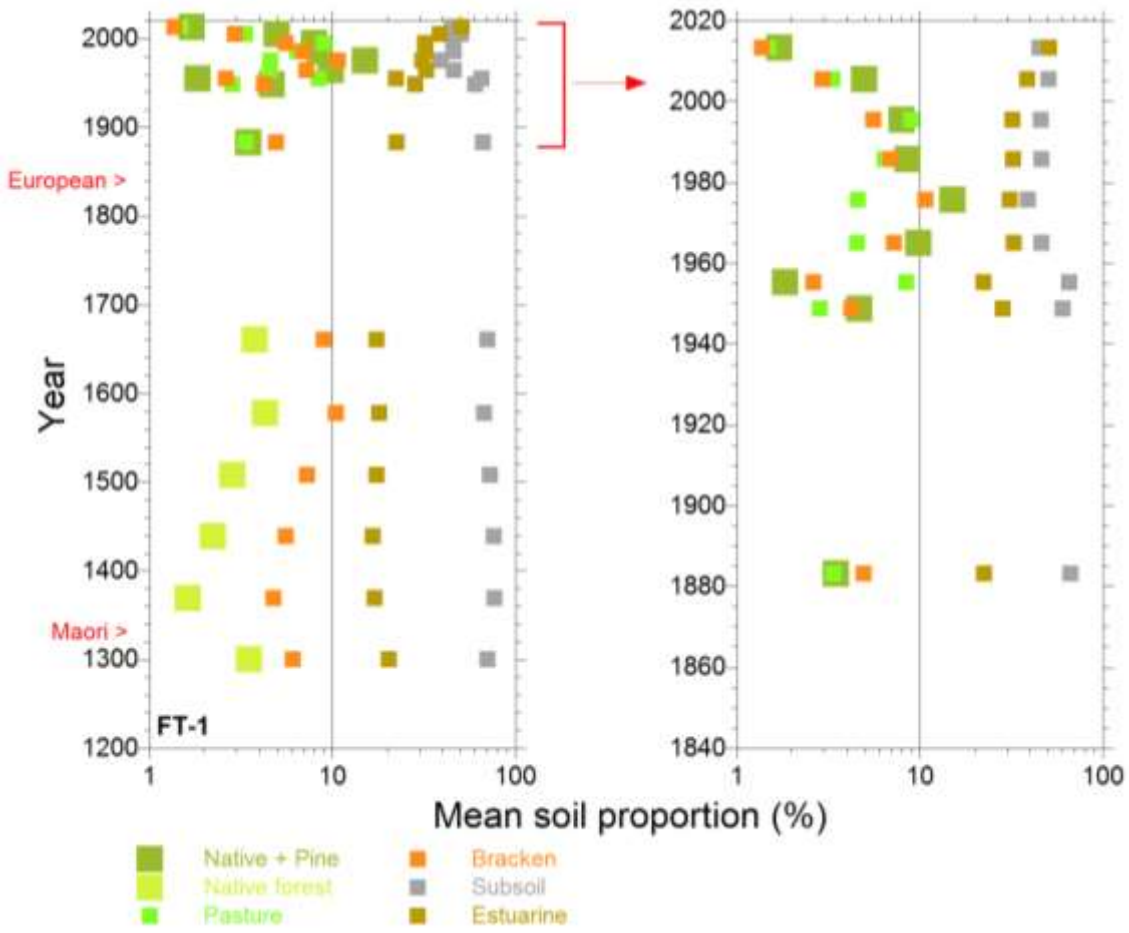

Figure 3-11: Core FT-1: temporal changes in mean soil proportions of major sediment sources to estuarine sedimentation (1300–2013 AD). Timing of Māori and European settlement indicated. Note: (1) right-hand plot provides more detail of the post-European time period; (2) log scale for mean soil proportions.

Table 3-7: Core FT-1: summary statistics of soil proportions (%) by source. Mean, median (standard deviation). Note: Data shown to nearest integer for mean values ≥ 10.

Depth (cm)	Year (AD)	Native+Pine Native	Bracken	Pasture	Subsoil	Estuarine
1–2	2014	**1.7**, 0.7 (2.6)	**1.4**, 0.9 (1.4)	**1.5**, 1.0 (1.6)	**45**, 47 (22)	**51**, 49 (25)
9–10	2000s	**4.9**, 3.6 (5.2)	**2.9**, 1.9 (3.2)	**3.3**, 1.8 (4.4)	**50**, 53 (28)	**38**, 35 (28)
19–20	1990s	**7.9**, 6.2 (7.7)	**5.5**, 3.7 (5.7)	**9.0**, 4.7 (10.6)	**46**, 44 (28)	**32**, 28 (28)
29–30	1980s	**8.5**, 7.1 (7.1)	**6.9**, 5.1 (6.4)	**6.4**, 3.4 (8.0)	**46**, 46 (27)	**32**, 29 (28)
39–40	1970s	**15.1**, 13.0 (9.4)	**10.7**, 7.4 (10.2)	**4.6**, 2.7 (5.5)	**39**, 37 (24)	**31**, 28 (24)
59–60	1960s	**9.8**, 8.0 (9.4)	**7.2**, 4.9 (6.9)	**4.5**, 2.4 (5.9)	**46**, 44 (29)	**33**, 28 (29)
77–78	1950s	**1.8**, 0.5 (3.6)	**2.6**, 1.7 (3.2)	**8.4**, 5.6 (8.9)	**65**, 73 (25)	**22**, 16 (28)
89–90	1940s	**4.7**, 1.1 (7.0)	**4.2**, 2.6 (4.9)	**2.8**, 1.4 (4.3)	**60**, 70 (29)	**28**, 20 (28)
108–109	1880s	**3.5**, 0.7 (6.5)	**4.9**, 3.1 (5.5)	**3.3**, 1.9 (5.0)	**66**, 77 (28)	**22**, 14 (27)
124–125	1660s	**3.7**, 1.3 (5.6)	**9.0**, 6.1 (9.4)		**67**, 79 (25)	**17**, 11 (25)
130–131	1570s	**4.3**, 2.0 (5.9)	**10.4**, 7.0 (10.6)		**67**, 77 (27)	**17**, 11 (27)
135–136	Early-1500s	**2.8**, 0.9 (4.5)	**7.2**, 5.1 (7.6)		**73**, 81 (23)	**17**, 12 (27)
140–141	1440s	**2.2**, 0.6 (3.8)	**5.6**, 3.8 (6.2)		**6**, 84 (22)	**17**, 11 (18)
145–146	1370s	**1.6**, 0.6 (3.0)	**4.7**, 3.6 (4.8)		**77**, 82 (19)	**17**, 13 (18)
150–151	Early-1300s	**3.5**, 1.4 (5.4)	**6.1**, 3.8 (7.3)		**70**, 79 (25)	**20**, 14 (25)

The sedimentation history preserved in core FT-2 (lower intertidal), like that at FT-1, shows a progressive increase (from 20 to 50%) in the contribution of estuarine sediments since the 1950s (Figure 3-12 and Figure 3-13). Likewise, subsoils dominate sedimentation at this site, averaging 60% of the mass deposition since the mid-1100s (

Table 3-6). Total contributions of eroded catchment topsoils during the pre-human and Māori period were relatively small (< 17%) by comparison to the last century. Figure 3-12 indicates that mass deposition at site FT-2 associated with eroded topsoils rapidly increased from 9% in the early-1900s and peaked at 65% in the 1940s. Most of this sediment was derived from bracken-labelled soils, indicative of erosion of catchment areas that had been disturbed by land clearance. Notably, the individual and total contributions of bracken, pasture and native and pine forest topsoil sources to sedimentation at FT-2 from the mid-1940s to mid-1990s (i.e., 22–26%) did not substantially change. The apparent contribution of catchment topsoils sources to mass deposition at site FT-2 has declined since the mid-1990s.

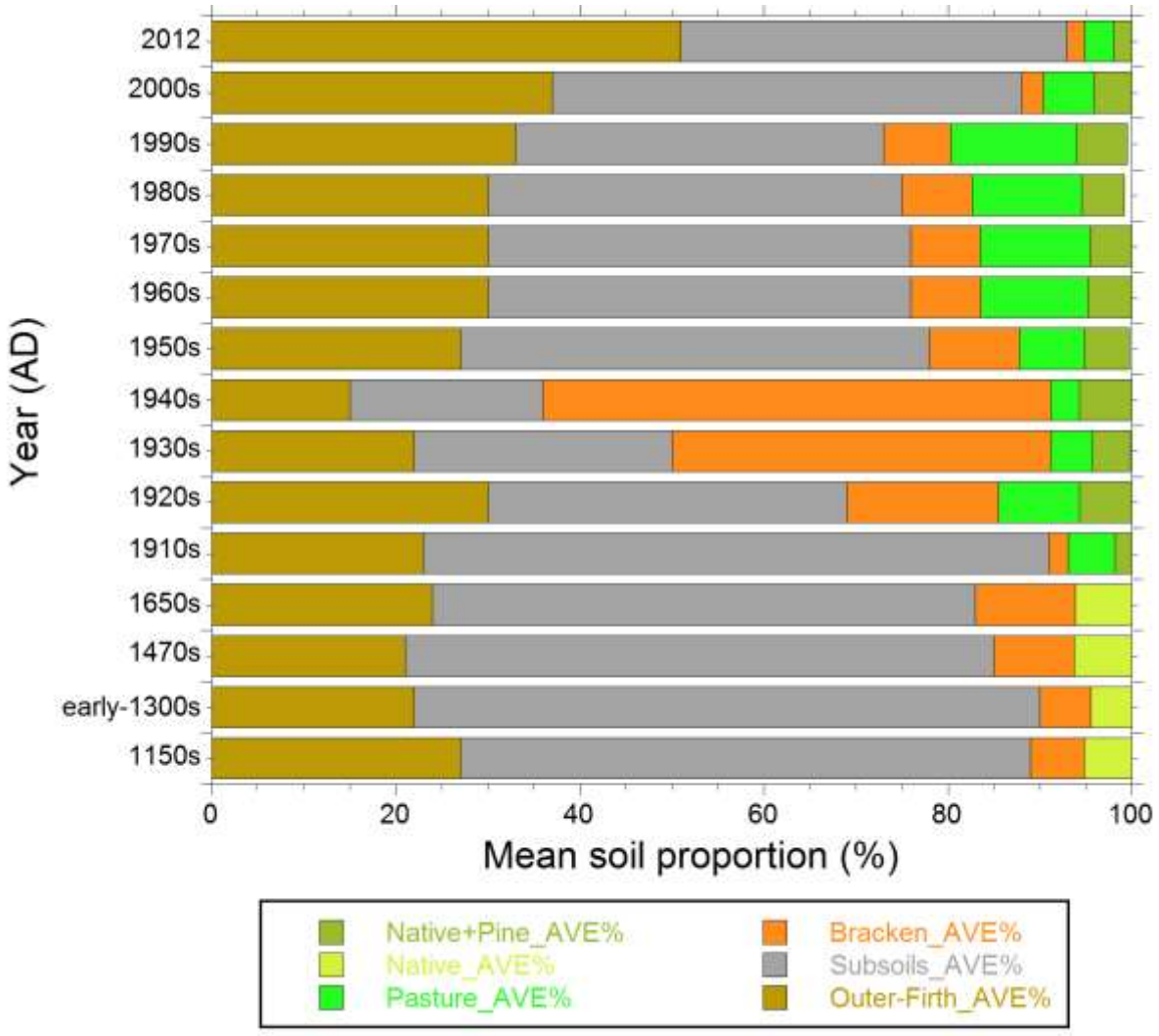

Figure 3-12: Core FT-2: summary stack plot of temporal changes in the contributions of major sediment sources to estuarine sedimentation (1150–2012 AD). Data are mean soil proportions calculated from isotopic source proportions determined using the MiXSIAR model. Notes: (1) Year of estimated sediment deposition indicated to the nearest decade, with exception of surface sample; (2) time scale on the y-axis is not linear.

Core FT-4 is more distant from the Waihou and Piako River outlets than cores FT-1 and FT-2, being located in the subtidal basin north of Thames. Despite this geographical separation, reconstruction of long-term source contributions to sedimentation at this site, show that eroded subsoils have also

dominated sedimentation at FT-4 since the mid-800s AD, averaging 68% of the mass deposition (Figure 3-14 and

Table 3-6). Estuarine sources show a general trend of increasing contributions over the last ~1,200 years (from ~15% to 40%). As observed at the other two core sites, total contributions of eroded catchment topsoils during the pre-human and Māori periods were relatively small (< 10%) by comparison to the last century. The contribution of topsoils to deposition since the mid-1920s increased to 15%, and peaking in the mid-1920s and again in the mid-1950s (~30%). Pasture and native + pine forest accounted for only ~6% and ~3% on average of the total mass deposition at site FT-4 since the mid-1920s (

Table 3-6).

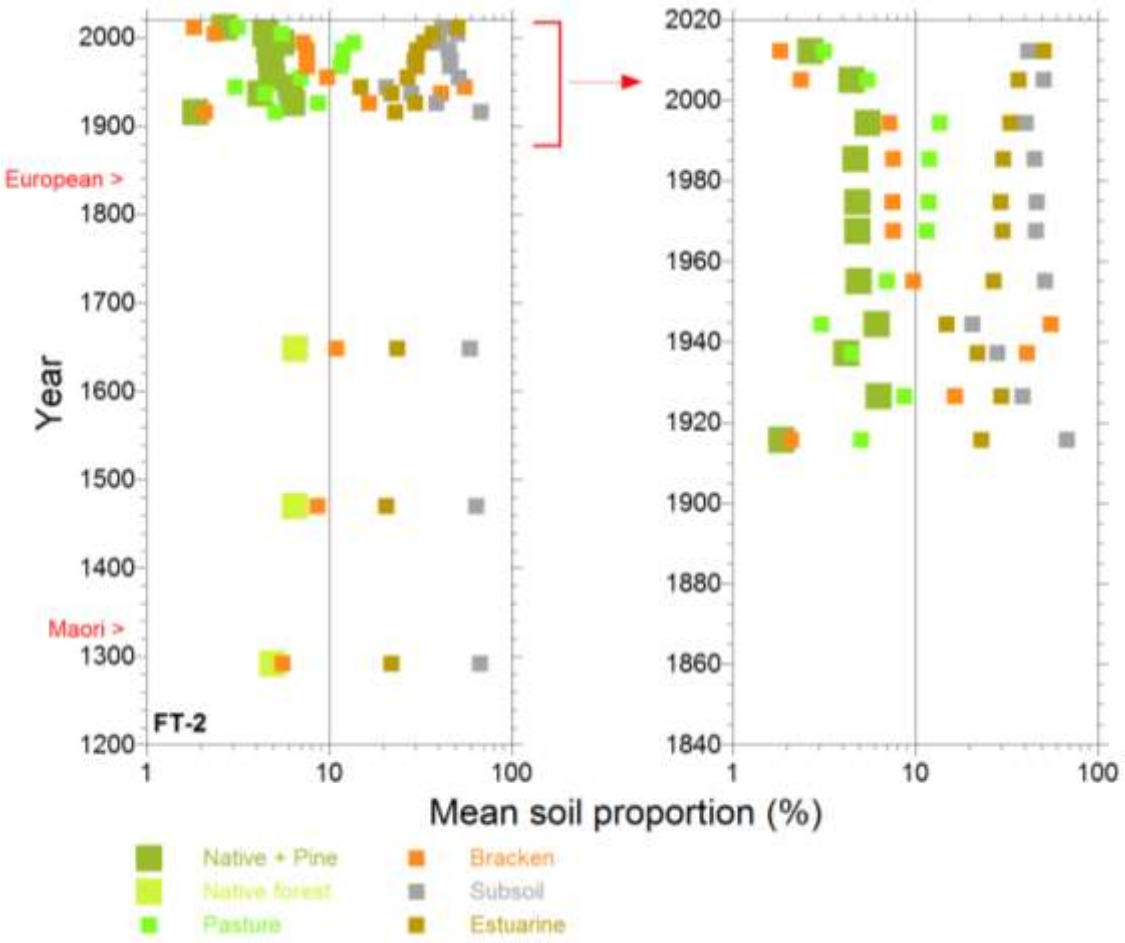

Figure 3-13: Core FT-2: temporal changes in mean soil proportions of major sediment sources to estuarine sedimentation (1300–2012 AD). Timing of Māori and European settlement indicated. Note: (1) right-hand plot provides more detail of the post-European time period; (2) log scale for mean soil proportions.

Table 3-8: Core FT-2: summary statistics of soil proportions (%) by source. Mean, median (standard deviation). Note: Data shown to nearest integer for mean values ≥ 10.

Depth (cm)	Year (AD)	Native+Pine Native	Bracken	Pasture	Subsoil	Estuarine
1–2	2012	**2.7**, 1.6 (3.5)	**1.8**, 1.2 (2)	**3.2**, 2 (3.4)	**42**, 42 (26)	**51**, 51 (23)
5–6	2000s	**4.5**, 2.1 (6.0)	**2.4**, 1.4 (3)	**5.5**, 3.1 (6.4)	**51**, 53 (29)	**37**, 33 (25)
11–12	1990s	**5.5**, 3.8 (5.7)	**7.3**, 5.6 (6.2)	**13.7**, 11.2 (12.2)	**40**, 38 (25)	**33**, 31 (21)
16–17	1980s	**4.7**, 3.2 (5.0)	**7.6**, 6.2 (6.2)	**11.9**, 8.6 (11.4)	**45**, 46 (26)	**30**, 27 (21)
22–23	1970s	**4.8**, 3.3 (5.3)	**7.5**, 6.1 (6.2)	**11.9**, 8.7 (11.4)	**46**, 47 (26)	**30**, 26 (21)
26–27	1960s	**4.8**, 3.2 (5.4)	**7.6**, 6.0 (6.5)	**11.6**, 8.7 (11)	**46**, 47 (26)	**30**, 26 (21)
33–34	1950s	**4.9**, 2.1 (6.5)	**9.8**, 8.6 (7.6)	**7**, 3.6 (9.4)	**51**, 54 (28)	**27**, 21 (22)
39–40	1940s	**6.2**, 3.2 (7.8)	**55.2**, 57.1 (20)	**3.1**, 1.9 (3.6)	**21**, 17 (17)	**15**, 12 (12)
43–44	1930s	**4.2**, 2.5 (5.0)	**41.2**, 40.7 (14.5)	**4.5**, 2.9 (5.1)	**28**, 25 (19)	**22**, 20 (15)
49–50	1920s	**6.3**, 4.6 (6.2)	**16.5**, 16 (10)	**8.8**, 4.9 (10)	**39**, 37 (24)	**30**, 27 (20)
55–56	1910s	**1.8**, 0.5 (3.6)	**2.1**, 1.3 (2.6)	**5.1**, 3.0 (6)	**68**, 75 (24)	**23**, 18 (19)
70–71	1650s	**6.5**, 5.0 (6.8)	**10.9**, 7.6 (10.8)		**59**, 64 (28)	**24**, 17 (21)
80–81	1470s	**6.5**, 4.5 (7.7)	**8.7**, 4.5 (10.6)		**64**, 73 (29)	**21**, 13 (20)
90–91	Early-1300s	**4.9**, 2.7 (6.4)	**5.6**, 2.7 (7.6)		**68**, 78 (27)	**22**, 14 (21)
98–99	1150s	**5.3**, 3.6 (6.4)	**5.8**, 3.5 (6.8)		**62**, 69 (29)	**27**, 20 (24)

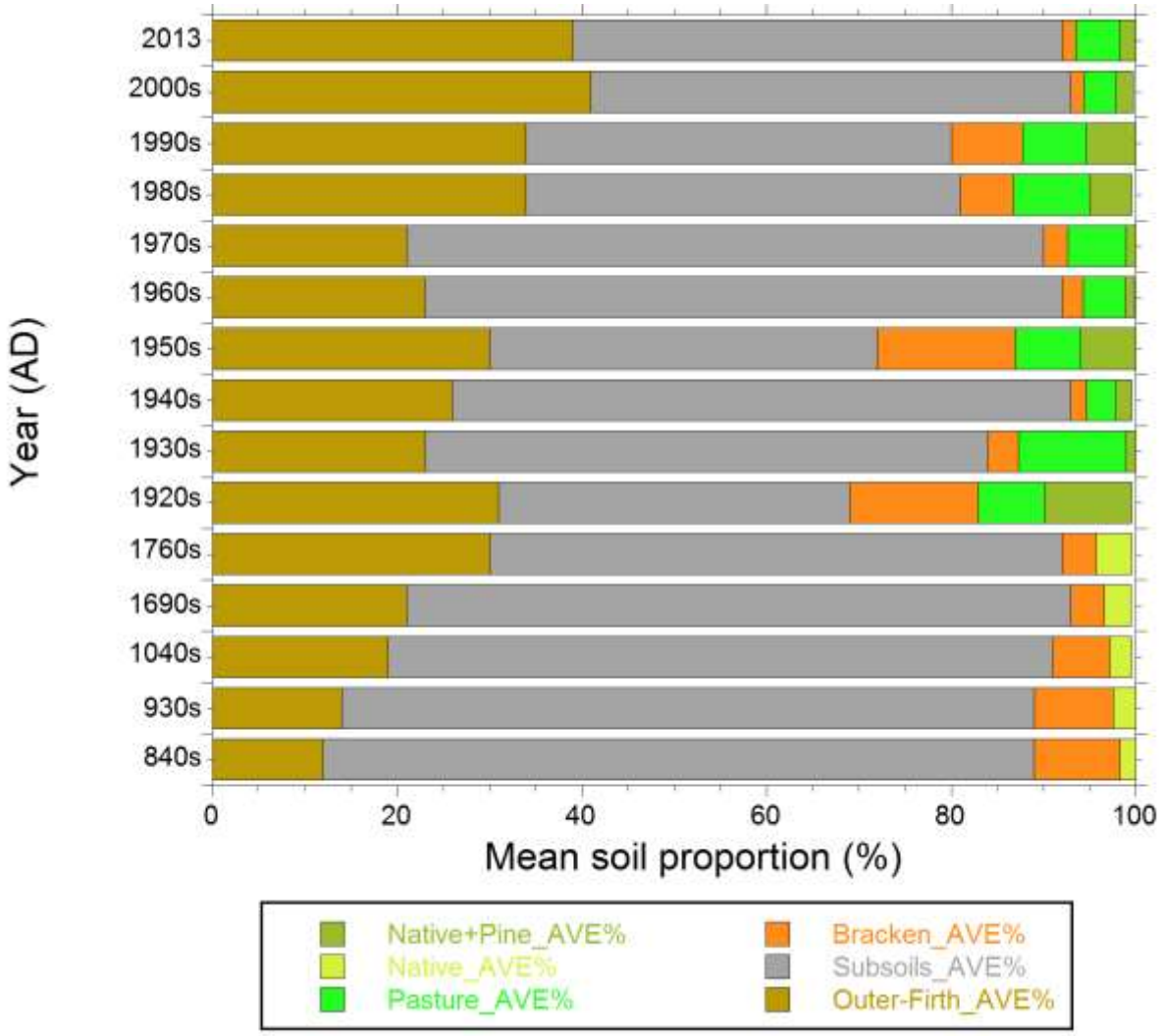

Figure 3-14: Core FT-4: summary stack plot of temporal changes in the contributions of major sediment sources to estuarine sedimentation (840–2013 AD). Data are mean soil proportions calculated from isotopic source proportions determined using the MiXSIAR model. Notes: (1) Year of estimated sediment deposition indicated to the nearest decade, with exception of surface sample; (2) time scale on the y-axis is not linear.

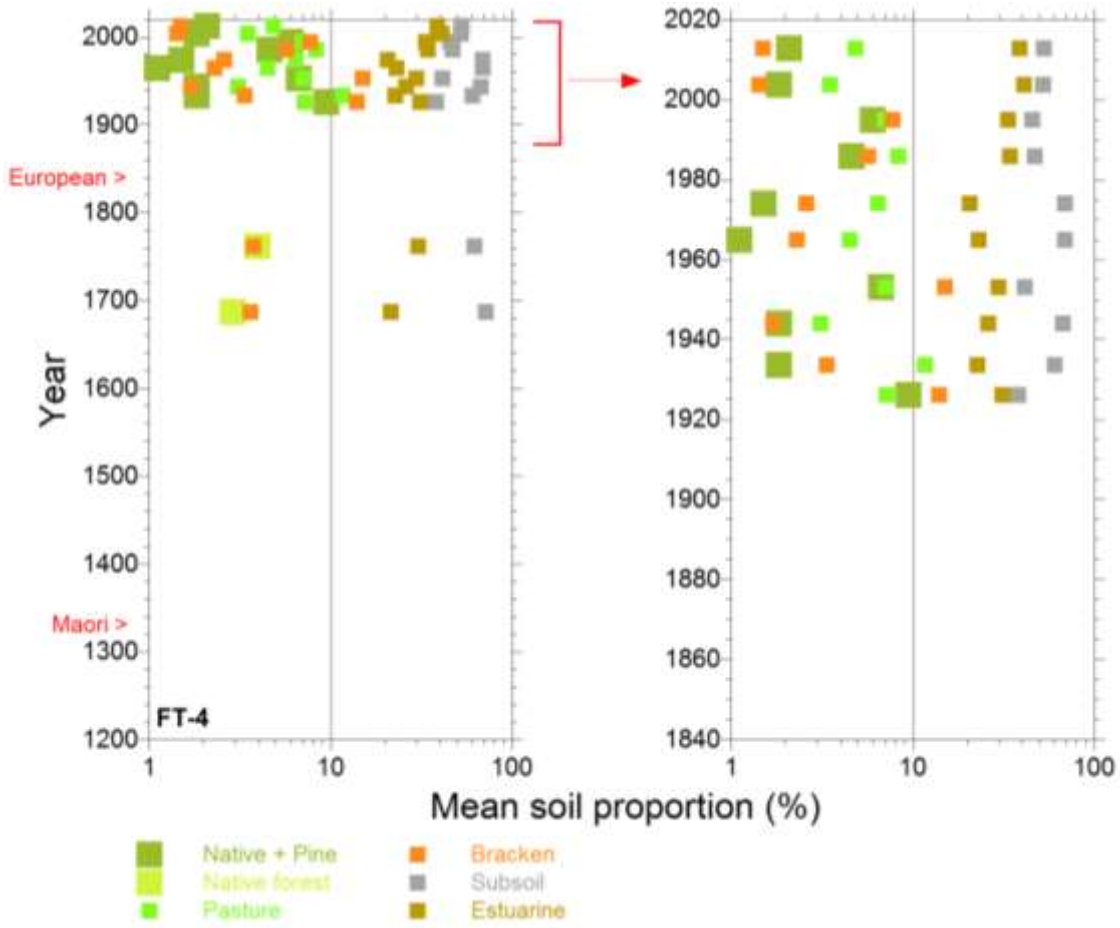

Figure 3-15: Core FT-4: temporal changes in mean soil proportions of major sediment sources to estuarine sedimentation (840–2013 AD). Timing of Māori and European settlement indicated. Note: (1) right-hand plot provides more detail of the post-European time period; (2) log scale for mean soil proportions.

Table 3-9: Core FT-4: summary statistics of soil proportions (%) by source. Mean, median (standard deviation). Note: Data shown to nearest integer for mean values ≥ 10.

Depth (cm)	Year (AD)	Native+Pine Native	Bracken	Pasture	Subsoil	Estuarine
1–2	2013	**2.1**, 0.5 (4)	**1.5**, 0.9 (2)	**4.8**, 3.3 (4.7)	**53**, 58 (28)	**39**, 35 (24)
7–8	2000s	**1.8**, 0.5 (3.3)	**1.4**, 1 (1.6)	**3.5**, 2.2 (3.7)	**52**, 57 (26)	**41**, 37 (23)
13–14	1990s	**6.0**, 4.8 (5.4)	**7.7**, 6.2 (6.4)	**7**, 4.2 (7.9)	**46**, 45 (26)	**34**, 31 (22)
19–20	1980s	**4.6**, 3.3 (4.8)	**5.7**, 4.4 (4.9)	**8.3**, 5.7 (8.4)	**47**, 48 (27)	**34**, 32 (22)
27–28	1970s	**1.5**, 0.5 (2.9)	**2.6**, 1.9 (2.7)	**6.4**, 4.2 (6.9)	**69**, 76 (23)	**21**, 16 (17)
33–34	1960s	**1.1**, 0.4 (2.3)	**2.3**, 1.7 (2.2)	**4.5**, 3.1 (4.8)	**69**, 75 (22)	**23**, 18 (18)
41–42	1950s	**6.7**, 5.3 (5.9)	**15**, 14.2 (9.7)	**7**, 4.1 (8.1)	**42**, 41 (25)	**30**, 27 (20)
47–48	1940s	**1.8**, 0.5 (3.5)	**1.7**, 1.1 (2.2)	**3.1**, 1.9 (3.8)	**67**, 73 (23)	**26**, 22 (19)
54–55	1930s	**1.8**, 0.6 (3.4)	**3.3**, 2.4 (3.4)	**11.7**, 8.7 (10.9)	**61**, 68 (26)	**23**, 18 (19)
59–60	1920s	**9.5**, 7.9 (8.9)	**13.9**, 12.7 (10.5)	**7.2**, 3.8 (9.2)	**38**, 36 (25)	**31**, 28 (21)
70–71	1760s	**3.9**, 2.3 (5.5)	**3.7**, 2.1 (5)		**62**, 70 (28)	**30**, 23 (25)
75–76	1690s	**2.9**, 0.9 (4.6)	**3.6**, 2 (4.9)		**72**, 80 (24)	**21**, 15 (20)
80–81	1040s	**2.4**, 0.8 (4.1)	**6.2**, 4.5 (6.2)		**72**, 80 (23)	**19**, 13 (18)
90–91	930s	**2.8**, 0.5 (4.9)	**8.6**, 5.6 (9.8)		**75**, 84 (24)	**14**, 8 (16)
98–99	840s	**1.7**, 0.4 (3.6)	**9.3**, 7.2 (8.5)		**77**, 84 (20)	**12**,8 (13)

These sediment source data can be re-scaled to quantify the overall contributions of the catchment sources (i.e., estuarine source excluded) and these re-scaled data are presented in Figure 4-2.

This analysis indicates that subsoils accounted for 84–88% of the fluvial sediments deposited in the southern Firth on average prior to European settlement. The next largest contributions of fluvial sediments, from bracken soils and native forest, accounted for 8–10% and less than 8% of the mass deposition respectively in the southern Firth. The contribution of subsoils to fluvial sediment deposition in the southern Firth over the last century has been lower (63–79%), primarily due to increasing contributions from eroded topsoils (21–37%). Soils eroded from native and pine forests and pasture have accounted for 5–8% and 6–9% respectively of this fluvial sediment mass deposition in the southern Firth over the last century. The contribution of bracken soils to the fluvial sediment mass deposition has averaged 7% at sites FT-1 and FT-4 and 23% at site FT-2 (derived from

Table 3-6). Again, in interpreting these results it is important to bear in mind that although the percentage contributions from forests and pasture are relatively small, the actual mass deposition associated with these and other sources over the last century has been as much as ten-fold higher than the previous ~1,200 years due to increases in sediment accumulation rates.

4 Discussion

4.1 Contemporary sources of eroded soils in the Waihou and Piako Rivers

The CSSI analysis and modelling of sediment sources at each of the major river confluences in the Waihou and Piako catchments enables the contributions of the main stem and main tributary sub-catchments to be estimated. As explained in section 2.6.3, some differentiation of sources using FA tracers are possible at the sub-catchment scale that are not possible at catchment scale. For example, native broadleaf forest and pine forest can be differentiated from each other in the upper Waihou catchment but not for the Waihou or Piako systems further downstream.

In the Waihou system, the Waiomou, Ohinemuri and Hikutaia tributaries made relatively small contributions (i.e., <16%) to the fluvial sediment deposited downstream of these major confluences (Figure 2-3, Table 3-1). In the upper catchment, at the Waihou-Waiomou confluence, these fluvial sediment deposits are mainly composed of eroded river bank material (75–80%, Table 3-2). In turn, CSSI analysis of the river bank material at this confluence indicates that 80–90% of this "bank erosion" source is composed of soil eroded from pine forest (Table 3-3). By contrast, at the Ohinemuri confluence, upstream deposits are composed of soils eroded from native broadleaf (75%) and sheep and beef (25%).

In the Piako system, two-thirds of the fluvial sediments downstream of the Piako–Waitoa confluence originate from the Waitoa River catchment (Table 3-1). Deconstruction of these sediments indicate that a large fraction of the Piako sediments are derived from bank erosion (~68%) and pine forest soils (27%), whereas 85% of the Waitoa sediments are dominated by eroded subsoils (85%). Soils eroded from dairying account for 75% of the Piako River "bank erosion" source.

On the river deltas at the catchment outlets, the two-endmember mixture modelling shows that ~70% of contemporary sediments accumulating on the Waihou delta are composed of fluvial sediments, with isotopically-enriched estuarine sediments accounting for the remainder. By contrast, estuarine sediments account for 80% of contemporary sediments accumulating on the Piako River delta (Table 3-1). These observed differences in fluvial sediment contributions are consistent with the relative differences in catchment size and discharges of the Waihou and Piako Rivers (Table 1-1). These results also suggest that the Waihou is the main contemporary source of eroded soils discharged to the Firth of Thames.

The number of feasible solutions and standard deviations about the mean soil proportions provide measures of uncertainty for the two-endmember and IsoSource mixing models' estimates. With only two-endmembers, the number of feasible solutions and standard deviations about the mean contributions for the tributary and main stem contributions are small. Assuming these fluvial sediment deposits were well mixed during transport then the proportions estimated from the main stem and tributaries should be accurate. Uncertainty increases with the number of potential sources (e.g., when land use is included). The number of feasible sources determined by the IsoSource modelling varies from one (i.e., unique solution) to several hundred, although in most cases standard deviations are less than 5% of the mean soil proportion. Importantly, reported uncertainty is likely to

be under-estimated for these river confluence samples given the minimal/lack of replication limits our ability to accurately describe the actual variation in the sources of fluvial sediment by land use.

4.2 Changes in sediment accumulation rates

Reconstruction of the sedimentation history of the southern Firth of Thames over the last 800 to 1,700 years indicates that SAR averaged less than 1.3 mm yr^{-1} before the arrival of people (i.e., pre-1300 AD, section 3.3). Radiocarbon dating of shell values from (two) individual animals preserved in discrete sediment layers as well as the close agreement in their ages (i.e., within 1–2 decades) and small σ–errors relative to their ^{14}C ages provide a high degree of confidence in these results. Pre-human SARs measured in the Firth are consistent with coring studies conducted in Northland, Auckland and Waikato estuaries (Hume and McGlone, 1986; Oldman and Swales, 1999; Sheffield et al. 1995; Swales et al. 1994, 1995, 1997, 2002a, 2002b, 2005a, b, 2007, 2012, 2013).

Evidence of land clearance by Māori was not detected through increased SAR or changes in sediment physical properties in the present study. This apparent absence of evidence of Māori land use activities reflects: (1) the coarse resolution of the core sampling; and (2) low SAR so that Māori to early-European era sediments (i.e., 1300–1800s AD) are represented by sediment layers only 20 to 50-cm thick (i.e., SAR ≤ 0.69 mm yr^{-1}).

Sediment core geochronology also demonstrates that time-average ^{210}Pb SARs during the European era of 3–18 mm yr^{-1} are typically an order of magnitude higher than pre-human rates. This large increase in SAR over the last ~150 years, coinciding with large-scale catchment deforestation during the mid–late 1800s, is consistent with sediment records from other North Island estuaries. Excluding the extremely high-SAR of 18 mm yr^{-1} measured in core FT-1 over a single decade during the mid-1960s to mid-1970s, the weighted-average (estuary) ^{210}Pb SAR in the southern Firth has been 5.5 mm yr^{-1} since the 1870s–1920s (i.e., SAR weighted by associated time period. The weighted-average (estuary) SAR in the Firth as a whole (including the deBaere (2006) data from the outer Firth, Figure 1-1) is 4.3 mm yr^{-1}. Both of these ^{210}Pb SAR estimates are at the upper range of weighted-average values measured for the post-European period in a number of other North Island estuaries (range 2.3–5.5 mm yr^{-1}, Figure 4-1). The variability in the weighted-average SAR is highest in the Kaipara Harbour and Firth of Thames, which partly reflects the size of these systems and range of sedimentary environments.

The most detailed sedimentation record in the southern Firth is preserved at site FT-1, located on the mid-intertidal flats (section 3.3.3). Here, SAR averaged ~3 mm yr^{-1} from the 1870s to early 1960s then abruptly increased to ~18 mm yr^{-1} over the next decade (1963–1974), then declining to average 10 mm yr^{-1} since the mid-1970s. Similar "s-shaped" sedimentation profiles with low–high–low SAR transitions are reported by Swales et al. (2015b) for the upper intertidal flats several hundred metres south of site FT-1, where a large mangrove forest has developed since the early 1960s. The timing of this initial transition from relatively low to high SAR on the upper-intertidal flat occurred during a similar period (i.e., 1950–1965) as observed at core site FT-1 on the mid-intertidal flat. Rates of accumulation on the upper intertidal flat during the high-SAR phase (33–100 mm yr^{-1}, Swales et al. 2015) were substantially higher than at FT-1 (18 mm yr^{-1}). This shift from a low to high SAR regime on the mid–upper intertidal flats indicates a fundamental change in environmental conditions on the mudflat. Physical processes that may have enhanced net sedimentation include increased bed

friction and fluid-mud attenuation of bed-shear stresses under shoaling waves as the tidal flat vertically accreted (Swales et al. 2015).

This progressive reduction in water depth over time would have increased the effectiveness of sediment resuspension by waves (Swales et al. 2004; Green and Coco, 2007; Talke and Stacey, 2008). This most likely explains, the transition from the high to low SAR regime that occurred at site FT-1 in the mid-1970s. By contrast, the high–low transition that occurred on the upper intertidal flat (1968–1972) in the mangrove forest was the result of the negative feedback between surface elevation gain and a progressive reduction in hydro period (i.e., frequency and duration of tidal submergence) and associated sediment delivery (Swales et al. 2015b). Hence, these observed patterns of changing sediment accumulation rates over the last 50 years or so are primarily driven by local estuarine processes rather than increases in inputs of fluvial sediments.

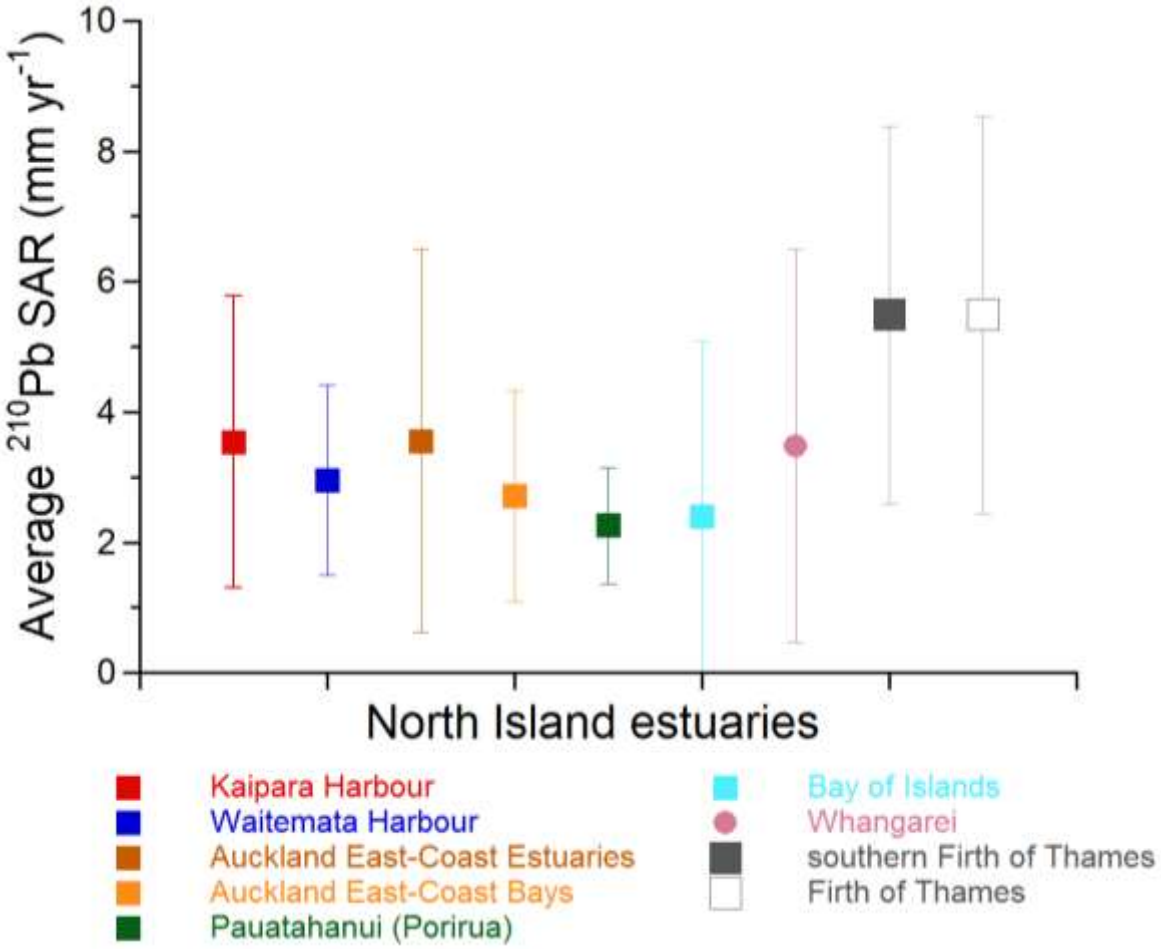

Figure 4-1: Comparison of estuary weighted-average ^{210}Pb sediment accumulation rates (SAR) in North Island estuaries (mid-1800s to present), including the Firth of Thames. Notes (1) total number of estuaries (16) and cores (99); (2) standard deviations shown; (3) southern Firth –present study and (4) including de Baere (2006) data. Source: NIWA.

In many North Island estuaries, an increase in SAR following deforestation has been accompanied by a shift from sand- to mud-dominated systems (e.g., Swales et al. 2002a, 2002b, 2012, 2013). The results of the present study indicate that mud-rich sediments have accumulated in the southern Firth for at least the last 1,700 years but mostly since the mid-1800s when SAR increased (section 3.3).

However, intertidal sand flats were present on the mid- to upper-intertidal flats before being buried by increasing onshore transport and deposition of mud that began in the 1950s (Swales et al. 2015b). These legacy fine sediments substantially composed of eroded catchment soils were largely delivered to the Firth of Thames by the early 1900s. Sediment accumulation rates of up to several cm yr^{-1} on the intertidal flats and in the fringing mangrove forest over the last several decades cannot be accounted for by contemporary fine sediment inputs from the Waihou and Piako Rivers alone (i.e., ~190,000 tonnes yr^{-1}, Hicks et al. 2011). This suggests that legacy sediments deposited in the Firth over the last 150 years in particular continue to drive rapid sedimentation in the southern Firth.

4.3 Changes in sources of eroded soils accumulating in the Firth of Thames

The CSSI analysis of the dated sediment cores indicates major changes in sediment sources, accompanying increased SAR, following the arrival of people in the 1300s (section 3.4). Pre-human sedimentation in the Firth of Thames was dominated by slow accumulation of fluvial sediment over centuries to millennia, primarily composed of subsoils (84–88%) supplied by rivers draining catchments with indigenous forest and scrub communities. Estuarine muds, with isotopically enriched signatures (i.e., FAs $\delta^{13}C$) were substantial secondary sources of sediment accumulating in the southern Firth (i.e., 15-27% of total). The isotopically enriched signatures of these estuarine muds in the Firth today suggest that these muds are composed of ancient fluvial sediments that have mixed with and have been modified by organic sediments supplied by marine primary production (e.g., phytoplankton, diatoms, sea grasses) (Dalsgaard et al. 2003, Alfaro et al. 2006). The presence of bracken-labelled sediments hundreds of years prior to human arrival suggests that frequent natural disturbance of the landscape was of feature of this system. Likely causes of forest disturbance include landslides during high-intensity rainfall events and/or fires triggered by lightning storms. Bracken-labelled sediments also occur in Bay of Islands sediments deposited hundreds of years prior to human settlement (Swales et al. 2012).

Contributions of eroded catchment topsoils substantially increased from the late 19th Century, although the precise timing of this change to greater land-use derived topsoil, along with declining but still larger subsoil contributions, is poorly constrained across the three cores, occurring between 1661 AD and 1883 AD in FT1. Regardless of the precise timing of this change, sedimentation in the Firth thereafter was composed of large amounts of subsoil and bracken soils (85–86% weighted averages), which suggest substantial coeval disturbance of the catchment indigenous forest landcover (McGlone et al. 2005). This may reflect progressive clearance by Māori of the foothills of the Coromandel and Kaimai ranges over time that were more distant from their settlements on the river banks (Phillips, 2000) but is more robust evidence of the impacts following European settlement, of markedly increased fluvial sediment loading. Figure 3-10 to Figure 3-15 and

Table 3-6 show that contributions of catchment subsoils to estuarine sedimentation declined following European settlement, although remained the largest single source of sediments accumulating at the core sites since the late-1800s/early 1900s (63–79% weighted averages).

As previously discussed, the $\delta^{13}C$ FA data collected in the present study do not enable these subsoils to be traced to a specific land use, but they are likely to be associated with processes such as slope failures during intense rainfall events and stream bank erosion and/or derived from road cuttings, unsealed roads and tracks or other major earthworks. It is also likely that a significant fraction of the subsoil that has accumulated in the southern Firth since the mid-1800s are legacy sediments associated with deforestation and gold-mining activities in the Waihou catchment. In particular, gold mining activities in the Ohinemuri sub-catchment discharged large quantities of mud to the southern Firth (section 1.2), with some 500–800 tonnes (i.e., 182,000–292,000 tonnes yr^{-1}) of tailings discharged per day to the river over a period of ~50 years (Hume and Dahm, 1992). For comparison, the contemporary suspended sediment loads delivered to the southern Firth by the Waihou and Piako Rivers of 190,000 tonnes yr^{-1} (Hicks et al. 2011). That contemporary load from the Waihou and Piako Rivers is not sufficient to account for rapid sedimentation of the intertidal flats over the last 50 years or so (Swales et al. 2015b). This suggests, that these legacy sediments have been progressively transported onshore under the influence of wind, wave and current action (Pritchard et al. 2015).

Further discrimination of subsoil sources by sub-catchment maybe possible using additional conservative tracers in a similar mixing model as applied in the present study. For example, Hume and Dahm (1992) reported elevated concentrations of metals occur in Waihou River and delta sediments as well as in estuarine sediments deposited since the mid-1800s. A number of metals (e.g., gold, silver, lead, copper, tin antimony, mercury) as well as the metalloid, arsenic, are associated with the hydrothermal ore deposits that were mined in the Coromandel ranges. However, discrimination of subsoils by land use origin is unlikely to be feasible without those land uses being restricted to subsoils of varying metal chemistry.

The relatively small contribution of pastoral top soils to sedimentation in the Firth of Thames over the last century, averaging 4–6%, is notable given the substantial areas of dairying, sheep and beef farming in the Waihou and Piako catchments. These pastoral land uses account for 73% of the combined area of the Waihou and Piako catchments. The combined contribution of native forest and pine averaged 5–8% during the same period from 20.3% of the catchment area. These top-soil sources are relatively minor compared to subsoil contributions averaging 63–79% per year. Figure 4-2 summarises and compares the weighted-average % contributions of fluvial sources, including pasture (dairy, beef and sheep), native and pine forest top soils, and subsoils to sedimentation in the southern Firth during the post-European period (i.e., 1880s onwards), based on CSSI analysis of the dated sediment cores.

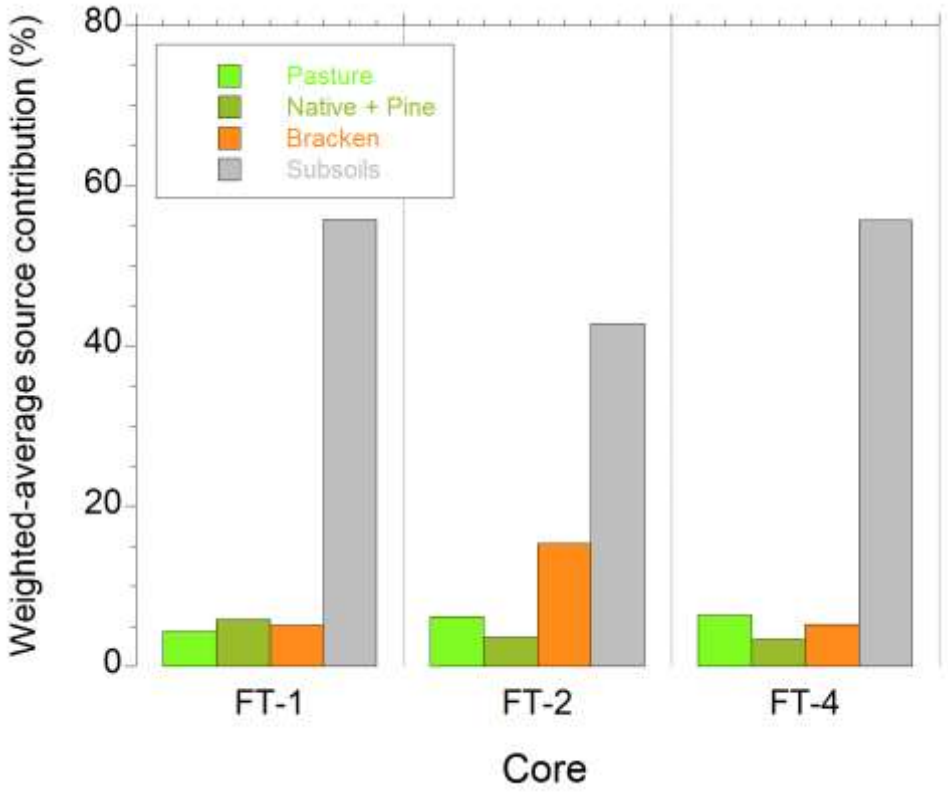

Figure 4-2: Weighted-average contributions (%) of major catchment soil sources for post-European period. Weighted-average soil source contributions for each core based on average values for individual samples in each dated cores based on length of record (time period). Refer to Tables 3-6 to 3-8 for data.

4.3.1 Comparison of contemporary sediment source contributions in fluvial and estuarine sediments

The results of the present study of the sources of sediments accumulating in the Waihou-Piako River system and the Firth of Thames indicates that:

- The largest contemporary source of sediment to both the Waihou and Piako River systems was from bank erosion (with the exception of the Waitoa and Ohinemuri Rivers). Analysis of bank erosion material from the upper reaches of the Waihou and Waiomou Rivers, which represents a major source of downstream sediment deposits, indicated that this bank sediment was mostly from pine forestry (Table 3-3). In contrast, soil eroded from dairy pasture and subsoils were the dominant sources of sediment in the banks of the Piako and Waitoa Rivers respectively.
- The largest contemporary source of river-borne sediment accumulating in the southern Firth of Thames are subsoils (including notable legacy contributions) with pastoral top soils being a secondary component. Moreover, analysis of the sediment cores collected in the Firth show that eroded subsoils have been the dominant source of fluvial sediments at least since the 1880s to early 1900s.

This apparent discontinuity between contemporary sources of sediment in the rivers and southern Firth can be explained by legacy subsoils that were originally delivered to the Firth by rivers during the period of mining and large-scale deforestation that occurred after European settlement (i.e., mid-1800s to early 1900s). These legacy subsoils have been progressively transported onshore under

the influence of wind, wave and current action and substantially account for the rapid accretion of the intertidal flats (i.e., centimetres per year) since the early 1900s.

4.3.2 Modelling of soil erosion sources - uncertainty

The present study of temporal changes in sources of eroded soils contributing to sedimentation in the Firth of Thames is the first to incorporate information about isotopic source-signature variability (i.e., $\delta^{13}C$ of FAs). Previous studies related to CSSI analysis of dated cores have employed IsoSource (Swales et al. 2012, 2015a).

Modelling of soil source contributions conducted using MixSIAR generated soil-source summary statistics with broad probability distributions and large standard deviation values (

Table 3-7 to

Table 3-9). This has resulted despite: (1) careful design of the field sampling of potential sources (section 2.2); (2) statistical analysis of the isotopic data to identify potential land use sources with measurably different signatures (Appendix D); (3) the number of sources always less than the degrees of freedom (*n*+1), where n = number of tracers, so that the model is not under-determined; (4) selection of tracers that satisfy the isotopic source polygon so that the isotopic values of mixtures are constrained within the isotopic area or hyper-volume defined by the source values (Section 2.6.2, Figure 2-9 to Figure 2-14); and (5) ensuring convergence of the MixSIAR solutions using diagnostic tests (Section 2.6.2).

Key sources of uncertainty in the modelling of soil source proportions are:

- The variability in the isotopic values of the FA tracers for each potential soil source.
- Sub-optimal isotopic arrangement of sources (i.e., source polygons) that result in "unavoidable model inadequacy" (Phillips et al. 2014). In particular, strong correlations between sources for modelled isotopic probability distributions.
- No prior information included. Informative priors can be used to guide model estimates. Highly informative priors will "sharpen" the range of distribution peaks (Moore and Semmens, 2008). The more data provided, the less influential priors become.

In the present study, the isotopic variability inherent in the catchment soil source data reflects the complexity of the environment, such as the relatively large catchment size (i.e., 1000s km^2) and the unavoidable limitations of the representativeness of sampling such a relatively large areas. The isotopic source polygons for the C14 to C18:1 FAs in particular provided reasonable separation between sources and mixtures (i.e., dated core sediments) and were generally constrained within the polygons. In some cases, strong negative correlations between sources for modelled isotopic probability distributions were also observed (e.g., subsoils and native, native and pine soils). The use of prior probabilities of source contributions to guide MixSIAR was not justified in the present study as reliable information on the timing and relative contributions of sources were not available. However, historical information and sedimentary records supported decisions about which sources to include to model a particular sediment mixture. An obvious example is that exotic plant communities, such as pasture and pine forest were only introduced from the mid-1800s onwards (section 1.2.1). Likewise, the inclusion of a bracken-fern soil source (forest disturbance indicator) in the modelling was justified by: (1) its ubiquitous occurrence, including in the study area (McGlone et al. 2005); (2) as well as the presence of bracken pollen in sediment cores analysed as part of an earlier study (Hume and Dahm, 1992).

Despite the limitations of the data and the modelling, the results are consistent with what is known about the pre-history and history of land use/ plant communities in the Waihou and Piako catchments. Temporal changes in soil source contributions reconstructed over the last 800–1200 years match the timing of human arrival (i.e., ~1300 AD), with estuarine sediment progressively displaced by catchment sources composed primarily of subsoils exposed by deforestation and associated bracken soils.

5 Conclusions

Contemporary and historical changes in the sources of fine sediment accumulating in the Firth of Thames have been determined from carbon isotopic analysis of catchment soils, river sediments and dated estuarine sediment cores. The cores, collected from the southern Firth, preserve records of environmental change over the last 1,800 years, including the effects of large-scale catchment deforestation and subsequent conversion to land uses including pastoral agriculture and production forestry since the mid-1800s. The specific objectives of the present study are:

- Determine the sources of eroded soils and their relative contributions to the sediment deposition in the Firth of Thames (by land use and sub-catchment), including an assessment of the variability in fatty acid $\delta^{13}C$ signatures (within end members).
- Determine how sedimentary contributions have changed by land use source over the recent past (present to 1000 years before present, BP).

Analysis of contemporary sediment sources within the Waihou–Piako Rivers system shows how source contributions vary between tributaries and which land uses are the dominant sources. In the Waihou system, the Waiomou, Ohinemuri and Hikutaia tributaries make relatively small contributions (i.e., <16%) to the fluvial sediments deposited downstream of their confluences. In contrast, the Waitoa dominates (65%) fluvial deposits downstream of the confluence with the Piako. Whilst eroding subsoils dominate fine sediment inputs to the Waitoa (~86%), bank erosion is the largest source of fluvial sediment in both the Waihou (~75-80%) and Piako Rivers (~68%). In both the Waihou and Piako, the origin by land use of bankside deposits differs. For instance, in the headwaters of the Waihou where the vast majority (>90%) of sediment carried downstream originates, soils eroded from pine forest dominate (i.e., ~80-90% of bankside eroded material). Minor contributing sources to bankside deposits within the Waihou include sheep and beef pasture, dairy pasture, native broadleaf forest and subsoils. In the Piako, eroding banks comprise sediment predominantly from dairy pasture (75%) with minor contributions by sheep and beef pasture, maize cropping, pine forest, broadleaf and podocarp native forest. Today, fluvial sediment from the Waihou and Piako Rivers account for 70% and 20% respectively of deltaic deposits, with the remainder composed of estuarine legacy sediments.

The CSSI analysis of the dated sediment cores indicate changes in sediment sources, particularly increases in topsoil contributions, accompanying increased SAR that followed the arrival of people in the 1300s. Pre-human sedimentation in the Firth of Thames was an order of magnitude lower and dominated by slow accumulation of mainly subsoils over centuries to millennia, supplied by rivers draining catchments with indigenous forest and scrub communities. Isotopically enriched and reworked estuarine sediments and bracken soils account for most of the remaining sedimentation at that time. The presence of these bracken-labelled sediments hundreds of years prior to human arrival suggests that frequent natural disturbance of the landscape was of feature of this system.

Sediment accumulation rates increased substantially from the late-1800s, by up to an order of magnitude, relative to the several centuries prior (i.e., ~post-1100s).

Relative contributions of eroded catchment soils also increased from the late-1800s, although the precise timing of this change to greater land-use derived subsoil and topsoil contribution is poorly constrained across the three cores, occurring between 1661 AD and 1883 AD in core FT-1.

Regardless of the precise timing of this change, sedimentation in the Firth thereafter was composed of large amounts of subsoil and bracken soils (85–86% weighted averages), which suggest substantial coeval disturbance of the catchment indigenous forest landcover. This may reflect progressive clearance by Māori of the foothills of the Coromandel and Kaimai ranges over time that were more distant from their settlements on the river banks (Phillips, 2000). There is more robust evidence of the impacts following European settlement, of markedly increased fluvial sediment loading. Contributions of catchment subsoils to estuarine sedimentation increased following European settlement, which have averaged 63–79% at the core sites since the late-1800s. In terms of catchment sources of sediments accumulating in the Firth over the last century (i.e., excluding reworked estuarine sediments), our analysis of individual dated samples from each core suggests that sub-soil erosion accounted for 21–69% of the sediment in each analysed layer.

The apparent discontinuity between contemporary sources of sediment in the rivers and southern Firth can be explained by legacy subsoils that were originally delivered to the Firth by rivers during the period of mining and large-scale deforestation that occurred after European settlement (i.e., mid-1800s to early 1900s). This suggest that legacy sediments continue to substantially contribute to present-day sedimentation in the southern Firth.

6 Acknowledgements

This project was co-funded by New Zealand dairy farmers through DairyNZ Incorporated (Schedule NP1401), Waikato Regional Council and NIWA Core Funding (FWCE1506).

The authors thank Waikato Regional Council staff for GIS analysis of catchment attributes to inform the selection of soil sampling locations (Dan Borman) and collection of soils for each land use class and fluvial sediments sampled in rivers (Pete Wilson, Justin Wyatt). Pete Wilson also provided review comments on the draft report. We also acknowledge Rod Budd, David Bremner and Sam Parkes (NIWA Hamilton) for assistance with collection of the estuarine sediment cores. We also thank Dr Sarah Bury and Julie Brown (NIWA Stable Isotope Facility) for isotopic analysis of bulk carbon and Dr David Thompson (NIWA) for reviewing the report.

Radioisotope dating was conducted at the ESR National Radiation Lab (Dr Nikolaus Hermansphan) and University of Waikato Radiocarbon Dating Lab (Dr Fiona Petchy). CSSI analysis of FAME samples was conducted at the University of California at Davis Stable Isotope Facility (Drs Chris Yarnes and Julian Herzage).

7 References

Alfaro, A.C., Thomas, F., Sergent, L., Duxbury, M. (2006) Identification of trophic interactions within and estuarine food web (northern New Zealand) using fatty acid biomarkers and stable isotopes. *Estuarine, Coastal and Shelf Science*, 70: 271–286.

Blake, W.H., Ficken, K.J., Taylor P., Russell, M.A., Walling, D.E. (2012) Tracing crop-specific sediment sources in agricultural catchments. *Geomorphology*, 139: 322–329. DOI: 10.1016/j.geomorph.2011.10.036

Brownell, B. (2004) Muddy feet: Firth of Thames RAMSAR-site update 2004. *Ecoquest Education Foundation*, Pokeno, New Zealand: 198.

Carter, L., Eade, J.V. (1980) Hauraki sediments. New Zealand Oceanographic Institute (now NIWA) Chart, *Coastal Series*, 1: 200 000.

de Baere, B.J.M. (2006) Silica diagenesis in New Zealand and Antarctic continental shelf sea sediments. Unpublished MOcean dissertation, *School of Ocean and Earth Science*, Faculty of Science, University of Southampton, United Kingdom: 103.

Dalsgaard, J., St. John, M., Kattner, G., Müller-Navarra, D., Hagen, W. (2003) Fatty acid trophic markers in the pelagic marine environment. *Advances in Marine Biology*, 46: 225–340.

Gibbs, M. (2008) Identifying source soils in contemporary estuarine sediments: a new compound specific isotope method. *Estuaries and Coasts,* 31: 344–359.

Gibbs, M.M., Swales, A., Olsen, G. (2014) Suess Effect on biomarkers used to determine sediment provenance from land use changes. In: L.K. Heng, K. Sakadevan, G. Dercon, M.L. Nguyen (eds). *Proceedings – International Symposium on Managing Soils for food Security and Climate Change Adaption and Mitigation*. Food and Agriculture Organization of the United Nations Rome, 2014: 371–375.

Giles, T., Newnham, R., Lowe, D., Munro, A. (1999) Impact of tephra fall and environmental change: a 1000 year record from Matakana Island, Bay of Plenty, North Island, New Zealand. *Geological Society, London*, Special Publications, 161: 11-26.

Green, M.O., Coco, G. (2007) Sediment transport on an estuarine intertidal flat: measurements and conceptual model of waves, rainfall and exchanges with a tidal creek. *Estuarine, Coastal and Shelf Science*, 72: 553–569.

Hancock, G.J., Revill A.T. (2013) Erosion source determination in a rural Australian catchment using compound-specific isotope analysis (CSIA). *Hydrological Processes*, 27: 923–932.

Healy, T.R. (2002) Muddy coasts of mid-latitude oceanic islands on an active plate margin - New Zealand. In Muddy Coasts of the World: Processes, Deposits and Function, Healy, T., Wang, Y., Healy, J.-A. (eds.). *Elsevier Science*, Amsterdam, 347–374.

Hicks, D.M., Shankar, U., McKerchar, A.I., Basher, L., Jessen M., Lynn, I., Page, M. (2011) Suspended sediment yields from New Zealand Rivers. *Journal of Hydrology (NZ)*, 50(1): 81–142.

Hogg, A.G., Higham, T.F.G., Dahm, J. (1998) Radiocarbon dating of modern marine and estuarine shellfish. *Radiocarbon*, 40: 975–984.

Hume, T.M., Dahm, J. (1992) An investigation of the effects of Polynesian and European Land Use on Sedimentation in Coromandel estuaries. *DSIR Marine and Freshwater Division Consultancy Report No. 6104 for Department of Conservation*: *73*.

Hume, T.M., McGlone, M.S. (1986) Sedimentation patterns and catchment use changes recorded in the sediments of a shallow tidal creek, Lucas Creek, Upper Waitemata Harbour, New Zealand. *Journal of the Royal Society of New Zealand,* 19: 305–317.

Jantschik, R., Nyffeler, F., Donard, OFX. (1992) Marine particle size measurement with a stream-scanning laser system. *Marine Geology*, 106: 239–250.

Manighetti, B., Carter, L. (1999) Across-shelf sediment dispersal, Hauraki Gulf, New Zealand. *Marine Geology*, 160: 271-300.

McGlone, M.S., Wilmshurst, J.M., Leach, H.M. (2005) An ecological and historical review of bracken (*Pteridium esculentum*) in New Zealand, and its cultural significance. *New Zealand Journal of Ecology*, 29(2): 165–184.

McGlone, M., Nelson, C., Todd, A. (1984) Vegetation history and environmental significance of pre-peat and surficial peat deposits at Ohinewai, Lower Waikato Lowland. *Journal of Royal Society of New Zealand*, 14: 233-244.

Moore, J.W., Semmens, B.X. (2008) Incorporating uncertainty and prior information into stable isotope mixing models. *Ecology Letters*, 11: 470–480.

Newnham, R., de Lange, P., Lowe, D. (1995) Holocene vegetation, climate and history of a raised bog complex, northern New Zealand based on palynology, plant macrofossils and tephrochronology. *The Holocene*, 5: 267-282.

Oldman, J.W., Swales, A. (1999) Maungamaungaroa Estuary numerical modelling and sedimentation. *NIWA Client Report* ARC70224, prepared for Auckland Regional Council.

Parnell, A., Phillips, D.L., Bearhop, S., Semmens, B.X., Ward, E.J., Moore, A.L., Jackson, J., Grey, D.J., Kelly, D.J., Inger, R. (2013). Bayesian stable isotope mixing models. *Environmetrics*, 24: 387–399.

Petchy, F., Anderson, A., Hogg, A., Zondervan, A. (2008) The marine reservoir effect in the Southern Ocean: an evaluation of extant and new DR values and their application to archaeological chronologies. *Journal of the Royal Society of New Zealand*, 38(4): 243–262.

Phillips, C. (2000) Waihou Journeys. The archaeology of 400 years of Maori settlement. *Auckland University Press*: 194.

Phillips, D.L., Gregg, J.W. (2001) Uncertainty in source partitioning using stable isotopes: coping with too many sources. *Oecologia,* 127: 171–179. (Also erratum, *Oecologia,* 128:204.)

Phillips, D.L., Gregg, J.W. (2003) Source portioning using stable isotopes: coping with too many sources. *Oecologia,* 136: 261–269.

Phillips, D.L., Inger, R., Bearhop, S., Jackson, A.L., Moore, J.W., Parnell, A.C., Semmens, B.X., Ward, E.J. (2014) Best practices for use of stable isotope mixing models in food-web studies. *Canadian Journal of Zoology*, 92: 823–835.

Pocknall, D., Gregory, M., Greig, D. (1989) Palynology of core 80/20 and its implications in understanding Holocene sea level changes in the Firth of Thames, New Zealand. *Journal of Royal Society of New Zealand*, 19: 171-179.

Pritchard, M., Swales, A., Green, M.O. (2015) Influence of buoyancy- and wind-coupling on sediment dispersal and deposition in the Firth of Thames, New Zealand. *Australasian Coasts and Ports Conference 2015*, 15–18 September 2015, Auckland, New Zealand.

Sheffield, A.T., Healy, T.R., McGlone, M.S. (1995) Infilling rates of a steepland catchment estuary, Whangamata, New Zealand. *Journal of Coastal Research,* 11(4): 1294–1308.

Smith, A.M., Nelson, C.S. (1994) Calcification rates of rapidly colonising bryozoans in Hauraki Gulf, northern New Zealand. *New Zealand Journal of Marine and Freshwater Research*, 28(2): 227–234.

Sommerfield, C.K., Nittrouer, C.A., Alexander, C.R. (1999) ^{7}Be as a tracer of flood sedimentation on the Northern California margin. *Continental Shelf Research,* 19: 335–361.

Stock, B.C., Semmens, B.X. (2015) *MixSIAR User Manual,* version 3.0. https://github.com/brianstock/MixSIAR/.

Stock B.C., Semmens, B.X. 2016. Unifying error structures in commonly used biotracer mixing models. *Ecology* doi: 10.1002/ecy.1517.

Stuiver, M., Polach, H.A. (1977) Discussion: reporting ^{14}C data. *Radiocarbon*, 19: 355–363.

Swales, A., Hume, T.M. (1994) Sedimentation history and potential future impacts of production forestry on the Whangamata Estuary, Coromandel Peninsula. *NIWA Client Report* CHH003, prepared for Carter Holt Harvey.

Swales, A., Hume, T.M. (1995) Sedimentation history and potential future impacts of production forestry on the Wharekawa Estuary, Coromandel Peninsula. *NIWA Client Report* CHH004, prepared for Carter Holt Harvey.

Swales, A., Hume, T.M., Oldman, J.W., Green, M.O. (1997) Holocene sedimentation and recent human impacts in a drowned-valley estuary: 895–900. In: J. Lumsden (ed.). *Proceedings of the 13th Australasian Coastal and Ocean Engineering Conference,* Centre for Advanced Engineering, University of Canterbury, Christchurch, New Zealand.

Swales, A., Williamson, R.B., Van Dam, L.F., Stroud, M.J. (2002a) Reconstruction of urban stormwater contamination of an estuary using catchment history and sediment profile dating. *Estuaries,* 25(1): 43–56.

Swales, A., Hume, T.M., McGlone, M.S., Pilvio, R., Ovenden, R., Zviguina, N., Hatton, S., Nicholls, P., Budd, R., Hewitt, J., Pickmere, S., Costley, K. (2002b) Evidence for the physical effects of catchment sediment runoff preserved in estuarine sediments: Phase II (field study). ARC Technical Publication 221. *NIWA Client Report* HAM2002-067.

Swales, A., MacDonald, I.T., Green, M.O. (2004) Influence of wave and sediment dynamics on cordgrass (*Spartina anglica*) growth and sediment accumulation on an exposed intertidal flat. *Estuaries*, 27(2): 225–243.

Swales, A., Hume, T.M. (2005a) Whaingaroa (Raglan) Harbour: Sedimentation and the effects of historical landcover changes. *NIWA Client Report* EVW05278.

Swales, A., Bentley, S.J., McGlone, M.S., Ovenden, R., Hermansphan, N., Budd, R., Hill, A., Pickmere, S., Haskew, R., Okey, M.J. (2005b) Pauatahanui Inlet: effects of historical catchment landcover changes on estuary sedimentation. *NIWA Client Report* HAM2004-149, for Wellington Regional Council and Porirua City Council.

Swales, A., Stephens, S., Hewitt, J.E., Ovenden, R., Hailes, S., Lohrer, D., Hermansphan, N., Hart, C., Budd, R., Wadhwa, S., Okey, M.J. (2007) Central Waitemata Harbour Study. Harbour Sediments. *NIWA Client Report* HAM2007-001, prepared for Auckland Regional Council.

Swales, A., Gibbs, M., Ovenden, R., Budd, R., Hermansphan, N. (2008) Sedimentation in the Okura – Weiti – Karepiro Bay system. *Auckland Regional Council Technical Report,* 2008/026.

Swales, A., Gibbs, M., Ovenden, R., Costley, K., Hermanspahn, N., Budd, R., Rendle, D., Hart, C., Wadhwa, S. (2011) Patterns and rates of recent sedimentation and intertidal vegetation changes in the Kaipara Harbour. *NIWA Client Report* HAM2011-040, prepared for Auckland Council and Northland Regional Council: 173.

Swales, A., Gibbs, M., Hewitt, J., Hailes, S., Griffiths, R., Olsen, G., Ovenden, R., Wadhwa, S. (2012) Sediment sources and accumulation rates in the Bay of Islands and implications for macro-benthic fauna, mangrove and saltmarsh habitats. *NIWA Client Report* HAM2012-048.

Swales, A., Gibbs, M., Pritchard, M., Budd, R., Olsen, G., Ovenden, R., Costley, K., Hermanspahn, N., Griffiths, R. (2013) Whangarei Harbour sedimentation. Sediment accumulation rates and present-day sediment sources. *NIWA Client Report* HAM2013–143, prepared for Northland Regional Council: 104.

Swales, A., Gibbs, M., Olsen, G., Ovenden, R. (2015a) Historical changes in sources of catchment sediment accumulating in Whangarei Harbour. *NIWA Client Report* HAM2015–037, prepared for Northland Regional Council: 39.

Swales, A., Bentley, S.J., Lovelock, C.E. (2015b) Mangrove-forest evolution in a sediment-rich estuarine system: Opportunists or agents of geomorphic change? *Earth Surface Processes and Landforms*, 40: 1672–1687, doi: 10.1002/esp.3759.

Talke, S.A., Stacey, M.T. (2008). Suspended sediment fluxes at an intertidal flat: The shifting influence of wave, wind, tidal and freshwater forcing. *Continental Shelf Research,* 28: 710–725.

Trustrum, N.A., Crippen, T.F. (1986) N49 Thames (2nd Edition): *New Zealand Land Resource Inventory Worksheet*, 1:63, 360, National water and Soil Conservation Authority, Wellington.

Turner, S., Hume, T., Gibberd, B., 2006 Waikato Region Estuaries — Information and Management Issues. *Environment Waikato Internal Series* 2006/09, Waikato Regional Council.

Van der Roovaart, J., Meihers, E., Weeber, M., Goorden, N., Tollenaar, D., Burger, D. (2016) Development of a water quality modelling framework for the Hauraki Plains Catchment. *Deltares client report* for DairyNZ Ltd. Reference 1210754-000-ZWS-0006. Pp.59.

Vant, B. (2011) Water Quality of the Hauraki Rivers and Southern Firth of Thames, 2000–09. *Waikato Regional Council Technical Report*, TR 2011/06.

Verburg, P. (2007) The need to correct for the Suess effect in the application of d13C in sediment of autotrophic Lake Tanganyika, a s a productivity proxy in the Anthropocene. *Journal of Paleolinology,* 37: 591–602.

Wildhaber, Y.S., Liechti, R., Alewell, C. (2012) Organic matter dynamics and stable isotope signatures of tracers of the sources of suspended sediment. *Biogeosciences*, 9: 1985–1996.

Wilmshurst, J.M., Anderson, A.J., Higham, T.F.G., Worthy, T.H. (2008) Dating the late prehistoric dispersal of Polynesians to New Zealand using the commensal Pacific rat. *Proceedings of the National Academy of Sciences*, 105: 7676–7680.

Appendix A Bulk carbon and fatty acid $\delta^{13}C$ data for catchment soils and sediments, and estuarine sediment cores.

Table A-1: Waihou and Piako catchment soils - bulk and CSSI $\delta^{13}C$ values. CSSI data corrected for: (1) methyl (MeOH) derivatisation effect; (2) inter-batch differences corrected using a NIWA FAME standard run with each batch.

Firth Catchment Sites												
Sample Description	**Site ID**	**Lab ID**	**%C**	**Bulk $d^{13}C$**	**C14:0**	**C16:0**	**C18:0**	**C18:1**	**C18:2**	**C20:0**	**C22:0**	**C24:0**
Waihou Kanuka (bottom of slope)	22	181/22	13.92	13.92	-35.73	-33.48	-31.98	-30.13	-31.77	-33.80	-34.14	-33.03
Piako Kahikatea	20	181/20	24.26	24.26	-33.54	-30.26	-29.77	-28.00	-28.58	-30.51	-30.81	-32.52
Piako Sheep/Beef	28	181/28	9.68	9.68	-31.99	-32.13	-32.92	-31.07	-30.15	-33.98	-35.88	-35.01
Piako Sheep/Beef	29	181/29	9.43	9.43	-30.70	-31.44	-32.86	-31.32	-30.26	-33.75	-33.92	-34.56
Piako Dairy (Floods)	31	181/31	9.95	9.95	-29.30	-30.00	-31.86	-28.40	-27.75	-30.35	-32.36	-33.09
Piako Dairy	31A	181/31A	5.53	5.53	-31.31	-31.92	-33.29	-30.29	-30.01	-33.93	-34.87	-35.34
Waihou Maize/Dairy	32	181/32	7.23	7.23	-29.58	-30.31	-34.16	-29.64	-29.16	-32.00	-32.59	-32.63
Waihou Dairy	32A	181/32A	8.36	8.36	-31.14	-31.15	-33.69	-28.78	-28.75	-33.96	-34.00	-34.21
Waihou Dairy	34	181/34	6.20	6.20	-29.97	-30.39	-32.78	-29.98	-28.29	-33.69	-33.88	-34.43
Maize (Piako)	35	181/35	4.72	4.72	-25.88	-22.29	-26.40	-19.92	-17.92	-28.46	-29.60	-29.64
Waihou Sheep/Beef	39	181/39	6.14	6.14	-31.57	-30.35	-31.79	no data	-30.60	-34.07	-33.45	-33.75
Piako Dairy	42	181/42	7.32	7.32	-31.49	-31.47	-33.91	-29.97	-29.71	-33.46	-33.26	-33.41
Piako Pine Forest	43	181/43	12.31	12.31	-34.08	-29.21	-28.62	-27.46	-27.96	-28.33	-26.98	-27.40
Piako Beef/Lifestyle	44	181/44	7.36	7.36	-33.79	-29.15	-29.49	-29.02	-28.31	-28.99	-27.59	-27.93
Kauri-Waihou	22A	181/22A	24.59	24.59	-26.96	-25.86	-27.06	-26.71	-26.52	-28.03	-25.96	-27.69
Waihou Dairy	24	181/24	12.35	12.35	-30.73	-30.87	-31.37	-27.84	-28.16	-31.46	-29.81	-30.59
Piako Dairy_40 years	25	181/25	36.32	36.32	2.33	-28.81	-30.04	-23.94	1.84	-30.06	-30.65	-33.00
Piako Dairy->20 years	26	181/26	10.22	10.22	-32.15	-30.56	-32.83	-29.75	-29.38	-31.65	-31.44	-32.15
Waihou Sheep/beef-10 years	27	181/27	15.06	15.06	-31.61	-29.25	-33.05	-29.44	-28.64	-33.10	-33.08	-33.06

Sample Description	Site ID	Lab ID	%C	Bulk $d^{13}C$	C14:0	C16:0	C18:0	C18:1	C18:2	C20:0	C22:0	C24:0
Waihou Dairy	30	181/30	13.39	13.39	-30.36	-29.72	-31.66	-28.57	-27.94	-32.20	-32.50	-32.41
Waihou Maize	33	181/33	4.81	4.81	-30.04	-28.46	-28.42	-26.37	-23.16	-30.91	-31.35	-32.40
Waihou Sheep	36	181/36	4.98	4.98	-31.76	-31.21	-33.18	-32.34	-32.24	-33.81	-33.76	-33.70
Waihou Dairy-Goat farm	38A	181/38A	16.64	16.64	-31.36	-31.07	-31.78	-30.87	-30.16	-31.83	-33.14	-33.15
Waihou-Dairy	38B	181/38B	11.47	11.47	-33.30	-31.58	-33.59	-31.75	-30.13	-32.53	-33.27	-33.14
Waihou-Dairy	40A	181/40A	19.76	19.76	-30.80	-29.57	-32.30	-27.95	-26.35	-33.27	-33.95	-34.41
Waihou-Dairy	40B	181/40B	13.18	13.18	-32.41	-30.79	-32.68	-29.64	-29.74	-33.04	-33.77	-33.87
Waihou-Dairy	40C	181/40C	13.01	13.01	-32.71	-31.71	-31.65	-30.79	-30.79	-35.21	-35.16	-35.54
Waihou Sheep/beef	41A	181/41A	10.49	10.49	-32.98	-30.95	-32.42	-30.10	-30.05	-34.34	-34.43	-34.60
Waihou Sheep/beef	41B	181/41B	18.56	18.56	-31.49	-29.40	-30.16	-28.47	-27.86	-33.55	-33.90	-33.96
Waihou Pine Forest-2002	45	181/45	18.88	18.88	-35.48	-31.27	-29.90	-32.46	-31.07	-32.04	-31.84	-32.45
Waihou Pine Forest-2008	46	181/46	13.79	13.79	-36.91	-30.88	-29.45	-30.79	-29.94	-30.46	-30.80	-31.04
Waihou Pine Forest-2014	46A	181/46A	5.65	5.65	-30.53	-30.24	-30.01	-29.42	-28.72	-31.65	-30.08	-31.27
Piako Maize	47	181/47	7.90	7.90	-29.35	-29.58	-30.24	-25.31	-22.50	-31.68	-31.82	-32.62
Piako Sheep/beef	48	181/48	7.04	7.04	-32.08	-31.01	-33.54	-31.22	-31.09	-34.35	-34.81	-35.05
Piako Beef grazing	49	181/49	10.30	10.30	-35.17	-32.40	-33.61	-31.40	-31.28	-34.32	-34.46	-34.63
Waihou Pine Forest	50	181/50	23.49	23.49	-34.37	-29.95	-29.05	-28.40	-27.10	-30.05	-29.84	-30.14
Waihou Sheep/beef	51	181/51	5.85	5.85	-33.54	-31.19	-33.16	-30.06	-30.00	-34.78	-34.70	-35.28
Piako Maize	52	181/52	5.66	5.66	-26.45	-20.81	-25.42	-21.11	-18.10	-28.87	-30.77	-32.65
Piako Maize	53	181/53	2.03	2.03	-23.93	-23.95	-28.85	-23.99	-27.14	-26.46	-27.99	-31.14
Piako Potatoes	54	181/54	2.59	2.59	-30.17	-29.01	-29.39	-28.76	-28.10	-31.88	-31.49	-32.76
Piako Sheep/beef	55	181/55	10.58	10.58	-31.15	-31.59	-33.72	-31.20	-31.57	-34.30	-34.81	-34.67
Waihou potato/onion/maize	56	181/56	4.48	4.48	-27.88	-29.43	-29.62	-26.80	-27.31	-27.66	-31.17	-30.81

Sample Description	Site ID	Lab ID	%C	Bulk $d^{13}C$	C14:0	C16:0	C18:0	C18:1	C18:2	C20:0	C22:0	C24:0
Piako-Patetonga Forest 1 – Pine	57	181/57	20.06	20.06	-34.81	-28.83	-27.78	-26.35	-27.17	-27.16	-26.43	-27.10
Piako-Patetonga Forest 2 – Pine	58	181/58	26.85	26.85	-36.33	-30.04	-27.77	-26.75	-26.16	-28.87	-28.54	-28.95
Waihou Forest – Pine	59	181/59	29.52	29.52	-31.90	-27.88	-28.47	-27.69	no data	-30.00	-29.40	-29.69
Waihou Native Bush	21A	181/21A	8.73	8.73	-32.11	-29.37	-27.96	-29.06	-27.41	-32.85	-32.53	-32.06
Waihou Native Bush	21B	181/21B	31.71	31.71	-35.54	-30.18	-29.02	-27.31	-27.52	-29.97	-29.46	-30.88
Piako Native Bush	21C	181/21C	44.83	44.83	-29.63	-25.76	-23.74	-25.73	-25.27	-28.81	-28.83	-27.23
Piako Native Bush	21D	181/21D	44.79	44.79	-36.24	-27.76	-26.59	-26.62	-25.60	-27.99	-28.59	-29.85
Piako Native Bush	21E	181/21E	44.50	44.50	-32.81	-30.47	-30.28	-30.15	-28.73	-32.92	-32.72	-32.18
Ohinemuri Subsoil 1	SUB-01	SUB-01	0.40	0.40	-31.07	-28.89	-28.27	-28.82	-27.82	-30.10	-31.03	-29.56
Waihou Subsoil 2	SUB-02	SUB-02	0.85	0.85	-29.75	-29.70	-33.29	-29.35	-27.47	-30.76	-31.65	-29.65
Piako Subsoil 3	SUB-03	SUB-03	0.42	0.42	-29.70	-30.41	-29.84	-28.75	-28.73	-29.91	-32.22	-28.73
Piako Subsoil 4	SUB-04	SUB-04	2.85	2.85	-31.96	-30.85	-30.99	-31.23	-30.10	-31.36	-30.61	-30.78
Waihou Subsoil 5	SUB-05	SUB-05	0.42	0.42	-28.49	-29.29	-29.02	-28.68	-28.29	-32.32	-30.93	-30.90
Waihou Subsoil 6	SUB-06	SUB-06	0.62	0.62	-28.10	-27.71	-28.77	-28.14	-26.66	-27.76	-30.20	no data

Table A-2: Waihou and Piako River sediment deposits - bulk and CSSI $\delta^{13}C$ values. CSSI data corrected for: (1) methyl (MeOH) derivatisation effect; (2) inter-batch differences corrected using a NIWA FAME standard run with each batch.

River sediments												
Sample Description	Site ID	Lab ID	%C	Bulk $d^{13}C$	C14:0	C16:0	C18:0	C18:1	C18:2	C20:0	C22:0	C24:0
Kaurenga River	1	181/1	2.56	2.56	-23.13	-23.49	-26.74	-25.11	-23.13	-28.17	-37.36	-28.13
Waihou down stream of confluence	2	181/2	0.66	0.66	-36.33	-34.15	-30.24	-29.43	-31.58	-31.02	-30.18	-30.52
Waiomoo Stream	3	181/3	1.14	1.14	-31.54	-30.83	-30.95	-30.08	-29.43	-31.70	-31.08	-31.19
Waiomoo Stream bank erosion	4	181/4	0.91	0.91	-28.79	-29.84	-29.09	-29.94	-32.46	-32.63	-30.67	-30.52
Waihou River (black) deposition	5	181/5	2.92	2.92	-35.67	-34.75	-31.69	-29.31	-30.39	-32.65	-33.21	-32.56
Waihou River (brown)	5A	181/5A	1.86	1.86	-29.64	-27.90	-30.91	-30.79	-30.70	-31.31	-33.01	-31.12
Ohinemuri River (d/s Karanagahake Gorge)	10	181/10	3.82	3.82	-31.56	-29.23	-31.39	-30.53	-30.21	-32.99	-34.47	-32.61
Waihou River (u/s)	11	181/11	2.23	2.23	-33.48	-33.14	-31.90	-31.03	-31.07	-32.59	-32.62	-33.20
Waihou River (D/S)	13	181/13	0.57	0.57	-33.33	-32.83	-32.85	-31.13	-31.79	-31.14	-31.84	-31.52
Bank erosion (@15-U/S of Hikutaia R	14	181/14	2.81	2.81	-30.65	-30.29	-28.65	-29.05	-27.74	-29.60	-30.43	-30.14
Waihou R (u/s/ of Hikutaia R)	15	181/15	2.52	2.52	-29.62	-29.34	-29.97	-29.57	-29.46	-28.55	-28.57	-28.52
Hikutaia River	16	181/16	2.28	2.28	-32.67	-31.66	-31.54	-29.77	-32.02	-28.70	-29.24	-28.93
Waihou River downstream confluence	17	181/17	2.56	2.56	-29.91	-29.39	-29.59	-29.84	-30.58	-28.08	-29.09	-29.00
Waitoa deposition	6	181/6	6.30	6.30	-32.94	-32.66	-29.69	-32.72	-36.34	-30.99	-31.76	-32.68
Waitoa erosion	6A	181/6A	3.38	3.38	-32.97	-30.58	-31.35	-32.21	-35.06	-30.78	-31.58	-31.87

Sample Description	Site ID	Lab ID	%C	Bulk $d^{13}C$	C14:0	C16:0	C18:0	C18:1	C18:2	C20:0	C22:0	C24:0
Piako downstream deposition	7	181/7	2.22	2.22	-32.12	-30.82	-29.95	-29.93	-32.79	-29.99	-28.24	-28.47
Piako upstream erosion	8	181/8	1.96	1.96	-27.40	-30.43	-32.97	-29.37	-28.48	-31.23	-31.58	-31.03
Piako upstream deposition	9	181/9	1.76	1.76	-27.38	-26.00	-29.42	-28.30	-27.52	-28.32	-28.16	-28.28
Waihou erosion	12	181/12	1.06	1.06	-25.84	-25.63	-27.18	-26.67	-25.10	-27.52	-28.28	-28.27
Hikutaia erosion	16A	181/16A	1.67	1.67	-29.44	-30.21	-28.38	-29.88	-29.22	-32.24	-31.24	-31.34

Table A-3: Firth of Thames surficial sediments - bulk and CSSI $\delta^{13}C$ values. CSSI data corrected for: (1) methyl (MeOH) derivatisation effect; (2) inter-batch differences corrected using a NIWA FAME standard run with each batch.

Firth surficial sediments												
Sample Description	Site ID	Lab ID	%C	Bulk $d^{13}C$	C14:0	C16:0	C18:0	C18:1	C18:2	C20:0	C22:0	C24:0
Waihou delta (sandy, cockles)	A1	181/A1	0.43	0.43	-20.41	-20.05	-25.66	-22.91	-10.54	-29.30	-29.24	-31.80
Waihou delta (sandy, cockles)	A2	181/A2	0.71	0.71	-23.32	-25.07	-29.08	-27.31	-21.18	-28.97	-28.14	-29.31
Waihou delta (mud)	A3	181/A3	1.82	1.82	-26.49	-26.78	-29.49	-26.34	-22.52	-30.70	-31.06	-30.84
Piako delta (mud, macomona)	A4b	181/A4b	1.25	1.25	-24.45	-26.65	-29.51	-26.88	-24.08	-29.74	-29.46	-31.01
Piako delta (mud)	A5b	181/A5b	1.96	1.96	-24.42	-26.21	-29.66	-26.36	-23.04	-29.90	-29.45	-30.18
Piako delta (mud)	A6b	181/A6b	1.85	1.85	-24.48	-27.03	-30.78	-26.46	-21.68	-31.17	-29.71	-32.00
Wilson-A Mussel Farm @ SE corner-1	WA1	181/WA1	2.30	2.30	-25.41	-25.11	-26.57	-23.87	-23.03	-29.02	-25.20	-28.14
Wilson-A Mussel Farm @ SE corner-2	WA2	181/WA2	2.36	2.36	-24.65	-25.11	-25.45	-23.44	-21.58	-30.28	-25.71	-26.48
Wilson-A Mussel Farm @ SE corner-3	WA3	181/WA3	2.09	2.09	-25.03	-25.38	-24.97	-23.79	-15.79	-28.20	-25.59	-26.51
Zeldis NIWA Buoy-1	SA3-1	181/SA3-1	0.77	0.77	-24.92	-23.08	-26.33	-24.08	-21.36	-27.36	-26.76	-25.27
Zeldis NIWA Buoy-2	SA3-2	181/SA3-2	0.54	0.54	-24.29	-22.41	-24.48	-23.86	-21.08	-27.69	-29.74	-25.58
Zeldis NIWA Buoy-3	SA3-3	181/SA3-3	0.77	0.77	-24.70	-23.25	-24.71	-23.79	-16.39	-28.86	-31.84	-25.85

Table A-4: Bracken soils (NIWA Mangemangeroa data) - bulk and CSSI $\delta^{13}C$ values. CSSI data corrected for: (1) methyl (MeOH) derivatisation effect; (2) inter-batch differences corrected using a NIWA FAME standard run with each batch.

Bracken soils - Mangemangeroa												
Sample Description	**Site ID**	**Lab ID**	**%C**	**Bulk $d^{13}C$**	**C14:0**	**C16:0**	**C18:0**	**C18:1**	**C18:2**	**C20:0**	**C22:0**	**C24:0**
Bracken topsoil	BK-A	OA153/34	4.87	4.87	-36.06	-33.94	-33.05	-32.78	-31.88	-37.31	-35.94	-36.02
Bracken topsoil	BK-B	OA153/35	3.72	3.72	-35.33	-33.43	-33.92	-33.87	-34.34	-37.42	-36.73	-36.39
Bracken topsoil	BK-C	OA153/36	5.08	5.08	-35.41	-31.97	-32.07	-31.43	-34.55	-34.15	52.49	-35.92
Bracken topsoil	BK-D	OA153/37	6.11	6.11	-35.79	-31.21	-31.35	-30.24	-37.74	-34.88	-23.63	-35.45
Bracken topsoil	BK-E	OA153/38	11.56	11.56	-34.82	-31.33	-31.76	-30.55	no data	-34.52	-33.99	-35.11
Bracken topsoil	BK-F	OA153/39	11.08	11.08	-36.32	-29.36	-27.17	-31.34	no data	-32.30	-34.33	-34.21

Table A-5: Core FT-1 (intertidal) - bulk and CSSI δ13C values.

CSSI data corrected for: (1) methyl (MeOH) derivatisation effect; (2) inter-batch differences corrected using a NIWA FAME standard run with each batch; and (3) Suess Effect –all data corrected to 2015 AD to enable direct comparison of data from contemporary soils and fluvial sediments with dated sediment cores.

Core FT-1 (2015)

Sample Description	Depth(cm	Year (AD)	%C	Bulk $\delta^{13}C$	C14:0	C16:0	C18:0	C18:1	C18:2	C20:0	C22:0	C24:0
FT-1	1.5	2013.5	1.56	-22.98	-28.46	-29.43	-28.23	-26.90	-24.78	-30.10	-29.91	-28.65
FT-1	9.5	2005.6	1.72	-23.63	-30.18	-30.92	-28.78	-26.71	-24.72	-30.65	-30.67	-28.96
FT-1	19.5	1995.7	1.65	-23.49	-31.15	-31.78	-30.00	-26.16	-25.16	-30.06	-29.91	-28.98
FT-1	29.5	1985.8	1.68	-23.51	-31.69	-31.94	-29.56	-26.63	-26.10	-29.18	-30.95	-29.14
FT-1	39.5	1975.9	1.69	-23.81	-33.47	-33.59	-28.62	-27.27	-25.90	-30.37	-30.77	-30.12
FT-1	59.5	1965.1	1.68	-24.11	-31.58	-33.77	-29.67	-27.05	-26.09	-30.00	-30.56	-28.83
FT-1	77.5	1955.4	1.59	-23.73	-29.26	-31.06	-30.92	-27.95	-27.12	-30.75	-32.11	-30.62
FT-1	89.5	1948.9	1.33	-23.93	-30.53	-33.30	-29.41	-27.77	-27.26	-29.06	-29.85	-29.04
FT-1	108.5	1883.3	1.23	-24.06	-30.75	-33.72	-30.21	-28.16	-27.43	-32.05	-31.81	-30.84
FT-1	124.5	1661.2	1.25	-24.58	-30.24	-32.08	-31.90	-28.89	-28.30	-31.87	-31.09	-31.08
FT-1	130.5	1577.9	1.53	-24.20	-30.29	-32.36	-32.20	-29.10	-29.21	-32.54	-32.34	-29.88
FT-1	135.5	1508.5	1.39	-25.41	-30.04	-31.87	-31.18	-28.61	-28.93	-31.83	-31.22	-29.41
FT-1	140.5	1439.1	1.37	-25.01	-29.58	-31.38	-30.94	-28.57	-30.37	-31.30	-32.06	-29.05
FT-1	145.5	1369.6	1.32	-24.82	-29.70	-31.00	-30.54	-28.49	-29.50	-31.14	-30.69	-30.07
FT-1	150.5	1300.2	1.28	-25.11	-29.76	-31.54	-31.17	-28.07	-28.94	-31.75	-30.86	-29.74

Table A-6: Core FT-2 (intertidal) - bulk and CSSI $\delta^{13}C$ values. CSSI data corrected for: (1) methyl (MeOH) derivatisation effect; (2) inter-batch differences corrected using a NIWA FAME standard run with each batch; and (3) Suess Effect –all data corrected to 2015 AD to enable direct comparison of data from contemporary soils and fluvial sediment with dated sediment cores.

Core FT-2 (2015)

Sample Description	Depth(cm	Year (AD)	%C	Bulk $\delta^{13}C$	C14:0	C16:0	C18:0	C18:1	C18:2	C20:0	C22:0	C24:0
FT-2	1.5	2012.3	1.66	-23.14	-29.33	-29.61	-28.96	-26.16	-25.50	-28.51	-30.14	-28.21
FT-2	5.5	2005.2	1.60	-23.31	-29.30	-30.57	-29.84	-25.87	-25.01	-29.98	-30.28	-28.64
FT-2	11.5	1994.5	1.59	-23.73	-31.86	-31.10	-30.51	-26.21	-26.43	-29.80	-30.82	-28.85
FT-2	16.5	1985.5	1.68	-24.27	-29.18	-29.72	-29.77	-26.58	-26.51	-29.93	-30.03	-28.37
FT-2	22.5	1974.8	1.51	-23.88	-31.66	-31.51	-30.45	-27.03	-27.46	-29.81	-30.03	-28.64
FT-2	26.5	1967.7	1.40	-24.07	-30.30	-31.22	-29.46	-27.66	-27.59	-30.09	-30.98	-28.84
FT-2	33.5	1955.2	1.25	-24.19	-31.68	-32.68	-30.38	-27.96	-28.35	-30.51	-30.71	-29.11
FT-2	39.5	1944.5	1.33	-19.67	-36.69	-33.50	-32.16	-29.14				
FT-2	43.5	1937.3	1.71	-16.21	-34.61	-33.16	-31.20	-28.34		-29.11	-30.94	-29.30
FT-2	49.5	1926.6	1.56	-24.43	-32.97	-32.08	-30.50	-27.31		-30.16	-30.32	-28.59
FT-2	55.5	1915.9	1.45	-24.77	-28.81	-30.80	-30.47	-27.70	-28.99	-29.89	-30.35	-28.45
FT-2	70.5	1648.7	1.35	-24.99	-30.66	-31.94	-33.44	-28.75		-30.69	-32.45	
FT-2	80.5	1470.6	1.45	-24.57	-29.38	-32.49	-32.64	-28.90		-31.84	-32.83	
FT-2	90.5	1292.4	1.62	-24.64	-28.46	-31.74	-31.59	-28.10	-29.76	-31.18	-32.64	-29.63
FT-2	98.5	1149.9	1.23	-25.96	-29.67	-31.52	-31.27	-27.32				

Table A-7: Core FT-4 (subtidal) - bulk and CSSI d^{13}C values. CSSI data corrected for: (1) methyl (MeOH) derivatisation effect; (2) inter-batch differences corrected using a NIWA FAME standard run with each batch; and (3) Suess Effect –all data corrected to 2015 AD to enable direct comparison of data from contemporary soils and fluvial sediment with dated sediment cores.

Core FT-4 (2015)

Sample Description	Depth(cm	Year (AD)	%C	Bulk δ^{13}C	C14:0	C16:0	C18:0	C18:1	C18:2	C20:0	C22:0	C24:0	Depth(cm
FT-4	1.5	2012.76	2.14	-22.46	-28.40	-29.80	-30.18	-26.44	-26.50	-30.22		-26.65	1.5
FT-4	7.5	2003.81	1.89	-22.46	-28.43	-29.66	-29.73	-26.65				-27.93	7.5
FT-4	13.5	1994.85	1.81	-22.37	-31.99	-31.27	-29.72	-27.02				-27.58	13.5
FT-4	19.5	1985.90	1.83	-23.61	-31.45	-30.89	-29.91	-26.91				-27.87	19.5
FT-4	27.5	1973.96	1.56	-22.43	-29.38	-30.89	-30.65	-28.38				-27.68	27.5
FT-4	33.5	1965.00	1.74	-22.98	-28.99	-30.15	-30.33						33.5
FT-4	41.5	1953.06	2.03	-23.54	-33.14	-31.76	-30.02	-27.64				-28.71	41.5
FT-4	47.5	1944.10	1.71	-23.55	-28.41	-30.41	-29.89	-27.49					47.5
FT-4	54.5	1933.66	1.60	-23.38	-29.91	-31.32	-31.13	-28.11					54.5
FT-4	59.5	1926.19	1.73	-24.05	-32.64	-33.01	-30.32	-26.83					59.5
FT-4	70.5	1761.62	1.75	-24.28	-29.11	-31.08	-30.10	-26.79	-28.93				70.5
FT-4	75.5	1686.81	1.73	-23.93	-28.78	-31.47	-30.11	-27.67					75.5
FT-4	80.5	1040.0	1.63	-24.38	-30.11	-31.40	-30.86	-28.30					80.5
FT-4	90.5	929.0	1.69	-24.68	-29.79	-32.16	-31.61	-29.44					90.5
FT-4	98.5	840.0	1.73	-24.93	-30.28	-31.90	-31.27	-29.94	-30.40				98.5

Appendix B Radioisotope dating

Radioisotopes are unstable atoms that release excess energy in the form of radiation (i.e., gamma rays, alpha particles) in the process of radioactive decay. The radioactive-decay rate can be considered fixed for each type of radioisotope and it is this property that makes them very useful as geological clocks. The half-life ($t_{1/2}$) of a radioisotope is one measure of the radioactive decay rate and is defined as the period of time taken for the quantity of a substance to reduce by exactly half. Therefore after two half-lives only 25% of the original quantity remains. The $t_{1/2}$ value of radioisotopes also defines the time-scale over which they are useful for dating. For example, ^{210}Pb has a half-life of 22 years and can be used to date sediments up to seven half-lives old or about 150 years. Dating by ^{210}Pb is based on the rate of decrease in unsupported or excess ^{210}Pb activity with depth in the sediment. Excess ^{210}Pb is produced in the atmosphere and is deposited continuously on the earth's surface, where it falls directly into the sea or on land. Like other radioisotopes, ^{210}Pb is strongly attracted to fine sediment particles (e.g., clay and silt), which settle out of the water column and are deposited on the sea bed. ^{210}Pb also falls directly on land and is attached to soil particles. When soils are eroded they may eventually by carried into estuaries and the sea and provide another source of excess ^{210}Pb. As these fine sediments accumulate on the sea bed and bury older sediments over time, the excess ^{210}Pb decays at a constant rate (i.e., the half-life). The rate of decline in excess ^{210}Pb activity with depth also depends on the local SAR. Slow declines in ^{210}Pb activity with depth indicate rapid sedimentation whereas rapid declines indicate that sedimentation is occurring more slowly.

Radioisotopes can occur naturally, such as ^{210}Pb, whereas others are artificially produced. Caesium-137 ($t_{1/2}$ = 30 yrs) is an artificial radioisotope that is produced by the detonation of nuclear weapon or by nuclear reactors. In New Zealand, the fallout of caesium-137 associated with atmospheric nuclear weapons tests was first detected in 1953, with peak deposition occurring during the mid-1960s. Therefore, caesium-137 occurs in sediments deposited since the early 1950s. The feeding and burrowing activities of benthic animals (e.g., worms and shellfish) can complicate matters due to downward mixing of younger sediments into older sediments. Repeated reworking of sea bed sediments by waves also mixes younger sediment down into older sediments. X-ray images and short-lived radioisotopes such as ^{7}Be ($t_{1/2}$ = 53 days) can provide information on sediment mixing processes.

Sediment accumulation rates

Time-averaged SAR were estimated from the unsupported ^{210}Pb ($^{210}Pb_{ex}$) concentration profiles preserved in cores. The rate of $^{210}Pb_{ex}$ concentration decrease with depth can be used to calculate a net sediment accumulation rate. The $^{210}Pb_{ex}$ concentration at time zero (C_0, Bq kg^{-2}), declines exponentially with age (t):

$$C_t = C_0 e^{-kt} \qquad \text{(A1)}$$

Assuming that within a finite time period, sedimentation (S) or SAR is constant then $t = z/S$ can be substituted into Eq. 2 and by re-arrangement:

$$\frac{\ln\left[\frac{C_t}{C_0}\right]}{z} = -k/S \qquad \text{(A2)}$$

Because $^{210}Pb_{ex}$ concentration decays exponentially and assuming that sediment age increases with depth, a vertical profile of natural log(C) should yield a straight line of slope $b = -k/S$. We fitted a linear regression model to natural-log transformed ^{210}Pb concentration data to calculate b. The SAR over the depth of the fitted data is given by:

$$S = -(k)/b \quad \text{(A3)}$$

An advantage of the ^{210}Pb-dating method is that the SAR is based on the entire $^{210}Pb_{ex}$ profile rather than a single layer, as is the case for ^{137}Cs. Furthermore, if the ^{137}Cs tracer is present at the bottom of the core then the estimated SAR represents a minimum value.

The ^{137}Cs profiles were also used to estimate time-averaged SAR based on the maximum depth of ^{137}Cs in the sediment column, corrected for surface mixing. The ^{137}Cs SAR is calculated as:

$$S = (M - L)/T - T_0 \quad \text{(A4)}$$

where S is the ^{137}Cs SAR, M is the maximum depth of the ^{137}Cs profile, L is the depth of the surface mixed layer (SML) indicated by the ^{7}Be profile and/or x-ray images, T is the year cores were collected and T_0 is the year (1953) ^{137}Cs deposition was first detected in New Zealand.

Pre 20th century time-average SAR, over time scales of several hundred years, were estimated from the radiocarbon dates (^{14}C) obtained from pairs of shell samples collected below the maximum depth of excess ^{210}Pb in each core. The time averaged ^{14}C SAR (mm yr^{-1}) was calculated as:

$$S_B = (D_{Pb} - D_C)/T_{Pb210} - T_{C14} \quad \text{(A5)}$$

Where D_{Pb} and D_C are respectively the depths (mm) below the top of each core of the maximum penetration of the $^{210}Pb_{ex}$ profile and mean AMS ^{14}C age of the dated shell samples. The matching ages of these layers (T_{Pb210}), T_{C14}) are estimates as years A.D., with the AMS 14C age (before present [BP = 1950]), adjusted to the year of core collection (2015). The S_B estimate integrate the effects of land disturbance and soil erosion by Māori and early Europeans over several hundred years as well as background SAR prior to human arrival.

Appendix C Summary of CSSI method

In this section we describe how stable isotopes are used to identify the sources of catchment sediments deposited in lakes, estuaries and coastal waters and explain how isotopic data are interpreted.

Stable isotopes are non-radioactive and are a natural phenomenon in many elements. In the NIWA Compound Specific Stable Isotope (CSSI) method, carbon (C) stable isotopes are used to determine the provenance of sediments (Gibbs 2008). About 98.9% of all carbon atoms have an atomic weight (mass) of 12. The remaining ~1.1% of C atoms have an extra neutron in the atomic structure, giving it an atomic weight (mass) of 13. These are the two stable isotopes of carbon. Naturally occurring carbon also contains an extremely small fraction (about two trillionths) of radioactive carbon-14 (^{14}C). Radiocarbon dating is also used in the present study to determine long-term sedimentation rates.

To distinguish between the two stable isotopes of carbon, they are referred to as light (^{12}C) and heavy (^{13}C) isotopes. Both of these stable isotopes of carbon have the same chemical properties and react in the same way. However, because ^{13}C has the extra neutron in its atom, it is slightly larger than the ^{12}C atom. This causes molecules with the ^{13}C atoms in their structure to react slightly slower than those with ^{12}C atoms, and to pass through cell walls in plants or animals at a slower rate than molecules with ^{12}C atoms. Consequently, more of the ^{12}C isotope passes through the cell wall than the ^{13}C isotope, which results in more ^{12}C on one side of the cell wall than the other. This effect is called isotopic fractionation and the difference can be measured using a mass spectrometer. Because the fractionation due to passage through one cell-wall step is constant, the amount of fractionation can be used to determine chemical and biological pathways and processes in an ecosystem. Each cell wall transfer or "step" is positive and results in enrichment of the ^{13}C content.

The amount of fractionation is very small (about one thousandth of a percent of the total molecules for each step) and the numbers become very cumbersome to use. A convention has been developed where the difference in mass is reported as a ratio of heavy-to-light isotope. This ratio is called "delta notation" and uses the symbol "δ" before the heavy isotope symbol to indicate the ratio i.e., $\delta^{13}C$. The units are expressed as "per mil" which uses the symbol "‰". The delta value of a sample is calculated using the equation:

$$\delta^{13}C = \left[\left(\frac{R_{sample}}{R_{standard}}\right) - 1\right] 1000$$

where *R* is the molar ratio of the heavy to light isotope $^{13}C/^{12}C$. The international reference standard for carbon was a limestone, Pee Dee Belemnite (PDB), which has a $^{13}C/^{12}C$ ratio of 0.0112372 and a $\delta^{13}C$ value of 0 ‰. As all of this primary standard has been consumed, secondary standards calibrated to the PDB standard are used. Relative to this standard most organic materials have a negative $\delta^{13}C$ value.

Atmospheric CO_2, which is taken up by plants in the process of photosynthesis, presently has a $\delta^{13}C$ value of about -8.5. In turn, the $\delta^{13}C$ signatures of organic compounds produced by plants partly depends on their photosynthetic pathway, primarily either C_3 or C_4. During photosynthesis, carbon passes through a series of reactions or trophic steps along the C_3 or C_4 pathways. At each trophic step, isotopic fractionation occurs and organic matter in the plant (i.e., the destination pool) is depleted by 1 ‰. The C_3 pathway is longer than the C_4 pathway so that organic compounds produced by C_3 plants have a more depleted $\delta^{13}C$ signature. There is also variation in the actual amount of

fractionation between plant species having the same photosynthetic pathway. This results in a range of $\delta^{13}C$ values, although typical bulk values for C_3 and C_4 plants vary around -26 ‰ and -12 ‰ respectively. The rate of fractionation also varies between the various types of organic compounds produced by plants. Thus, by these processes a range of organic compounds each with unique $\delta^{13}C$ signatures are produced by plants that can potentially be used as natural tracers or biomarkers.

The instruments used to measure stable isotopes are called "isotope ratio mass spectrometers" (IRMS) and they report delta values directly. However, because they have to measure the amount of ^{12}C in the sample, and the bulk of the sample C will be ^{12}C, the instrument also gives the percent C (%C) in the sample.

When analysing the stable isotopes in a sample, the $\delta^{13}C$ value obtained is referred to as the bulk $\delta^{13}C$ value. This value indicates the type of organic material in the sample and the level of biological processing that has occurred. (Biological processing requires passage through a cell wall, such as in digestion and excretion processes and bacterial decomposition.) The bulk $\delta^{13}C$ value can be used as an indicator of the likely source land cover of the sediment. For example, fresh soil from forests has a high organic content with %C in the range 5% to 20% and a low bulk $\delta^{13}C$ value in the range -28‰ to -40‰. As biological processing occurs, bacterial decomposition converts some of the organic carbon to carbon dioxide (CO_2) gas which is lost to the atmosphere. This reduces the %C value and, because microbial decomposition has many steps, the bulk $\delta^{13}C$ value increases by ~1‰ for each step. Pasture land cover and marine sediments typically have bulk $\delta^{13}C$ values in the range -24‰ to -26‰ and -20‰ to -22‰, respectively. Waste water and dairy farm effluent have bulk $\delta^{13}C$ values more enriched than -20‰. Consequently, a dairy farm where animal waste has been spread on the ground as fertilizer, will have bulk $\delta^{13}C$ values higher (more enriched) than pasture used for sheep and beef grazing.

There are occasions when the inorganic component of the soil imparts a highly modified $\delta^{13}C$ isotopic signature to the soil such that the $\delta^{13}C$ value cannot be used for modelling of soil sources. This phenomenon occurs for example in Karst (limestone) soils, such as in the upper Whangarei Harbour associated with the Portland sediment.

In addition to the bulk $\delta^{13}C$ value, organic carbon compounds in the sediment can be extracted and the $\delta^{13}C$ values of the carbon in each different compound can be measured. These values are referred to as compound-specific stable isotope (CSSI) values. A forensic technique recently developed to determine the provenance of sediment uses both bulk $\delta^{13}C$ values and CSSI values from each sediment sample in a deposit for comparison with signatures from a range of potential soil sources for different land cover types. This method is called the CSSI technique (Gibbs, 2008).

The CSSI technique is based on the concepts that:

1. land cover is primarily defined by the plant community growing on the land, and
2. all plants produce the same range of organic compounds but with slightly different CSSI values because of differences in the way each plant species grows and also because each land cover type has a characteristic composition of plant types that contribute to the CSSI signature.

The compounds commonly used for CSSI analysis of sediment sources are natural plant fatty acids (FAs) which bind to the soil particles as labels called biomarkers. While the amount of a biomarker may decline over time, the CSSI value of the biomarker does not change. The CSSI values for the range of biomarkers in a soil provides positive identification of the source of the soil by land cover type.

The sediment at any location in an estuary or harbour can be derived from many sources including river inflows, coastal sediments and harbour sediment deposits that have been mobilised by tidal currents and wind-waves. The contribution of each sediment source to the sediment mixture at the sampling location will be different. To separate and apportion the contribution of each source to the sample, a mixing model is used. The CSSI technique uses the mixing model IsoSource (Phillips and Gregg, 2003). The IsoSource mixing model is described in more detail in a following section.

While the information on stable isotopes above has focused on carbon, these descriptions also apply to nitrogen (N), which also has two stable isotopes, ^{14}N and ^{15}N. The bulk N content (%N) and bulk isotopic values of N, $\delta^{15}N$, also provide information on land cover in the catchment but, because the microbial processes of nitrification and denitrification can cause additional fractionation after the sediment has been deposited, bulk $\delta^{15}N$ cannot be used to identify sediment sources. The fractionation step for N is around +3.5‰ with bulk $\delta^{15}N$ values for forest soils in the range +2‰ to +5‰. Microbial decomposition processes result in bulk $\delta^{15}N$ values in the range 6‰ to 12‰ while waste water and dairy effluent can produce bulk $\delta^{15}N$ values up to 20‰. However, the use of synthetic fertilizers such as urea, which has $\delta^{15}N$ values of -5‰, can result in bulk $\delta^{15}N$ values <0‰.

Sample analyses

An aliquot of each dry sediment sample was acidified with 1 N hydrochloric acid to remove inorganic carbonate before analysing for bulk organic C and N stable isotopes. About 50 mg of each acidified sample was combusted in a helium gas stream in a Fisons N1500 Elemental Analyser coupled via a ConFlo-II interface to a Thermo-Finnegan Continuous Flow Isotope Ratio Mass Spectrometer (CF-IRMS).

For $\delta^{13}C$, CF-IRMS measurements typically have a precision of ± 0.1 ‰ or better and the instrument also provides the proportion of organic C and N (%) in each sample.

Aliquots (20 to 40 g) of the non-acidified dry sediment were extracted with hot dichloromethane (100 ºC) under high pressure (2000 psi) in a Dionex Accelerated Solvent Extractor (ASE 2000) to extract the fatty acids bound to the sediment particles. The FAs were methylated using 5% boron trifluoride catalyst in methanol to produce fatty acid methyl esters (FAMEs). These FAMEs were analysed by gas chromatography (GC)-combustion-IRMS to produce compound-specific stable isotope $\delta^{13}C$ values i.e., CSSI values. Method details and data interpretation protocols were described previously by Gibbs (2008).

Data processing and presentation

The %C and suite of CSSI values for the extracted FAMEs were assembled into a matrix table and modelled using IsoSource to estimate the number (*n*) of isotopically feasible proportions of the main sediment sources at each sampling location. In successive model iterations, potential sources were added or removed to find an isotopic balance where the confidence level was high (lowest *n* value) and uncertainty was low. The isotopically feasible proportions of each soil source are then converted to soil proportions using the %C of each soil on a proportional basis. That is to that the higher the %C in the soil, the less of that soil source is required to obtain the isotopic balance. In general, soil proportions less than 5% were considered possible but potentially not present. Soil proportions >5% were considered to be present within the range of the mean ± SD.

CSSI Method

The CSSI method applies the concept of using the $\delta^{13}C$ signatures of organic compounds produced by plants to distinguish between soils that develop under different land-cover types. With the exception of monocultures (e.g., wheat field), the $\delta^{13}C$ signatures of each land-cover type reflects the combined signatures of the major plant species that are present. For example, the isotopic signature of the Bay's lowland native forest will be dominated by kauri, rimu, totara and tānekaha. A monoculture, such as pine forest, by comparison will impart an isotopic signature that largely reflects the pine species, as well as, potentially, any understory plants.

The application of the CSSI method for sediment-source determination involves the collection of sediment samples from potential sub-catchment and/or land cover sources as well as sampling of sediment deposits in the receiving environment. These sediment deposits are composed of mixtures of terrigenous sediments, with the contribution of each source potentially varying both temporally and spatially. The sampling of catchment soils provides a library of isotopic signatures of potential sources that is used to model the most likely sources of sediments deposited at any given location and/or time.

Straight-chain FAs with carbon-chain lengths of 12 to 24 atoms (C12:0 to C24:0) have been found to be particularly suitable for sediment-source determination as they are bound to fine sediment particles and long-lived (i.e., decades). Fatty acids including myristic (C14:0); palmitic (C16:0); stearic (C18:0); aachidic (C20:0) and behenic (C22:0) have commonly been used to evaluate present and historical sources of terrigenous sediments. Although breakdown of these FA to other compounds eventually occurs, the signature of a remaining FA in the mixture does not change.

The stable isotope compositions of N and C and the CSSI of carbon in the suite of fatty acid (FA) biomarkers are extracted from catchment soils and marine sediments. It is the FA signatures of the soils and marine sediments that are used in this study to determine sediment sources. Gibbs (2008) describes the CSSI method in detail.

Correction of the CSSI signatures for the Suess Effect

The reconstruction of changes in sources of terrigenous sediment deposited in the BOI system is derived from dated cores using the FA isotope signatures preserved in the sediments. Before the feasible sources of these sediments could be evaluated using the IsoSource package, the isotope (i.e., input) data required correction for the effects of the release of "old carbon" into the biosphere over the last 300 years, associated with the burning of fossil fuels and deforestation.

Specifically, the release of old carbon with a depleted $\delta^{13}C$ signature has resulted in a decline in $\delta^{13}C$ in atmospheric CO_2 ($\delta^{13}CO_2$). The changing abundance of carbon isotopes in a carbon reservoir associated with human activities is termed the Suess Effect (Keeling 1979). This depletion in atmospheric $\delta^{13}CO_2$ is of the order of 2 ‰ since 1700 and has accelerated substantially since the 1940s (Verburg 2007). Thus, the $\delta^{13}C$ signatures of plant biomarkers, such as Fatty Acids have also changed due to the Suess Effect. Consequently, the isotopic signatures of estuarine sediments (i.e., the mixture) deposited in the past must be corrected to match the isotopic signatures of present-day source soils.

Figure C-1 presents the atmospheric $\delta^{13}C$ curve reconstructed by Verburg (2007) using data collected in earlier studies and includes measurements of material dating back to 1570 AD. These data indicate that the atmospheric $\delta^{13}C$ signature was stable until 1700 AD, with subsequent depletion of $\delta^{13}C$ due to release of fossil carbon.

In the present study, we use this atmospheric $\delta^{13}C$ curve to correct the isotopic values of the FAs in sediment samples of varying ages taken from cores to equivalent modern values. This is required because the $\delta^{13}C$ values of the FAs from the potential catchment sources are modern (i.e., 2010 AD), and are therefore depleted due to the Suess Effect. For example, the $\delta^{13}C$ value of a Fatty Acid derived from a kauri tree growing today will be depleted by -2.15 ‰ in comparison to a kauri that grew prior to 1700 AD (Fig. 8.1). It can be seen that the isotopic correction for the period since 1700 is variable depending on age. Examples of this correction process for isotopic data for sediments taken from a sediment core collected in the Bay of Islands are presented in Table C-1: Examples of the linear correction method to convert the isotopic proportions to soil proportions. Using sodium (Na) salt compounds as analogies to various soil sources present in a mixture. Error! Reference source ot found.

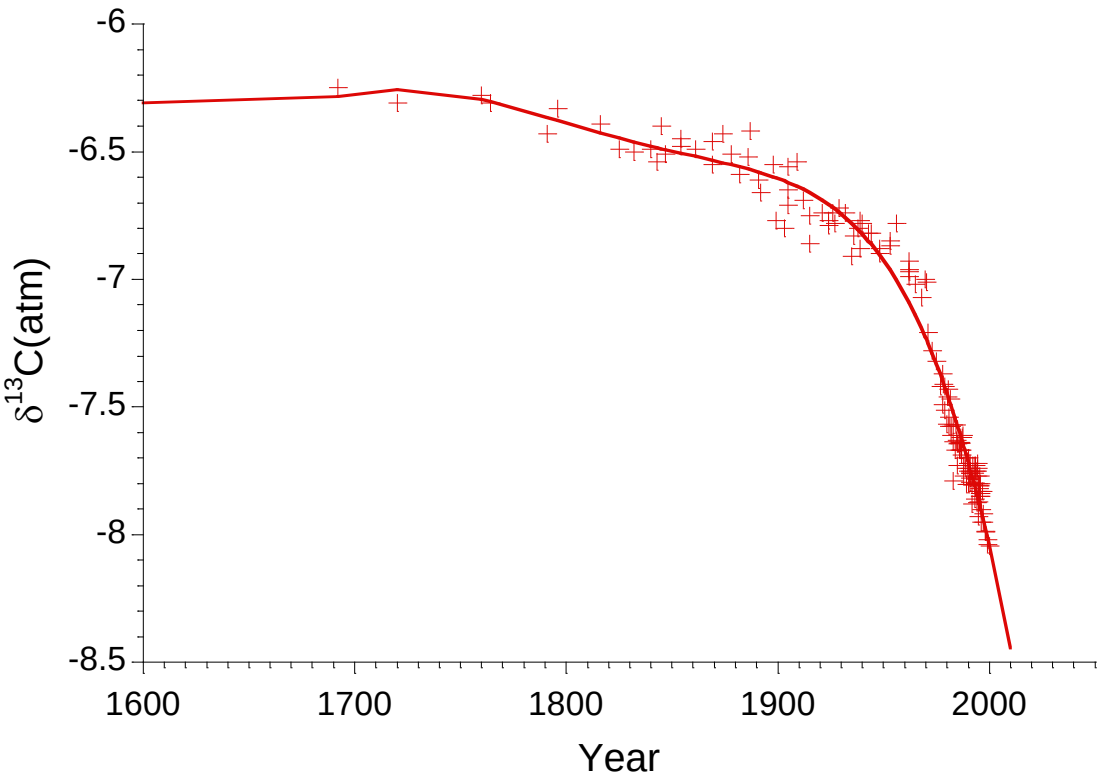

Figure C-1: Historical change in atmospheric $\delta^{13}C$ (per mil) (1570–2010 AD) due to release of fossil carbon. The release of this fossil carbon is associated with anthropogenic activity (the so-called Suess Effect), Source: Verburg (2007).

IsoSource mixing model

IsoSource (Phillips and Gregg, 2003) is not a conventional mixing model in that it iteratively constructs a table of all possible combinations of isotopic source proportions that sum to 100% and compares these predicted isotopic values with the isotopic values in the sediment mixture (i.e., deposit). If the predicted and observed stable isotope values are equal or within some small tolerance (e.g., 0.1 ‰, referred to as the mass-balance tolerance by Phillips and Gregg, 2003) then that predicted stable-isotope signature represents a feasible solution. Within a given tolerance, there may be few or many feasible solutions.

The total number of feasible solutions (*n*) provides a measure of the confidence in the result. High values of *n* indicate many feasible solutions and hence there is low confidence in the result. As the value of *n* reduces towards 1 the level of confidence increases until *n* = 1, which represents a unique solution. It is rare to have an exact match or unique solution. In most cases there will be many feasible solutions and these can be statistically evaluated to assess the most likely combination of sources in the sediment sample. These feasible solutions are expressed as isotopic feasible proportions (%) with an uncertainty value equivalent to the standard deviation about the mean.

In practice, the tolerance is reduced by iteration within the IsoSource model to obtain the lowest *n* and therefore the highest confidence in the result. The tolerance required to obtain any feasible solutions will be greater than 0.1 ‰ if the isotopic values of the source tracers differ markedly from those of the sediment mixture in the receiving environment. Together, the tolerance and number of feasible solutions (*n*) for each sediment mixture provide measures of uncertainty in the results in addition to the standard deviation and the range of the isotopic proportions for each soil source. A

An example result from an IsoSource analysis is shown in Table C-1 below. The feasible isotopic proportions of the three major sediment sources are shown in the table (range = 0–1, where 1 = 100%). Although mean, median and standard deviation values are shown, minimum and maximum values of the feasible isotopic proportions for each source are also calculated. **The reporting solely of mean values is not adequate** and a measure of uncertainty, such as the minimum, maximum and/or standard deviation should be included in the results (Phillips and Gregg 2003).

Table C-1: Example of IsoSource model result. Core RAN-5B (Waikare Inlet, Bay of Islands), estimated year of deposition - 1914 AD. Mean, median and standard deviation (SD) values are shown.

Tolerance	n	Nikau			Kauri			Bracken		
		mean	median	SD	mean	median	SD	mean	median	SD
0.9	3	0.317	0.32	0.006	0.55	0.55	0.01	0.133	0.13	0.006

The results indicate that the soils that make up the sediment-core sample are largely derived from native forest (kauri and nikau associations), with a small contribution from bracken. The presence of bracken is a key indicator of catchment disturbance/forest clearing. The presence of bracken pollen in sediment deposits has long been used in historical reconstructions of the New Zealand environment (e.g., McGlone 1983). However, bracken pollen reflects the presence of these plants growing in the general area and may or may not be indicative of bracken soils being eroded. By comparison, the presence of a CSSI bracken signature in a deposit positively indicates that some proportion of the sediment sample is composed of eroded bracken soil. The tolerance at 0.9 ‰ is a mid-range value, with values as low as 0.01 ‰ possible in some of the samples that were analysed. The number of feasible solutions (*n* = 3) is low, which also provides high confidence in these results.

Typically less than 5% of most sediment samples is composed of carbon, and the isotopic balance evaluated by IsoSource is only applicable to the carbon content of each source. These isotopically feasible proportions must therefore be converted to soil proportions using a linear scaling factor to estimate the percent contribution of each feasible soil source. This conversion of feasible isotopic source proportions to soil source proportions is described in a following section.

Conversions of isotopic proportions to soil proportions

The IsoSource model provides estimates of the isotopic-proportional contributions of each land-cover (i.e., soil) type in each marine sample. Thus, these results are in terms of carbon isotopic proportions and not source soil proportions. Furthermore, the stable isotope tracers account for a small fraction, typically less than 2%, of total organic carbon (OC) in the soil and OC accounts for typically <10% of the soil by weight. These factors mean that the contribution of each source soil to a sediment mixture will scale with the soil carbon content. Consequently, a linear correction based on the soil OC is required to estimate the proportion of each soil source in a sediment sample from a receiving environment (Gibbs 2008).

To convert the isotopic proportions to soil proportions (S_n%) the simple linear correction equation below was used:

$$S_n\% = \frac{{}^{I_n}/_{C_n\%}}{\sum_n^1 \left({}^{I_n}/_{C_n\%}\right)} * 100$$

Where I_n is the mean feasible isotopic proportion of source soil *n* in the mixture estimated using an isotopic mixing model and C_n% is the percentage organic carbon in the source soil.

Because this calculation only uses the OC% in the source soils for linear scaling, the proportional contribution of each source soil is not influenced by any loss of carbon (e.g., total carbon, FAs etc.,) in the sediment mixture due to biodegradation. The level of uncertainty in the mean soil proportion is the same as that defined by the standard deviation about the mean isotopic proportion.

A simple example of this linear correction is illustrated here by considering a solution composed of a mixture of three different sodium (Na) salts which provide equal proportions of Na to the mixture (3 x 1/3 each): sodium chloride (NaCl, molecular weight 58.45); sodium nitrate ($NaNO_3$, mw 85.0); and sodium sulphate (Na_2SO_4, mw 142.0). Consider each of these salts to represent a different source soil, each of which are present in a sediment mixture. The %Na represents the % carbon in each source soil. The %Na in each salt is calculated by dividing the atomic weight of sodium (23) by the molecular weight of each salt compound, but also recognising how many atoms of sodium are present in the molecule.

Error! Reference source not found. below presents the calculations required to apply the linear orrection equation using the sodium salts example in order to determine how much of each salt is in the mixture. The ratio M%/S% for each salt and sum of this ratio (3.11) represent the numerator and denominator respectively in the conversion equation. Thus, for example the proportion of NaCl salt in the mixture is given by (0.85/3.11)*100 = 27.3%.

Table C-2: Example of the linear correction method to convert the isotopic proportions to soil proportions. Using sodium (Na) salt compounds as analogies to various soil sources present in a mixture.

Salt type	%Na in salt (S%)	%Na in mixture (M%)	M%/S%	% salt in mixture
NaCl	39.4	33.3	0.85	20.5
$NaNO_3$	27.1	33.3	1.23	29.8
Na_2SO_4	32.4	33.3	1.03	33.1
SUM			3.11	

Appendix D Statistical analysis of sources and tracers

The library of $\delta^{13}C$ soil source signatures used in these analyses are identical to those used to model source contributions to the fluvial and estuarine sediments (i.e., bulk, C14:0, C16:0, C18:0, C18:1, C18:2, C20:0, C22:0, C24:0). Outlier signatures within each FA type were identified as >±4‰ of the arithmetic mean within land-use class $\delta^{13}C$ signature. Both subsoil and Wilson mussel farm classes were added to land uses. A lack of "Goat" replicates precluded inclusion of sample 181/38A (thereby excluding the class altogether and sample 181/32 which was mixed "Dairy" and "Goat"), whilst two samples within the "Maize" class were also excluded for having repeated outlying signatures across multiple fatty acids (e.g., 181/47, 181/33). Following exclusion of outliers this amounted to 53 library samples distributed into 9 sediment source classes (Table D-1).

Table D-1: Summary information on δ13C geochemistry of 53 land cover soil library samples distributed into 9 classes. Catchment codes are: P = Piako; W = Waihou; W&P = Waihou and Piako. Values exclude outliers in all classes and $\delta^{13}C$ compounds.

Land use class	Catchment	*n*	Mean $\delta^{13}C$ signature								
			Bulk	C14:0	C16:0	C18:0	C18:1	C18:2	C20:0	C22:0	C24:0
Dairy	W&P	13	-28.2	-28.9	-30.7	-32.4	-29.0	-26.7	-32.7	-30.7	-31.2
Lifestyle	P	2	-28.4	-34.5	-30.8	-31.6	-30.2	-29.8	-31.7	-31.0	-31.3
Maize	W&P	3	-23.0	-25.4	-22.3	-29.9	-21.7	-12.0	-19.1	-20.1	-31.1
Mussel	Firth	3	-22.1	-25.0	-25.2	-25.7	-23.7	-14.9	-29.2	-25.5	-27.0
Native	W&P	7	-28.6	-28.6	-24.8	-24.4	-23.8	-27.1	-26.1	-26.1	-26.4
Other crops	W&P	2	-24.7	-29.0	-29.2	-29.5	-27.8	-27.7	-29.8	-31.3	-31.8
Pine	W&P	8	-28.3	-30.5	-29.8	-28.9	-28.7	-24.8	-29.8	-29.2	-29.8
Sheep & beef	W&P	10	-28.1	-31.9	-30.9	-32.7	-27.5	-30.2	-34.0	-34.3	-34.4
Subsoil	W&P	5	-26.0	-29.6	-29.6	-23.7	-29.2	-28.2	-30.4	-31.1	-24.0

Methods

Discrimination of similar and dissimilar land cover classes based on their stable carbon isotopic composition was pursued in graphical and statistical approaches, in two steps.

Step 1: Graphical analyses involved generation of Tukey boxplots for each of bulk $\delta^{13}C$ and the eight FAs, across the nine cover classes in R (R Core Development Team, 2016). Linear unconstrained ordinations (PCA) were also performed on centred and standardised variation in the bulk and eight FA $\delta^{13}C$ signatures of 42 samples, in R using the VEGAN package (Oksanen, 2015). The reduced sample number relative to the 53 original filtered samples reflects the need for an observed $\delta^{13}C$ signature across all 9 bulk and FA before inclusion in ordination – hence, 11 samples lacked one or more $\delta^{13}C$ signatures in any of the FA and bulk carbon compounds, following filtering for outliers. PCA (principal components analysis) determines the underlying pattern of change (variance) in the eight FA and bulk $\delta^{13}C$ signatures, and then spreads the 42 individual land cover samples as widely as possible along these gradients or 'principal components' of isotopic variation. A biplot of the 42 samples distributed along the first and second principal components, using symmetric scaling, was utilised to determine which land cover classes were alike or dissimilar, as well as which FA or bulk isotopic signature varied most between land cover classes.

ANalysis Of VAriance (ANOVA) was employed in single factor designs on all samples bar outliers (e.g., n = 49 to 53), to test if statistically significant (p<0.05) differences in mean $\delta^{13}C$ signatures exist between the nine land cover classes, repeated for each of FA and bulk indicator. Residuals were inspected for normality and equivalence of variance. Post-hoc testing of between-class differences was undertaken using Tukey Honest Significant Difference routines. All analyses were undertaken in R using inbuilt functions (R Core Development Team, 2016).

Step 2: Using information provided by Tukey post-hoc testing and the PCA biplot, a subjective decision was made to include, exclude or merge the nine land cover classes to optimise variation between classes across all nine $\delta^{13}C$ indicators. Following this decision, the revised (fewer) land cover classes were again subjected to 1-way ANOVA using revised land cover class as the factor examined, across all nine $\delta^{13}C$ indicators (as before inspecting output for residual normality and equivalence of variance between classes).

Tukey boxplots were generated for the revised land cover classes in R.

Bottom-up, hierarchical cluster analysis was also performed on the full suite of nine $\delta^{13}C$ indicators following standardisation, using the STATS package in R (R Core Development Team, 2016). Clustering requires information on all 8 FA and bulk $\delta^{13}C$, so was conducted on 41 samples (omitting outliers as above, samples lacking any one or more of C14:0-C24:0, and omitting any samples excluded following Step 1). Whereas ANOVA considers each water quality indicator separately, hierarchical classification is multivariate, attempting to discriminate groups of land cover samples whose members are similar within their class but dissimilar between classes, across all 9 $\delta^{13}C$ indicators simultaneously. The dataset of $\delta^{13}C$ signatures was standardised to zero unit mean deviation (to weight the importance of the nine $\delta^{13}C$ indicators equally) before computing a Euclidean distance matrix. Clustering was performed using six linkage functions (e.g., complete, average, Ward-linear, Ward-squared, single median). The optimal linkage function was selected to minimise cophenetic distance and maximise cophenetic correlations (e.g., Gower, 1983). A confusion table was generated in R to demonstrate the degree of similarity (coherence) between the top-down and bottom-up discriminant approaches (i.e., whether the 41 library samples differed markedly in their $\delta^{13}C$ due to corresponding land cover class only, or whether additional factors are also likely to have driven observed differences in the nine $\delta^{13}C$ indicators).

The revised land cover samples were also subject to subset 1-way ANOVA with “catchment” as the factor (two classes: Waihou or Piako). Output examined whether statistically significant (p<0.05) differences in geochemistry exist within each revised land use class (across the nine $\delta^{13}C$ indicators) due to location (i.e., whether a sample was collected in the Waihou or Piako catchment).

Results: output from the 1-way ANOVA in Step 1 demonstrated significant differences (p<0.05) attributable to land use as a single factor, in all nine $\delta^{13}C$ indicators (e.g., p<0.001 for each FA or bulk $\delta^{13}C$ indicator (Table D-2). Inspection of residuals demonstrated normality whilst variance was not equal between classes on account of few samples being available in the “lifestyle” and “other cropping” land cover classes. Transformation of the original data could benefit the ANOVA performance, but the limited use of output here in Step 1 to simply determine which classes to merge, makes this unnecessary.

Table D-2: Summary statistics for one-way ANOVA of land use (nine classes) for each of nine δ13C indicators. Note that all 9 indicators offer significant differences between at least two land uses (e.g., p <0.05).

Factor	δ^{13}C indicator	Source	df	F	Sig. (p)
Land use	Bulk	Land use	8	39.23	<0.0001
		Residuals	44		
	C14:0	Land use	8	23.55	<0.0001
		Residuals	41		
	C16:0	Land use	8	22.27	<0.0001
		Residuals	43		
	C18:0	Land use	8	22.63	<0.0001
		Residuals	42		
	C18:1	Land use	8	11.7	<0.0001
		Residuals	42		
	C18:2	Land use	8	22.82	<0.0001
		Residuals	40		
	C20:0	Land use	8	7.605	<0.0001
		Residuals	42		
	C22:0	Land use	8	15.1	<0.0001
		Residuals	41		
	C24:0	Land use	8	12.48	<0.0001
		Residuals	41		

Whilst overall output highlights significant differences in δ^{13}C geochemistry are present between **at least** two of the nine land uses, post-hoc testing between the land classes reveals the frequency of significant differences to other land uses varied, from a mode of 1 of 8 pairings for "Other Cropping" (potato, onion) to 7 of 8 possible pairings for "Mussel" and "Maize" classes (i.e., mode calculated across full suite of nine δ^{13}C indicators – Table D-3). If instead the percentage of significantly different (p<0.05) pairings between each of the nine land use classes is inspected, performance appears better ranging from 24% of 72 possible pairings with "Lifestyle" through to 76% of the 72 possible pairings with "Mussel" differing significantly (i.e., the "Mussel" class differing in 55 of 72 pairings across the nine δ^{13}C indicators – Table D-3). Overall in terms of the nine land use classes, both "Lifestyle" (24%) and "Other Cropping" (26%) were poorly discriminated from others whilst only Sheep & beef" (49%), "Maize" (57%) and "Mussel" (76%) were well-discriminated – note, this is in the context of having a full suite of nine possible land use classes and performance would improve by agglomeration.

Performance of each δ^{13}C indicator to discriminate between land use classes also varied markedly (Table D-3). For instance, modal differences between land uses within each compound varied from 1 for C20:0 and C24:0 through to 3 for C14:0 and 4 for bulk δ^{13}C. A general pattern was evident that when comparing between the nine land use classes, better discrimination was possible with shorter carbon-chain FA. In terms of the percentage of 72 pairings possible between the nine land uses but within each compound, the number that were significantly different varied from 25% (C20:0) to 64% of pairings (bulk δ^{13}C).

Table D-3: Summary table of post-hoc Tukey significant differences (p<0.05). For all 504 possible relationships between: (1) each of the 9 land use classes; and (2) the nine FA $\delta^{13}C$ tracers. Note the summary performance measures by land use class (horizontal base) and $\delta^{13}C$ indicator (vertical right).

$\delta^{13}C$ tracer	Count of significantly different pairing to other of 8 land uses									Total count	Mode	% of 72 pairs
	Bush	Other Cropping	Dairy	Lifestyle	Mussel	Maize	Pine	Sheep & Beef	Subsoil			
Bulk	4	6	4	4	7	6	4	4	7	46	4	64
C14:0	4	3	3	4	6	6	6	3	5	40	3	56
C16:0	2	2	2	2	7	7	2	2	2	28	2	39
C18:0	3	2	5	2	7	3	3	6	3	34	3	47
C18:1	2	1	2	2	6	7	2	2	2	26	2	36
C18:2	3	2	2	2	7	7	2	3	2	30	2	42
C20:0	1	1	3	0	2	2	2	6	1	18	1	25
C22:0	3	1	3	1	8	2	3	5	2	28	3	39
C24:0	3	1	4	0	5	1	2	4	2	22	1	31
Total count	25	19	28	17	55	41	26	35	26			
Mode	3	1	3	2	7	7	2	4	2			
% of 72 pairings	35	26	39	24	76	57	36	49	36			

Table D-4 has been produced to guide reduction of the nine land use classes into a better discriminated subset. It presents the pairwise differences between each land use. From this, “Bush” fails to differ significantly from “Lifestyle” and “Pine” in any of the nine $\delta^{13}C$ indicators, but otherwise does differ from remaining land classes across two or more indicators (typically shorter-chain FAs). “Dairying”, “Sheep & Beef” and “Lifestyle” also fail to differ significantly from each other in any of the nine $\delta^{13}C$ indicators. “Lifestyle” also fails to differ significantly from “Bush” and “Pine” in any of the nine $\delta^{13}C$ indicators (differing significantly with “Other cropping” and “Subsoil” in only two of nine indicators). “Other cropping” also is poorly discriminated from other land use classes, differing significantly from “Maize” in only three short-chain FAs (e.g., C16:0, C18:1, C18:2). Oddly, “Maize” and “Mussel” whilst significantly different to every other land use class on short and long-chain FA $\delta^{13}C$, are only different to each other in terms of their C22:0 $\delta^{13}C$ signature (i.e., are otherwise similar to each other).

Table D-4: Post-hoc Tukey output displaying compounds that differed significantly between pairs of land use classes (p<0.05). Note the better discrimination of some classes (i.e., those with greatest number of the nine $\delta^{13}C$ FA tracers observing a significant difference to another class [e.g., "Maize" and "Mussel"]).

	Bush	Other cropping	Dairying	Lifestyle	Mussel	Maize	Pine	Sheep & Beef	Subsoil
Bush		Bulk C14:0	C18:0 C22:0 C24:0		Bulk C14:0 C16:0 C18:0 C18:1 C18:2 C22:0 C24:0	Bulk C14:0 C16:0 C18:1 C18:2		C18:0 C18:2 C20:0 C22:0 C24:0	Bulk C14:0
Other cropping			Bulk	Bulk C14:0	Bulk C16:0 C18:0 C18:2 C22:0 C24:0	C16:0 C18:1 C18:2	Bulk C14:0	Bulk C18:0 C20:0	
Dairying					Bulk C14:0 C16:0 C18:0 C18:1 C18:2 C20:0 C22:0 C24:0	Bulk C14:0 C16:0 C18:0 C18:1 C18:2 C20:0	C14:0 C18:0 C20:0 C22:0 C24:0		Bulk C18:0 C24:0
Lifestyle					Bulk, C14:0 C16:0 C18:0 C18:1 C18:2 C22:0	Bulk C14:0 C16:0 C18:0 C18:1 C18:2			Bulk C14:0
Mussel						C22:0	Bulk C14:0 C16:0 C18:0 C18:1 C18:2 C22:0	Bulk C14:0 C16:0 C18:0 C18:1 C18:2 C20:0 C22:0 C24:0	Bulk C14:0 C16:0 C18:0 C18:1 C18:2 C20:0 C22:0
Maize							Bulk C14:0 C16:0 C18:0 C18:1 C18:2	Bulk C14:0 C16:0 C18:0 C18:1 C18:2 C20:0 C22:0	Bulk C14:0 C16:0 C18:1 C18:2

	Bush	Other cropping	Dairying	Lifestyle	Mussel	Maize	Pine	Sheep & Beef	Subsoil
Pine								C14:0 C18:0 C20:0 C22:0 C24:0	Bulk C14:0
Sheep & Beef									Bulk C18:0 C20:0 C22:0 C24:0
Subsoil									

Inspection of the PCA biplot, where Axes 1 and 2 explained 88% of the variance in $\delta^{13}C$ FA tracers between library samples tested, supports above findings (Figure D-1). For instance, the majority of differences between all 42 samples were expressed in the mid-to-short chain FA (PCA Axis 1 which explained 68% of total geochemical variance is driven by changes to $\delta^{13}C$ of C18:0, C18:1 and C18:2; PCA Axis 2 which explained 20% of total geochemical variance is driven by change to $\delta^{13}C$ of C14:0). From the position of the land use classes, "Dairying" and "Sheep & Beef" clearly overlap, suggesting their merger into a combined pastoral class would better discriminate differences to other land uses, but also that this combined class would vary little in terms of C14:0 or bulk $\delta^{13}C$ whilst exhibiting larger within-class variation amongst C18:0 and longer FA. "Mussel" and "Maize" classes are also highly alike but as before, markedly dissimilar to the other land use classes. Merging both would be illogical given their distinctly different pathways for sediment to travel (i.e., from the sea and land respectively). Other notable features of Figure D-1 are that "Bush" and "Pine" classes also overlap, precluding the ability to separately model their contributions to Firth sediment cores reliably. However, note that pre-European sediments will naturally exclude "Pine" soil contributions (e.g., Newnham et al. 1995; Giles et al. 1999; Wilmshurst et al. 2008). Similarly, that "Other cropping" signatures are markedly dissimilar from "Maize" and "Mussel" but otherwise overlap with many other classes, on both shorter and longer FA. Hence, although poorly distinguished "Other cropping" cannot be readily merged with any other land use class, which combined with its overlapping other sources precludes it inclusion in Step 2. By excluding "Other cropping", the geochemistry of "Subsoils" is also better distinguished although the latter overlap somewhat with "Bush" signatures. Much broader overlap with other classes limits the ability to discriminate the "Lifestyle" samples that are distributed very widely in terms of their $\delta^{13}C$ signatures on short and longer chain FAs. This wide variance in geochemistry coupled to overlapping with "Dairying", "Sheep & Beef", "Bush" and "Pine" classes precludes inclusion of "Lifestyle" to mixture modelling of Firth sediments.

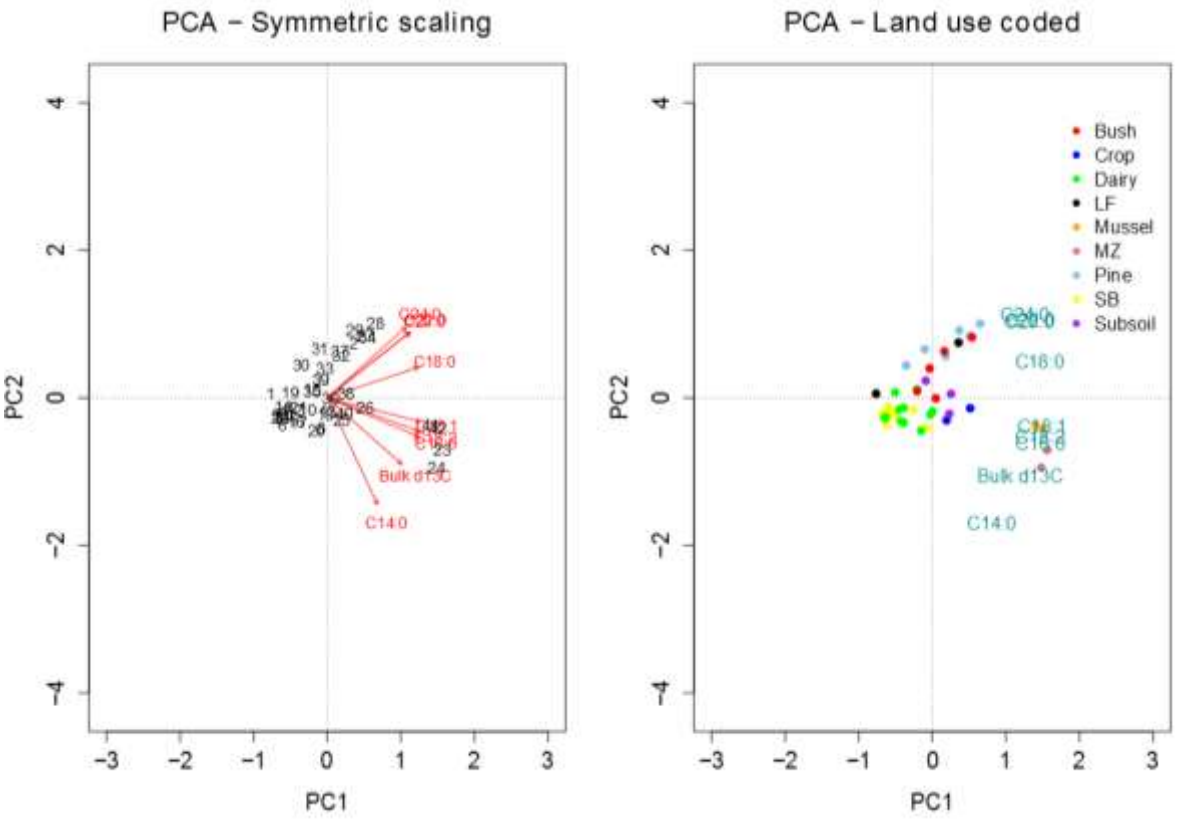

Figure D-1: PCA biplot of 42 land use samples distributed into nine classes, by corresponding fatty acid and bulk δ13C indicator. The direction of arrows indicates the effect on each axis (greater effect if line drawn from arrow tip perpendicular to axis is lengthiest on that axis). Position of land use samples indicates their degree of similarity across the nine $\delta^{13}C$ indicators (greater similarity if overlapping or position close together in biplot).

Combining the information from Table D-1 to Table D-4 with Figure D-1, it is clear that several land uses were infrequently discriminated from others. "Other cropping" and "Lifestyle" classes differed least significantly amongst all possible pairings (i.e., differing significantly only in <20 of 72 relationships possible across the nine $\delta^{13}C$ indicators). Based on their varying geochemistry and limited replicates, neither class can be merged reliably with others so both should be excluded from Step 2. Likewise the lack of any significant difference between "Dairying" and "Sheep & Beef" in any of the nine $\delta^{13}C$ indicators but the marked differences between both and other land uses in over half of all possible relationships, suggests a merged pastoral class will be effectively discriminated from others. Based on the lack of any significant difference between "Bush" and "Pine" in any of the nine $\delta^{13}C$ indicators, and their distinction from most other classes (with the exception of "Subsoil"), a combined forest class should perform better in later mixture modelling. Hence, five distinct classes were selected for Step 2: "Forest" (pine and bush combined), "Maize", "Mussel", "Pastoral" (dairying and sheep & beef combined) and "Subsoil".

Step 2: Significant (p<0.05) differences were observed in all nine $\delta^{13}C$ indicators by **at least** two of the five land uses (Table D-5). Inspection of residuals demonstrated normality and variance was equivalent between the five land cover classes, an improvement on Step 1.

Table D-5: Summary statistics for one-way ANOVA of revised land use (five classes) for each of nine δ13C indicators.

Factor	$\delta^{13}C$ indicator	Source	df	F	Sig. (*p*)
Land use	Bulk	Land use	4	72.78	<0.0001
		Residuals	44		
	C14:0	Land use	4	39.4	<0.0001
		Residuals	41		
	C16:0	Land use	4	45.55	<0.0001
		Residuals	43		
	C18:0	Land use	4	50.72	<0.0001
		Residuals	42		
	C18:1	Land use	4	19.71	<0.0001
		Residuals	42		
	C18:2	Land use	4	37.63	<0.0001
		Residuals	40		
	C20:0	Land use	4	15.1	<0.0001
		Residuals	42		
	C22:0	Land use	4	33.5	<0.0001
		Residuals	41		
	C24:0	Land use	4	30.14	<0.0001
		Residuals	41		

Post-hoc testing revealed that the five revised land classes generally performed equally well to each other (

Table D-6). The frequency of significant differences varied little, from a mode of 2 of 4 possible land use pairings for “Forest” and “Subsoil”, to a mode of 3 for “Maize”, “Mussel” and “Pasture” (i.e., that the latter generally differed significantly from all bar one of the other land uses across the nine $\delta^{13}C$ indicators). When examined as a percentage, performance is markedly better than in Step 1 meaning the exclusion and merger of the earlier nine land use classes into just five has improved discriminant ability for later mixture modelling. For instance, the proportion of significantly different relationships between revised land use classes varied from 56% for “Subsoil” to 83% in “Pasture”, compared to between 24% for “Lifestyle” and 76% for “Mussel” for the original nine land uses.

Table D-6: Summary table of post-hoc Tukey significant differences (p<0.05). For all 180 possible relationships between each of 5 land use classes and another, over the nine $\delta^{13}C$ indicators. Note the summary performance measures by land use class (horizontal base) and $\delta^{13}C$ indicator (vertical right).

$\delta^{13}C$ Indicator	Count of significantly different pairing to other of 4 land uses					Total count	Mode	% of 20 pairings
	Forest	Maize	Mussel	Pasture	Subsoil			
Bulk	3	3	3	3	4	16	3	80
C14:0	4	3	3	3	3	16	3	80
C16:0	3	4	4	3	2	16	3	80
C18:0	2	2	3	4	3	14	2	70
C18:1	2	3	3	2	2	12	2	60
C18:2	3	4	4	3	2	16	3	80
C20:0	1	1	1	4	1	8	1	40
C22:0	2	2	4	4	2	14	2	70
C24:0	2	2	3	4	1	12	2	60
Total count	22	24	28	30	20			
Mode	2	3	3	3	2			
% of 20 pairings	61	67	78	83	56			

All five land use classes are significantly different from each other in at least two of the nine $\delta^{13}C$ indicators, but most often in seven $\delta^{13}C$ indicators. From

Table D-7: Post-hoc Tukey output displaying compounds that differed significantly between pairs of land use classes ($p<0.05$)., the revised "Pasture" class is significantly different from every other land use in at least seven of nine $\delta^{13}C$ indicators. The "Mussel" and "Maize" classes perform equally well being significantly different from every other land use class, in at least four of the $\delta^{13}C$ indicators. However, both classes are insignificantly different to each other in five $\delta^{13}C$ indicators (i.e., "Mussel" and "Maize" are generally alike in the majority of $\delta^{13}C$ indicators). With the exception of "Subsoil" the revised "Forest" class was significantly different from "Maize", "Mussel" and "Pasture" in at least five $\delta^{13}C$ indicators – "Forest" and "Subsoil" were quite alike differing only in terms of their C14:0 and bulk $\delta^{13}C$. Figure D-2 to Figure D-4 display these apparent similarities and dissimilarities more clearly, showing the great distinction of "Pasture" from every other class across most $\delta^{13}C$ indicators, the similarity of "Forest" and "Subsoil" in all bar two indicators and the similarity of "Mussel" and "Maize" in the majority of $\delta^{13}C$ indicators.

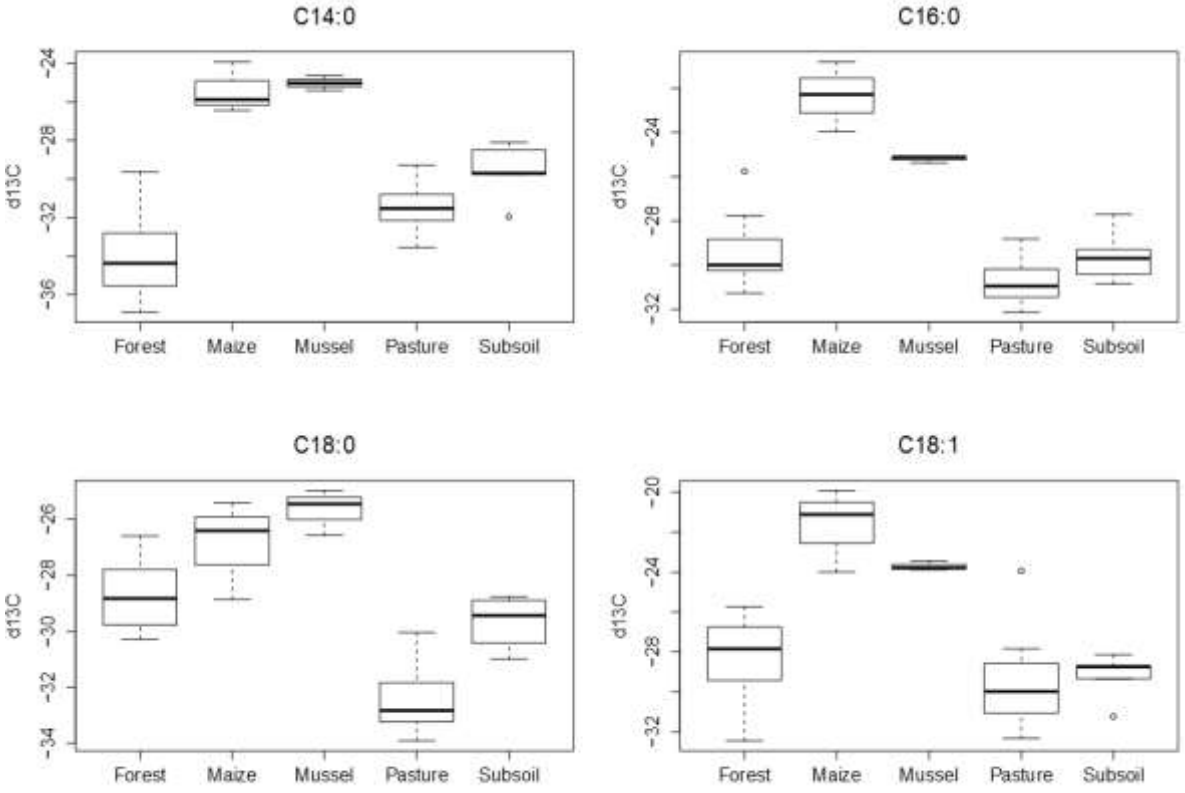

Figure D-2: Boxplots of the five revised land use classes for C14:0, C16:0, C18:0 and C18:1 fatty acid δ13C. Vertical axes are δ13C (‰).

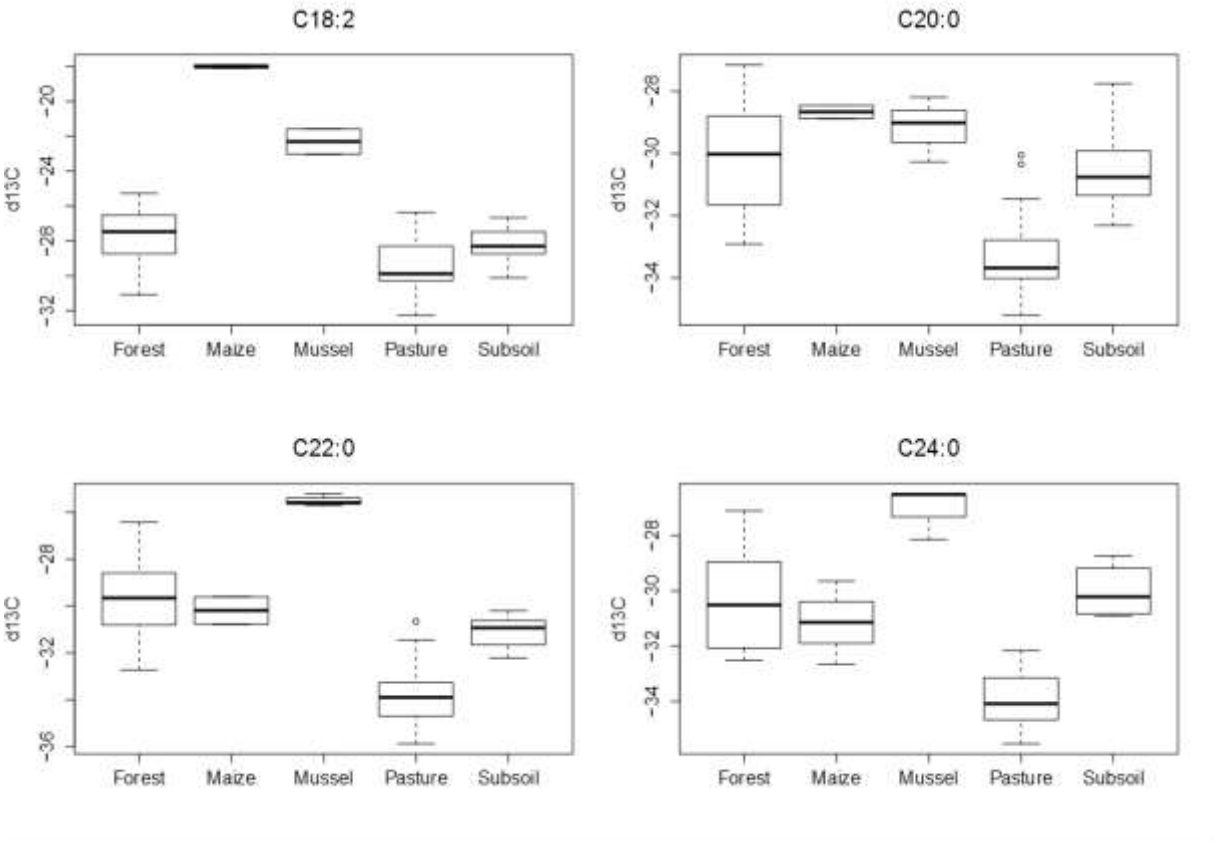

Figure D-3: Boxplots of the five revised land use classes for C18:2, C20:0, C22:0 and C24:0 fatty acid δ13C. Vertical axes are δ13C (‰).

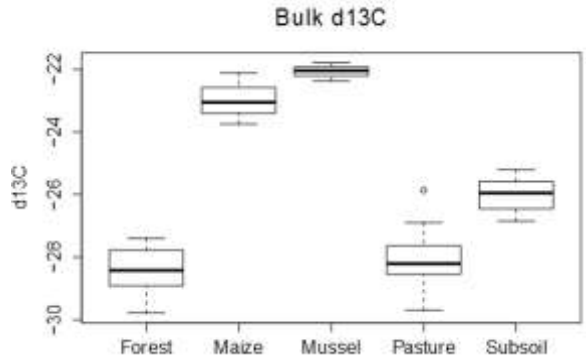

Figure D-4: Boxplot of the five revised land use classes for bulk δ13C. Vertical axis is δ13C (‰).

Table D-7: Post-hoc Tukey output displaying compounds that differed significantly between pairs of land use classes (p<0.05). Note the good discrimination of all five classes (i.e., compared to Table D-4).

	Forest	Maize	Mussel	Pasture	Subsoil
Forest		Bulk C14:0 C16:0 C18:1 C18:2	Bulk C14:0 C16:0 C18:0 C18:1 C18:2 C22:0 C24:0	C14:0 C16:0 C18:0 C18:2 C20:0 C22:0 C24:0	Bulk C14:0
Maize			C16:0 C18:2 C22:0 C24:0	Bulk C14:0 C16:0 C18:0 C18:1 C18:2 C20:0 C22:0 C24:0	Bulk C14:0 C16:0 C18:0 C18:1 C18:2 C22:0
Mussel				Bulk C14:0 C16:0 C18:0 C18:1 C18:2 C20:0 C22:0 C24:0	Bulk C14:0 C16:0 C!8: C18:1 C18:2 C22:0
Pasture					Bulk C18:0 C20:0 C22:0 C24:0
Subsoil					

As above, shorter-chain FAs perform better at discriminating between the five revised land use classes (

Table D-7). For instance, C14:0, C16:0 and C18:2 offer equivalent performance, with 80% of possible pairings being significantly different (e.g., 16 of 20). Performance drops in mid-chain and long-chain FAs but is otherwise good (e.g., ≥60% or 12 of 20 possible pairings). Importantly, revising the land use classes has improved the ability to discriminate between the revised sediment sources; the percentage of significant between-class differences in any one $\delta^{13}C$ indicator has risen from between 25% and 64% (with nine distinct classes) to between 40% and 80% (with five distinct classes).

Efficacy of revised land cover classification at discriminating sediment sources

Bottom-up clustering demonstrated greater performance for average-linkage (UPGMA) hierarchical clusters, than for the other five linkage functions tested (e.g., least Gower distance [512] and greatest Cophenetic Kendall correlation [0.76] from average linkage Euclidean distance matrix). Utilising 'revised' land cover classes and comparing these to the average-linkage dendrogram cut at five leaves, resulted in a low misclassification rate of 18%. That is, based on no more than their observed $\delta^{13}C$ across the nine indicators, 31 of 38 soil library samples would correctly be assigned into a cluster of like-class samples). Both the "Maize" and "Mussel" samples were correctly clustered into two unique groups. All 20 "Pasture" samples were clustered into a single group albeit, with two of eleven "Forest" and all three "Subsoil" samples also included – likely due to variation between "Pasture" samples and overlap of this variance with that of "Subsoils", particularly on shorter chain FAs (e.g.,C14:0, C16:0, C18:1, C18:2). "Forest" samples are the least well clustered, being distributed into three separate clusters of which only seven samples were uniquely clustered together (Figure D-5). However, when examining those seven "Forest" samples, they comprise three bush and three pine signatures from Step 1 so the merger of both prior classes into the revised "Forest" class remains supported. Overall, the low misclassification rate does suggest that that vast majority of differences in $\delta^{13}C$ signatures between the 38 soil library samples clustered, can be explained solely on account of their 'revised' land use proving that Step 2 has been effective at improving subsequent discrimination of land uses in mixture modelling.

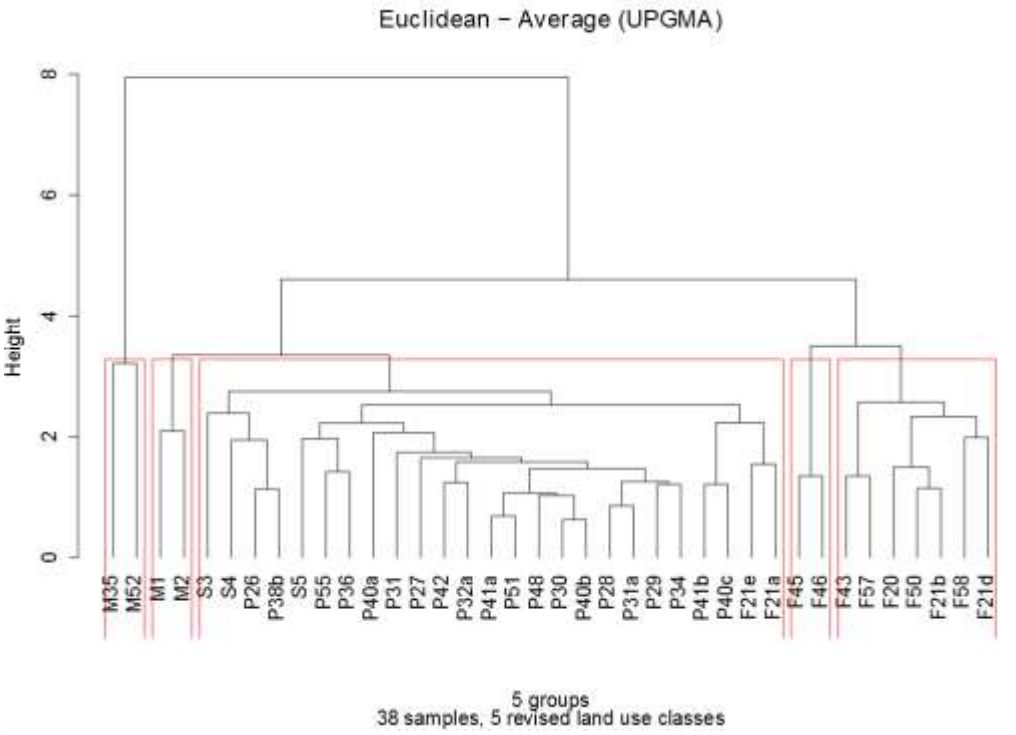

Figure D-5: Average-linkage dendrogram (on Euclidean distance) of 38 soil library samples distributed across nine δ13C indicators. The dendrogram has been cut to five leaves for comparison to revised land use classes, but fusion level plots suggest six would be the optimal number of groups.

Catchment-specific effects on $\delta^{13}C$ signatures

Only two of the five revised land cover classes offered a sufficient number of replicates distributed in both Waihou and Piako catchments, to test catchment type was able to explain significant differences in observed $\delta^{13}C$ (i.e., n >10). This subset 1-way ANOVA revealed that collecting a sample in the Waihou or Piako had no significant effect on the corresponding $\delta^{13}C$ of all nine indicators for "Pasture" and eight indicators for "Forest". The only $\delta^{13}C$ indicator to vary significantly between catchments within "Forest" was C18:1 (p=0.04). Taken together, this implies very little likelihood that catchment rather than land use, is important in determining the $\delta^{13}C$ of FAs. Hence, splitting revised land cover classes into Waihou or Piako specific variants is unwarranted for mixture modelling.